SKI Report 2008:47

Research

# Selected Models for Key Processes in a Nuclear Waste Repository

## Temperature field – Bentonite drying/resaturation

Johan Claesson

December 2007

ISSN 1104-1374
ISRN SKI-R-08/47-SE

SKI

# SKI Perspective

## Background

The conceptual design of the disposal of spent nuclear fuel in Sweden is based on a multi-barrier system. In the KBS-3 concept, the bentonite buffer is a barrier with the primary purpose of surrounding and protecting the canister. The bentonite buffer is expected to prevent or minimise the water exchange with the surrounding rock and protect the canister against mechanical damages caused by possible shear movements in the immediate surroundings.

For a number of years, the researchers at Chalmers University of Technology have studied the buffer, with special emphasis on the drying and saturation phases of the buffer evolution. As a complement to the detailed numerical models for coupled thermal-hydrological-mechanical-chemical (THMC) processes, simplified models have been developed within the current project in order to improve the conceptual understanding of relevant physical processes and their interactions.

## Purpose

The main purpose of this project is to: 1) develop new tools to quantify the drying and the resaturation stages, 2) study parameter sensitivity and identify key parameters, and 3) provide independent methods to test other numerical models. The study is restricted to the moisture flow in the bentonite annulus. The project is a complementary study with focus on understanding and an endeavour to provide handy models.

## Results

A compact formula for the temperature level and gradient in the bentonite is presented. The key radial moisture flow process at a canister is shown to be governed by two flow coefficient functions. These depend on water and bentonite properties in a rather complicated way, but they are determined quite handily by one of the models.

The main results of this work are new complete analytical solutions for the linearized wet-rock and dry-rock cases. The solutions involve two key parameters only, a time scale and a thermo-diffusive parameter a. The largest drying at the canister wall and the resaturation in the wet-rock case are obtained from a single set of curves with a dimensionless time and a as the only parameter. Explicit formulas for the largest drying and for the resaturation process are presented.

The studies of parameter sensitivity show that the hydraulic conductivity at full saturation is a key parameter. Other important parameters are the temperature level and the intensity of the heat release from the canister. The initial degree of saturation is important, in particular in the dry-rock case with no water supply from the rock. The ratio between dry vapour conductivity and saturated liquid conductivity is important. These results are summarized as two rules of thumb.

## Effect on SKI work

This work will be used in the SKI evaluation of the SKB work on drying and resaturation of bentonite. The report will also be used as one basis in SKI's forthcoming reviews of SKB's safety assessments of long-term safety and RD&D programmes.

## Project information

Responsible for the project at SKI has been Christina Lilja and Anna Cato.
SKI reference: SKI 2006/698/200710223

SKI Report 2008:47

Research

# Selected Models for Key Processes in a Nuclear Waste Repository

## Temperature field – Bentonite drying/resaturation

Johan Claesson
Chalmers University
Sweden

December 2007

## Summary

The bentonite, which surrounds and protects the canisters in a nuclear waste repository deep down in rock, experiences a complex, coupled heat and moisture flow process. The emitted heat from the canisters will cause an initial drying from the warmer canister side. The water in cracks and fractures in the rock will on the other hand cause successive saturation of the bentonite from the outer rock side. These processes will interact and one key question is the degree of initial drying and the time it takes to saturate the bentonite.

This paper studies this problem and presents new handy tools of analysis. A compact formula for the temperature level and gradient in the bentonite is presented. The key radial moisture flow process around a canister is shown to be governed by two flow coefficient functions. These depend on water and bentonite properties in a rather complicated way, but they are determined quite handily by one of the models.

The moisture flow may have a time scale of a few years, while the canister heat emission and temperature process involve a time scale of decades. Steady-state solutions are therefore of interest. One model solves the general case of coupled nonlinear differential equations for water saturation $S(r)$ and temperature $T(r)$. An analysis of the equations shows that there is a direct relation between *S* and *T*, with the initial degree of saturation as a parameter. We get a set of curves that gives the (steady-state) drying for any temperature level, canister heat emission, and water saturation level. These very instructive diagrams are generated for any set of data in a few seconds.

The second part of the analysis concerns the transient moisture flow process. There are two limits. In the wet-rock case, full saturation ($S = 1$) is maintained at the rock boundary. The moisture flux is zero at the rock boundary in the dry-rock case. The equation for the water saturation $S(r,t)$ involves two free flow coefficient functions which are functions of *S* and *T*. It is shown that the highly non-linear equation may, when formulated in a special way, be linearized with a loss of accuracy of some 10% only. The paper presents new complete analytical solutions for the linearized wet-rock and dry-rock cases. The solutions involve two key parameters only, a time scale and a thermo-diffusive parameter *a*. The largest drying at the canister wall and the resaturation in the wet-rock case are obtained from a single set of curves with a dimensionless time and *a* as the only parameter. Explicit formulas for the largest drying and for the resaturation process are presented.

The steady-state equation may also be linearized with a modest loss of accuracy. A compact explicit formula for the saturation as function of radius is obtained. The largest drying, which occurs at the canister boundary, is given by a handy formula that involves the initial degree of water saturation and the parameter *a* only

All mathematical programs are implemented in Mathcad. They involve each a few pages. The computer time is typically a few seconds up to a minute only. The models are easy to understand, implement and use.

The studies of parameter sensitivity show that the hydraulic conductivity at full saturation is a key parameter. Other important parameters are the temperature level and the intensity of the heat release from the canister. The initial degree of saturation is important, in particular in the dry-rock case with no water supply from the rock. The ratio between dry vapor conductivity and saturated liquid conductivity is important. These results are summarized as two rules of thumb.

# Contents


1 Nuclear waste repository ..... 1
2 Heat and moisture flow problem ..... 2
3 Outline of the study and the analyses ..... 4
4 Formula for the bentonite temperature level ..... 7
5 Temperature from canister heat sources ..... 8
5.1 Time-dependent point heat source ..... 8
5.2 Time-dependent line heat source ..... 8
5.3 Field of canister heat sources ..... 9
5.4 Tunnel line heat source ..... 9
5.5 Rectangular global heat source ..... 10
5.6 Effect of ground surface and undisturbed temperature ..... 10
5.7 Mixed solution ..... 11
5.8 Final fast solution ..... 12
6 Equations for heat and moisture flow ..... 13
6.1 Flow equations ..... 13
6.2 Data for bentonite and water ..... 13
6.3 General form for flow equations ..... 14
6.4 Temperature over the bentonite annulus ..... 15
6.5 Thermo-diffusive coefficient function A(S,T) ..... 15
6.6 Moisture balance equation ..... 16
7 Steady-state analyses ..... 18
7.1 General steady-state equations ..... 18
7.2 Coordinate-independent relation between S and T ..... 19
7.3 Solution for the reference case ..... 19
7.4 Charts for S(T) ..... 21
7.5 Linearized equation for S(r) ..... 23
8 Assessing drying, wetting and resaturation ..... 27
8.1 Linearization of the equation for S(r,t) ..... 27
8.2 Solution of linearized equation ..... 29
8.3 An example. The reference case ..... 30
8.3.1 Dry-rock case ..... 30
8.3.2 Wet-rock case ..... 31
8.4 Dependence on saturation and temperature level ..... 32
8.5 Graphs for the full solution for different a-values ..... 33
8.5.1 Dry-rock case ..... 34
8.5.2 Wet-rock case ..... 34
8.6 Drying at the canister wall in the dry-rock case ..... 36
8.7 Drying and resaturation at the canister wall in wet-rock case ..... 37
8.7.1 Drying and resaturation for different a-values ..... 37
8.7.2 Formulas for drying ..... 38
8.7.3 Formulas for resaturation ..... 39
9 Key parameters and sensitivity analysis ..... 41
9.1 Key factors for the thermo-diffusive parameter a ..... 41
9.2 Key factors for the time scale $t_0$ ..... 41
10 Survey of models ..... 43
11 Boltzmann solution ..... 44
11.1 General step-response problem ..... 44

11.2 Boltzmann solution ..... 44
12 Conclusion ..... 46
References ..... 47
Nomenclature ..... 49
Appendix 1. Temperature field ..... 51
A1.1 Temperature field from heat emitting canisters ..... 51
A1.2 Temperature during the first years ..... 52
A1.3 Simplified formula ..... 53
Appendix 2. Equations for heat and moisture flow ..... 55
A2.1 Data for water ..... 55
A2.2 Flow coefficient functions ..... 55
A2.3 Temperature solution ..... 56
A2.4 Moisture balance equation ..... 56
Appendix 3. Transient solution for dry and wet rock ..... 57
A3.1. Dimensionless form of linearized equation ..... 57
A3.2. Solution for the wet-rock case ..... 58
A3.3. Steady-state solution for the dry-rock case ..... 59
A3.4. Solution for the dry-rock case ..... 60
Appendix 4. Steady-state solution of coupled nonlinear equations for water saturation S(r) and temperature T(r), $r_c<r<r_r$ ..... 61
Appendix 5. Steady-state solution of coupled nonlinear equations to give $S(T;S_0)$ for $T>T_0$, $S(T_0;S_0)=S_0$. ..... 66
Appendix 6. Calculation of thermal diffusivity D, basic time scale $t_{0y}$ and thermo-diffusive parameter A as functions of S and T ..... 69
Appendix 7. Core formulas for σ(s,t) in the dry-rock case. The solution S(r, t). Figure for S(r,t) in reference case ..... 72
Appendix 8. Core formulas for σ(s,t) in the wet-rock case. The solution S(r,t). Figure for S(r,t) in reference case ..... 75

# 1 Nuclear waste repository

Figure 1.1 shows a nuclear waste repository, where the canisters with nuclear waste are buried deep down in rock. The canisters with the radius $r_c$ and height $H_c$ are placed in boreholes with the radius $r_r$ (rock) along parallel tunnels. The canisters are imbedded in bentonite, Fig. 1.2. Each canister emits heat at a rate $Q_c(t)$ (W), which decays slowly with time. The emitted heat will cause a temperature increase in the repository and surrounding rock. The canisters are evenly spread out over a large rectangular area so that too high temperatures are avoided at the canisters.

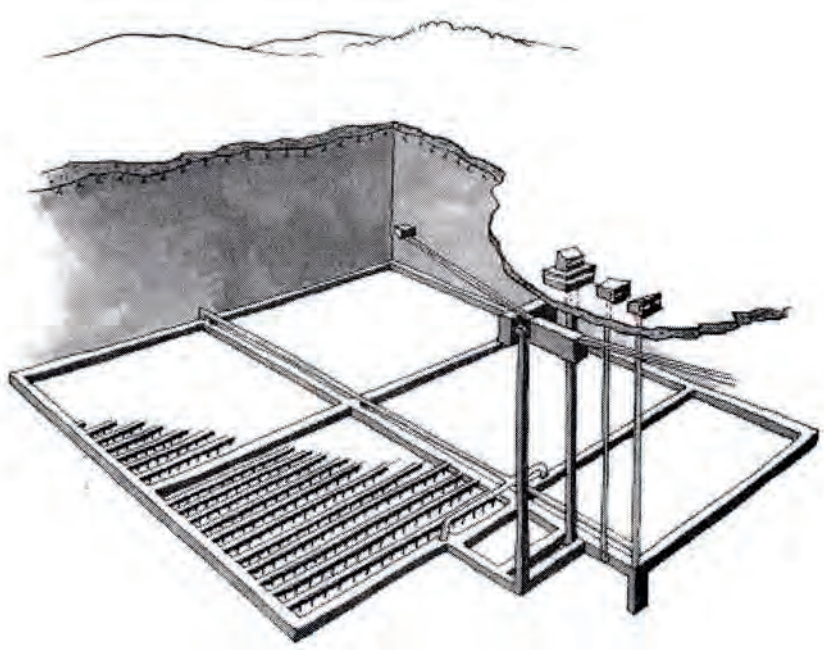

Figure 1.1. SKB concept for nuclear waste repository.

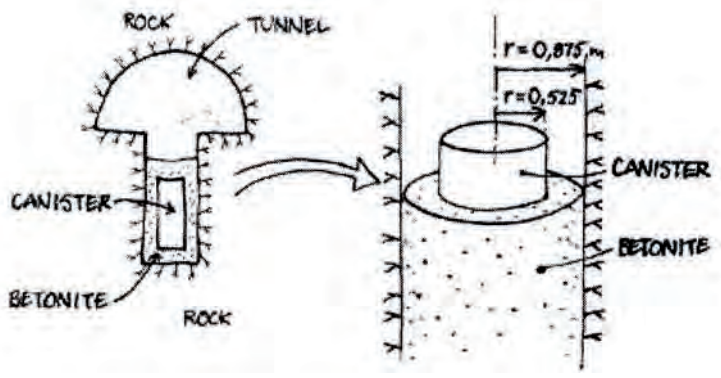


Figure 1.2. Canister imbedded in bentonite in a borehole from a tunnel.

# 2 Heat and moisture flow problem

The bentonite, which surrounds and protects the canisters in a nuclear waste repository deep down in rock, experiences a complex coupled heat and moisture flow process. The emitted heat from the canisters will cause an initial drying from the warmer canister side. The water in cracks and fractures in the rock will on the other hand cause successive saturation of the bentonite from the outer rock side. These processes will interact and a key question is the degree of initial drying and the time it takes to saturate the bentonite under various scenarios. Too much drying of the bentonite may damage its swelling and sealing capacity. The worst case with the strongest drying will occur for a canister in completely dry rock without any water supply from the adjacent rock.

The goal of this study for the moisture flow processes in the bentonite are: (1) find methods to quantify the drying and resaturation, (2) study parameter sensitivity and identify key parameters, and (3) provide independent methods to test other numerical models. These coupled heat and mass processes have been studied with large numerical codes. This is a complementary study with a focus on *understanding* and with an endeavor to provide *handy models*.

The paper gives a survey of our studies and results from the last few years. Formulas, models and other tools of analysis are presented without derivations. The details of derivations are presented in other reports and, to some extent, in appendices.

The canisters of the repository shown in Fig. 1.1 lie in large a rectangular area, $-L < x < L$, $-B < y < B$, $z = 0$, deep down in rock. The horizontal *x*-axis lies perpendicular to the tunnels, and the y-axis lies along the central tunnel The ground surface lies at $z = D_{\mathrm{gr}}$. The canisters are placed along tunnels with the spacing $D_c$. The distance between the parallel tunnels is $D_{\mathrm{t}}$. See Figure 2.1.

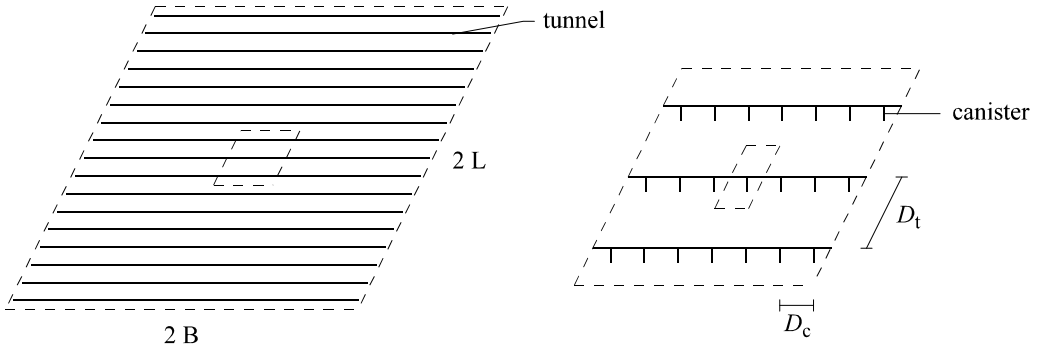


Figure 2.1. Canisters in a rectangular grid along parallel tunnels.

We will use a reference case, from which parameters are varied in the sensitivity analyses. The following data are used in the reference case use:

$$
\begin{aligned}
&L = 500 \text{ m}, \quad B = 500 \text{ m}, \quad D_{\mathrm{gr}} = 500 \text{ m}, \quad \lambda_{\mathrm{r}} = 3.5 \text{ W/(mK)}, \quad a_{\mathrm{r}} = 1.6 \cdot 10^{-6} \text{ m}^2/\text{s}, \\
&D_{\mathrm{c}} = 6 \text{ m}, \quad D_{\mathrm{t}} = 25 \text{ m}, \quad r_{\mathrm{c}} = 0.525 \text{ m}, \quad r_{\mathrm{r}} = 0.875 \text{ m}, \quad H_{\mathrm{c}} = 6 \text{ m}, \\
&T_{\mathrm{rep}} = 15^{\mathrm{o}} \text{ C}, \quad Q_{\mathrm{c}}(0) = 1000 \text{ W}, \quad Q_{\mathrm{c}}(t) = Q_1 \cdot e^{-t/t_1} + Q_2 \cdot e^{-t/t_2} + \ldots \text{ W}.
\end{aligned}
\tag{2.1}
$$

Here, we consider a homogeneous rock with the thermal conductivity $\lambda_r$ W/(m,K)), the density $\rho_r$ (kg/m$^3$), the heat capacity $c_r$ (J/(kg,K)), and the thermal diffusivity $a_r = \lambda_r /(\rho_r c_r)$ (m$^2$/s). The undisturbed ground temperature (without heat emitting canisters) at the repository depth is $T_{rep}$. The heat release $Q_c(t)$ may be any function of time. It may as indicated in (2.1) consist of a number of exponentials, where the smallest decline time is $t_1 = 46$ years.

# 3 Outline of the study and the analyses

The largest drying occurs in the center of the repository with the highest temperatures. We consider in particular the central canister. The drying is driven by water vapor diffusion. The highest drying occurs for the largest temperature gradient in the bentonite around the canister. This largest gradient from the warm canister will occur at the mid level of the canister, since heat may "escape" more easily from top and bottom of the canister. At the mid level of the canister, the heat and moisture flow process in the bentonite annulus is radial without any vertical component. We have only to consider *a radial, one-dimensional process* in the bentonite. This is an important simplification.

The first step in the analysis is to determine the temperature distribution over the bentonite annulus $(r_c < r < r_r,\ z = 0)$ as function of time. The temperature depends on the heat release $Q_c(t)$ from the central canister and from neighboring canisters. More and more canisters must be accounted for as time goes. The heat release decays exponentially with a time scale of some thirty years. The time scale to approach steady-state temperature conditions over the bentonite annulus is below 24 hours. This means that the temperature distribution over the annulus is virtually a steady-state one with a slow change on a time scale of years. A remarkably simple explicit formula for the temperature $T_r(t)$ in the bentonite at the rock boundary $(r = r_r)$ is presented in next section. The quasi steady-state temperature distribution in the bentonite is determined by $T_r(t)$ and $Q_c(t)$. The thermal process is essentially *decoupled* from the moisture flow process.

The equations for moisture flow in the bentonite annulus are discussed in Section 6. The total moisture flux has a liquid and a vapor component. The description of the flow involves data and functions for water and bentonite, and in particular for liquid and vapor flow in the bentonite. The moisture flux is determined by gradients in moisture state variables and temperature. We will choose the degree of water saturation in the bentonite $S$, $0 \le S \le 1$, as our basic moisture state variable. The flow coefficients before the gradients in $S$ and $T$ become functions of $S$ and $T$.

We will restrict this study to the moisture flow in the bentonite annulus. The inner boundary against the canister is certainly watertight with zero moisture flux at $r = r_c$. At the outer boundary $r = r_r$, there are two limits. The rock may be sufficiently wet to maintain full saturation at the surface of the bentonite: $S_r = 1$. We will call this the *wet-rock case*. The other limit, which is the worst possible case, is that the water inflow from the rock is zero: $G_r = 0$. We will call this the *dry-rock case*. (The possibility that the rock sucks water from the bentonite is ruled out, since the suction pressures are so high in bentonite.) The case with high water pressure at the outer bentonite boundary from a water table well above the repository is not discussed here, since it is a more favorable case, which will occur after a longer period of water recovery on repository scale.

With the reference data (2.1), we will find that the time scale to approach (exponentially) steady-state moisture conditions is around 4 years in the wet-rock case, and around 1 year in the dry-rock case. The temperature and the heat release from the canisters have, except for the first few years, a distinctly longer time scale. This means that the *steady-state* solutions for the moisture distribution over the bentonite annulus are quite interesting to us.

The steady-state solutions for the moisture distribution are studied in Section 7. One model deals with the general solution for $S(r)$ and $T(r)$ from two coupled, highly nonlinear, ordinary differential equations. The model that has been implemented in Mathcad is given in full in Appendix 4. From the structure of the coupled differential equations we find that there

is an intrinsic relation between $S$ and $T$ that is *independent* of the radius $r$. We get a set of curves for $S = S(T; S_r)$ for different degree of water saturation $S_r$ at the rock boundary $r = r_r$. These diagrams give directly the drying and moisture distribution over the bentonite annulus in steady state for any moisture level and any temperature interval over the bentonite. The program in Appendix 5 generates a new diagram for any particular set of assumptions and data in a few seconds.

The time-dependent moisture process in the bentonite is studied in Section 8. The basic equation for $S(r,t)$ has a convective-diffusive character with a diffusivity function $D(S,T)$ and a convective-diffusive or thermo-diffusive coefficient function $A(S,T)$. The model that calculates these functions for any particular set of assumptions and data shows that the variations of these functions are rather moderate. In a process within a temperature span of $10^oC$ and a degree of saturation from 0.75 to 1, the two coefficient functions vary some 20%. We may use *constant mean values* with an error below 10%. The model that has been implemented in Mathcad is given in full in Appendix 6.

These constant mean values depend on the saturation and temperature levels in the bentonite for the considered process. We have two basic parameters: the *mean diffusivity* $D_0$ ($m^2/s$) for moisture flow and a dimensionless *thermo-diffusive parameter a*. The diffusivity determines the time scale to attain steady-state conditions. The time scale is inversely proportional to the diffusivity. The second basic parameter $a$ depends on the ratio between vapor and liquid diffusion coefficients. It is also proportional to the heat flux $Q_c(t)$. It increases with the temperature level.

We have in this approximation obtained a *linear* partial differential equation for $S(r,t)$. The general solutions of this equation have been derived for the dry-rock and wet-rock cases. From these solutions, explicit expressions for the maximum drying at the canister and the subsequent resaturation in the wet-rock case are derived. From these solutions, we have formulas and diagrams that give the complete transient process for any parameter values and initial degree of saturation ( $D_0$ or $t_0$, $a$, $S_{in}$ ). The two solutions have been implemented in Mathcad. They are given in full in Appendix 7 and 8.

The linear approximation may also be used as a quite good approximation for the steady-state moisture profiles. In steady state, full saturation $S = 1$ prevails through the bentonite annulus in the wet-rock case. In steady state for the dry-rock case, we get, in the linear approximation, a neat *explicit formula* for the degree of saturation as function of the radius. *The only parameters* are $a$ and $S_{in}$ (and the ratio of radii $r_c / r_r$). The *largest possible drying* in the bentonite occurs in steady state at the canister boundary for the dry-rock case. We get a single, very handy formula and diagram for the largest possible drying under any circumstances with $a$ and $S_{in}$ as parameters.

Section 11 presents briefly a particular so-called Boltzmann solution for the key case of a step change of boundary values at $x = 0$. The coupled highly nonlinear partial differential equations for moisture and heat are reduced to ordinary differential equations with $x/\sqrt{t}$ as variable. These equations may be solved with very high and controlled accuracy.

Section 10 gives a survey of the new models and tools of analysis. All models involve a number of explicit formulas. They have been implements in Mathcad, and they are given in full detail in the Appendices 4 to 8. It should be straightforward to implement the formulas in any other program such as Matlab or Maple.

Any calculation with the models require a few seconds only, except for the full solution of the linearized equations for $S(r,t)$, which may require a few minutes to determine the complete transient moisture flow process.

All models may easily be changed for other assumptions about flow coefficients, data, etc.

# 4 Formula for the bentonite temperature level

The temperature field in the ground consists of an undisturbed ground temperature $T_{\text{undist}}(z)$ with temperature $T_{\text{undist}}(0) = T_{\text{rep}}$ at the repository level and a temperature contribution from some 6 000 heat-emitting canisters as indicated in Fig. 2.1. We are in particular interested in the temperature $T_{\text{r}}(t)$ at the mid-level of the central canister, i.e. for $r = r_{\text{r}}$ and $z = 0$. The formulas for the rock temperatures are discussed further in Appendix 1. Further analyses and full derivations of the formulas are presented Claesson and Probert (1996), Probert and Claesson (1997), and Hökmark and Claesson (2005).

After the first year (or two), we may use the following remarkably simple formula:

$$T_{\text{r}}(t) \approx T_{\text{rep}} + T_{\text{gl}}(t) + Q_{\text{c}}(t) \cdot R_{\text{local}}. \tag{4.1}$$

Here, we have a global temperature field obtained from a surface heat source over the repository rectangle $z = 0$, $-L < x < L$, $-B < y < B$ with the strength $Q_{\text{c}}(t)/\left(D_{\text{c}}D_{\text{t}}\right)$ (W/m$^2$):

$$T_{\text{gl}}(t) = \int_0^t \frac{Q_{\text{c}}(t')/\left(D_{\text{c}}D_{\text{t}}\right)}{\rho_{\text{r}}c_{\text{r}}\sqrt{\pi}\cdot s} \cdot \text{erf}\left(\frac{\text{L}}{s}\right) \cdot \text{erf}\left(\frac{B}{s}\right) \cdot \left(1 - e^{-4D_{\text{gr}}^2/s^2}\right) dt', \qquad s = \sqrt{4a_{\text{r}}(t-t')}\,. \tag{4.2}$$

We have replaced the array of line sources by smearing out the heat source $Q_{\text{c}}(t)$ evenly over the corresponding rectangle with the area $D_{\text{c}}D_{\text{t}}$. See Fig.2.1. The error function erf($x$) is defined in (5.5). The last exponential involving $D_{\text{gr}}$ accounts for the effect of the ground surface. The integral (4.2) in time is easily solved numerically for any time-dependent heat source $Q_{\text{c}}(t)$.

The remaining temperature field involves *balanced* heat sources between the array of line sources and the rectangular source (with negative sign). This part may, after rather intricate calculations, be represented by a single thermal resistance $R_{\text{local}}$ (K/W) in the last term of (4.1):

$$R_{\text{local}} = \frac{1}{2\pi\lambda_{\text{r}}} \cdot \left\{ \frac{1}{H_{\text{c}}} \cdot \ln\left(\frac{\text{H}_{\text{c}}}{\sqrt{1.5}\cdot r_{\text{r}}}\right) + \frac{1}{D_{\text{c}}} \cdot \left[\gamma + \ln\left(\frac{D_{\text{t}}}{4\pi D_{\text{c}}}\right)\right]\right\}, \qquad \gamma = 0.577. \tag{4.3}$$

Here, $\gamma$ is Euler's constant.

The solution (4.1)-(4.3) is valid with good accuracy compared to the full expression (13.1)-(13.2) in App. 1 after a year or two until infinite time. The effects of spacing $D_{\text{t}}$ between tunnels and spacing $D_{\text{c}}$ between canisters along a tunnel are shown in a very clear way.

A formula suitable for the first few years is in Appendix A1.2. It involves the original line sources from the central canister and a suitable number of its closer neighbors. The two closest tunnels are also accounted for by equivalent line heat sources along the two tunnels.

The formulas for the temperature $T_{\text{r}}(t)$ at the rock-bentonite boundary are easily implemented in Mathcad. Any particular case is readily solved. We obtain the temperature level $T_{\text{r}}$ as an input to the further analysis.

# 5 Temperature from canister heat sources

This section presents the formulas derived in the new report Claesson (2007). The formulas are studied in four appended Mathcad calculation sheets.

## 5.1 Time-dependent point heat source

The starting point for all formulas for the temperature is a time-dependent point heat source with the heat release $Q(t)$ (W) from time $t = 0$ in the point $(0,0,0)$ in an infinite solid material with the thermal conductivity $\lambda_r$ (W/(m,K)), the density $\rho_r$ (kg/m$^3$), the heat capacity $c_r$ (J/(kg,K)) and the thermal diffusivity $a_r = \lambda_r/(\rho_r c_r)$ (m$^2$/s). The undisturbed temperature at $t = 0$ is zero throughout the solid. The temperature is

$$T(x,y,z,t) = \int_0^t \frac{Q(t')}{\rho_r c_r} \cdot \frac{1}{\left[4\pi a_r (t-t')\right]^{1.5}} \cdot e^{-\frac{x^2+y^2+z^2}{4a_r(t-t')}}\, dt'. \tag{5.1}$$

We make the substitution

$$u = \frac{\sqrt{t}}{\sqrt{t-t'}}, \qquad t-t' = \frac{t}{u^2}, \qquad dt' = \frac{2t}{u^3}du, \qquad \begin{cases} t' = 0 \leftrightarrow u = 1 \\ t' = t \leftrightarrow u = \infty \end{cases}. \tag{5.2}$$

Then we get a basic integral for the temperature field from a point heat source with the continuous heat release $Q(t)$ (W) from the time $t = 0$ at $(0,0,0)$:

$$T(x,y,z,t) = \frac{1}{4\pi\lambda_r\sqrt{\pi a_r t}} \cdot \int_1^\infty Q\left(t - \frac{t}{u^2}\right) \cdot e^{-\frac{x^2}{4a_r t}\cdot u^2} \cdot e^{-\frac{y^2}{4a_r t}\cdot u^2} \cdot e^{-\frac{z^2}{4a_r t}\cdot u^2} du. \tag{5.3}$$

## 5.2 Time-dependent line heat source

The next step is to consider a time-dependent *line* heat source. The heat $q(t)$ (W/m) is released from time $t = 0$ along the $z$-axis in the interval $-H \le z \le H$. The solution is

$$T(x,y,z,t) = \frac{1}{4\pi\lambda_r\sqrt{\pi a_r t}} \cdot \int_1^\infty 2H \cdot q\left(t - \frac{t}{u^2}\right) \cdot e^{-\frac{x^2}{4a_r t}\cdot u^2} \cdot e^{-\frac{y^2}{4a_r t}\cdot u^2} \cdot E\left(\frac{z}{H}, \frac{Hu}{\sqrt{4a_r t}}\right) du. \tag{5.4}$$

Here, we use the function $E(p,v)$ and the error function erf($x$):

$$E(p,v) = \frac{\sqrt{\pi}}{4} \cdot \frac{\mathrm{erf}\left[(1-p)\cdot v\right] + \mathrm{erf}\left[(1+p)\cdot v\right]}{v}, \qquad \mathrm{erf}(x) = \frac{2}{\sqrt{\pi}} \cdot \int_0^x e^{-s^2} ds. \tag{5.5}$$

We are in particular interested in a *canister line heat source*. The temperature from a canister at the center $(0,0,z)$, $-H < z < H$, $H = H_c/2$, with the heat release $Q_c(t) = 2H \cdot q(t)$ becomes from (5.4)

$$T_{\text{clhs}}(x,y,z,t)=\frac{1}{4\pi\lambda_{\text{r}}\sqrt{\pi a_{\text{r}}t}}\int_1^{\infty}Q_{\text{c}}\left(t-\frac{t}{u^2}\right)\cdot e^{-\frac{x^2+y^2}{4a_{\text{r}}t}\cdot u^2}\cdot E\left(\frac{z}{H},\frac{Hu}{\sqrt{4a_{\text{r}}t}}\right)du. \tag{5.6}$$

## 5.3 Field of canister heat sources

The canisters in the nuclear waste repository lie along tunnels. The distance between the tunnels is $D_{\text{t}}$, and the spacing between canisters along a tunnel is $D_{\text{c}}$. Canister number *n* in tunnel number *m* lies at $x=mD_{\text{t}}$ and $y=nD_{\text{c}}$. The temperature field from this canister becomes

$$T_{\text{can},m,n}(x,y,z,t)=\frac{1}{4\pi\lambda_{\text{r}}\sqrt{\pi a_{\text{r}}t}}\int_1^{\infty}Q_{\text{c}}\left(t-\frac{t}{u^2}\right)\cdot e^{-\frac{(x-mD_{\text{t}})^2+(y-nD_{\text{c}})^2}{4a_{\text{r}}t}\cdot u^2}\cdot E\left(\frac{z}{H},\frac{Hu}{\sqrt{4a_{\text{r}}t}}\right)du. \tag{5.7}$$

The total temperature field from all canister heat sources involves a sum over all tunnels and all canisters along each tunnel:

$$T_{\text{sum}}(x,y,z,t)=\frac{1}{4\pi\lambda_{\text{r}}\sqrt{\pi a_{\text{r}}t}}\int_1^{\infty}Q_{\text{c}}\left(t-\frac{t}{u^2}\right)\cdot\sum_{m=-N_{\text{t}}}^{N_{\text{t}}}\sum_{n=-N_{\text{c}}}^{N_{\text{c}}}e^{-\frac{(x-mD_{\text{t}})^2+(y-nD_{\text{c}})^2}{4a_{\text{r}}t}\cdot u^2}\cdot E\left(\frac{z}{H},\frac{Hu}{\sqrt{4a_{\text{r}}t}}\right)du. \tag{5.8}$$

Here, we consider a case with a central tunnel ($m=0$) and $N_{\text{t}}$ tunnels to the left and to the right. The total number of tunnels in the repository is $2N_{\text{t}}+1$. In each tunnel there is a central canister and $N_{\text{c}}$ canisters on each side. The total number of canisters in a tunnel is $2N_{\text{c}}+1$, and the total number of canisters in the rectangular repository is $(2N_{\text{t}}+1)\cdot(2N_{\text{c}}+1)$.

The double sum (5.8) is a sum over all canisters, i.e. over some 6000 terms. The number of terms to compute can be reduced considerably by writing it as a product. We introduce the sum

$$S(p,v,N)=\sum_{n=-N}^{N}e^{-(p-n)^2\cdot v^2}. \tag{5.9}$$

The temperature field from all canisters may be written:

$$T_{\text{sum}}(x,y,z,t)=\int_1^{\infty}\frac{Q_{\text{c}}\left(t-t/u^2\right)}{4\pi\lambda_{\text{r}}\sqrt{\pi a_{\text{r}}t}}S\left(\frac{x}{D_{\text{t}}},\frac{D_{\text{t}}u}{\sqrt{4a_{\text{r}}t}},N_{\text{t}}\right)S\left(\frac{y}{D_{\text{c}}},\frac{D_{\text{c}}u}{\sqrt{4a_{\text{r}}t}},N_{\text{c}}\right)E\left(\frac{z}{H},\frac{Hu}{\sqrt{4a_{\text{r}}t}}\right)du. \tag{5.10}$$

This summation as a product reduces the number of terms to sum from $(2N_{\text{t}}+1)\cdot(2N_{\text{c}}+1)$ to $2N_{\text{t}}+2N_{\text{c}}+2$. The time to compute a temperature is typically reduced by a factor of 25.

## 5.4 Tunnel line heat source

The temperature from the canisters in a tunnel is obtained by a sum over *n.* For the central tunnel ($m=0$) we have:

$$T(x,y,z,t)=\frac{1}{4\pi\lambda_{\mathrm{r}}\sqrt{\pi a_{\mathrm{r}}t}}\int_1^{\infty}Q_{\mathrm{c}}\left(t-\frac{t}{u^2}\right)\cdot\sum_{n=-N_{\mathrm{c}}}^{N_{\mathrm{c}}}e^{-\frac{x^2+(y-nD_{\mathrm{c}})^2}{4a_{\mathrm{r}}t}\cdot u^2}\cdot E\left(\frac{z}{H},\frac{Hu}{\sqrt{4a_{\mathrm{r}}t}}\right)du. \quad (5.11)$$

This formula may be simplified for points far away from the tunnel. The row of vertical line heat sources may then be replaced by a horizontal line heat source along the tunnel axis. The heat $Q_{\mathrm{c}}(t)$ from a canister is placed along the tunnel axis over the length $D_{\mathrm{c}}$ around the center of the canister. Let $q_{\mathrm{tunnel}}(t)=\mathrm{Q_c}(t)/D_{\mathrm{c}}$ (W/m) denote the strength of the tunnel line heat source. The line heat source for the central tunnel lies along $(0,y,0),\ -B<y<B$. The tunnel length $2B$ is given by $(2N_{\mathrm{c}}+1)\cdot D_{\mathrm{c}}$.

The temperature for an equivalent tunnel line heat source along the *x*-axis becomes in analogy with (5.6):

$$T_{\mathrm{tlhs}}(x,y,z,t)=\frac{1}{4\pi\lambda_{\mathrm{r}}\sqrt{\pi a_{\mathrm{r}}t}}\cdot\frac{2B}{D_{\mathrm{c}}}\int_1^{\infty}Q_{\mathrm{c}}\left(t-\frac{t}{u^2}\right)\cdot e^{-\frac{x^2+z^2}{4a_{\mathrm{r}}t}\cdot u^2}\cdot E\left(\frac{y}{B},\frac{Bu}{\sqrt{4a_{\mathrm{r}}t}}\right)du. \quad (5.12)$$

This solution is a good approximation of (5.11) for points that lie at a certain distance from the tunnel.

## 5.5 Rectangular global heat source

The canisters lie in a grid in a rectangular area: $-L<x<L,\ -B<y<B,\ z=0$. The solution for all canisters is given by (5.8) or (5.10). For points at a certain distance from the rectangular repository area, we may derive a much simpler formula by replacing the vertical canister line heat sources by an equivalent surface heat source $q_{\mathrm{surface}}(t)$ over the rectangular repository area. We have

$$q_{\mathrm{surface}}(t)=\frac{\mathrm{Q_c}(t)}{D_{\mathrm{t}}D_{\mathrm{c}}},\quad -L<x<L,\ -B<y<B,\ z=0. \quad (5.13)$$

$$L=(N_{\mathrm{t}}+0.5)\cdot D_{\mathrm{t}},\ B=(N_{\mathrm{c}}+0.5)\cdot D_{\mathrm{c}}. \quad (5.14)$$

The solution is then:

$$T_{\mathrm{gl}}(x,y,z,t)=\frac{1}{4\pi\lambda_{\mathrm{r}}\sqrt{\pi a_{\mathrm{r}}t}}\cdot\frac{4LB}{D_{\mathrm{t}}D_{\mathrm{c}}}\int_1^{\infty}Q_{\mathrm{c}}\left(t-t/u^2\right)E\left(\frac{x}{L},\frac{Lu}{\sqrt{4a_{\mathrm{r}}t}}\right)E\left(\frac{y}{B},\frac{Bu}{\sqrt{4a_{\mathrm{r}}t}}\right)e^{-\frac{z^2}{4a_{\mathrm{r}}t}\cdot u^2}du. \quad (5.15)$$

We will call this the global solution. It is the same formula as (4.2) but with a different form for the variable of integration. It is valid at a certain distance from the rectangular canister area.

## 5.6 Effect of ground surface and undisturbed temperature

The temperature variation at the ground surface $z=D_{\mathrm{gr}}$ may be neglected. We can use the annual mean temperature $T_0$ as boundary condition at the ground surface. The undisturbed ground temperature increases downwards with the geothermal gradient to the temperature $T_{\mathrm{rep}}$ at the repository level $z=0$. Using a linear geothermal gradient, we have:

$$T(x,y,D_{\rm gr},t)=T_0,\qquad T_{\rm undist}(z)=T_{\rm rep}-\frac{z}{D_{\rm gr}}\cdot\left(T_{\rm rep}-T_0\right). \tag{5.16}$$

The temperature field due to the heat emitting canisters is to be added to the above undisturbed ground temperature:

$$T_{\rm total}(x,y,z,t)=T_{\rm undist}(z)+T_{\rm canisters}(x,y,z,t). \tag{5.17}$$

The temperature field from the canisters becomes zero at the ground surface $z=D_{\rm gr}$. This is achieved by putting negative mirror heat sources at $z=2D_{\rm gr}$. We can certainly use the global solution for the mirror canisters, since they are at the distance $D_{\rm gr}$ from our ground region $z<D_{\rm gr}$. We have:

$$T_{\rm canisters}(x,y,D_{\rm gr},t)=0,\qquad T_{\rm canisters}(x,y,z,t)=T(x,y,z,t)-T_{\rm gl}(x,y,z-2D_{\rm gr},t). \tag{5.18}$$

Here, $T(x,y,z,t)$ is the solution for the repository canisters (in an infinite ground region) as discussed in the preceding subsections.

## 5.7 Mixed solution

We now again consider the solution from the heat emitting canisters in an infinite ground with zero ground temperature at $t=0$. We consider the solution around the central canister (or a canister not too close to the periphery of the repository):

$$-D_{\rm t}\le x\le D_{\rm t},\qquad -D_{\rm c}\le y\le D_{\rm c},\qquad D_{\rm gr}>z>-\infty. \tag{5.19}$$

Above a certain vertical distance from above the canisters, $d_{\rm glz}$, we use the global solution:

$$T(x,y,z,t)=T_{\rm gl}(x,y,z,t),\qquad |z|>d_{\rm glz}. \tag{5.20}$$

For $|z|<d_{\rm glz}$, we proceed in the following way. Let $-L'<x<L',\ -B'<y<B'$ be a smaller rectangular area around the central canister. In this region we use the solutions for canister and tunnel line heat sources. In the rectangular repository region outside this smaller rectangle, we use the surface heat source of the type (5.13). The global solution for the smaller region is:

$$T'_{\rm gl}(x,y,z,t)=\frac{1}{4\pi\lambda_{\rm r}\sqrt{\pi a_{\rm r}t}}\cdot\frac{4L'B'}{D_{\rm t}D_{\rm c}}\int_1^\infty Q_{\rm c}\left(t-t/u^2\right)E\left(\frac{x}{L'},\frac{L'u}{\sqrt{4a_{\rm r}t}}\right)E\left(\frac{y}{B'},\frac{B'u}{\sqrt{4a_{\rm r}t}}\right)e^{-\frac{z^2}{4a_{\rm r}t}\cdot u^2}\,du. \tag{5.21}$$

The solution for the surface heat source in the region between the repository rectangle and the cutout smaller rectangle in obtained by subtraction $T'_{\rm gl}(x,y,z,t)$ from $T_{\rm gl}(x,y,z,t)$.

The smaller rectangular region covers $2N'_{\rm t}+1$ tunnels and $2N'_{\rm c}+1$ canisters in each tunnel around the central canister. So we have: $L'=(N'_{\rm t}+0.5)\cdot D_{\rm t},\qquad B'=(N'_{\rm c}+0.5)\cdot D_{\rm c}$.

The central tunnel and $N'_{\text{tcan}}$ tunnels on each side, i.e. $2N'_{\text{tcan}}+1$ tunnels, retain the canister line heat sources ( $0 \le N'_{\text{tcan}} < N'_{\text{t}}$ ). The temperature from these canisters is obtained from a summation of the type (5.8), which involves much fewer canisters. We get:

$$T'_{\text{can}}(x,y,z,t) = \int_1^{\infty} \frac{Q_{\text{c}}\left(t - t/u^2\right)}{4\pi\lambda_{\text{r}}\sqrt{\pi a_{\text{r}} t}} S\left(\frac{x}{D_{\text{t}}}, \frac{D_{\text{t}}u}{\sqrt{4a_{\text{r}}t}}, N'_{\text{tcan}}\right) S\left(\frac{y}{D_{\text{c}}}, \frac{D_{\text{c}}u}{\sqrt{4a_{\text{r}}t}}, N'_{\text{c}}\right) E\left(\frac{z}{H}, \frac{Hu}{\sqrt{4a_{\text{r}}t}}\right) du. \quad (5.22)$$

For the tunnels further away in the smaller rectangle, $m = \pm(N'_{\text{tcan}}+1), \ldots, \pm N'_{\text{t}}$, we use tunnel line heat sources. We get a sum of solutions of the type (5.12):

$$T'_{\text{tunnel}}(x,y,z,t) = \frac{1}{4\pi\lambda_{\text{r}}\sqrt{\pi a_{\text{r}} t}} \cdot \frac{2B}{D_{\text{c}}} \int_1^{\infty} Q_{\text{c}}\left(t - \frac{t}{u^2}\right) \cdot \sum_{m \in \mathbf{M}} e^{-\frac{(x - mD_{\text{t}})^2}{4a_{\text{r}}t} \cdot u^2} \cdot E\left(\frac{y}{B'}, \frac{B'u}{\sqrt{4a_{\text{r}}t}}\right) \cdot e^{-\frac{z^2}{4a_{\text{r}}t} \cdot u^2} du \quad (5.23)$$

$$\mathbf{M} = \left\{ m = \pm(N'_{\text{tcan}}+1), \ldots, \pm N'_{\text{t}} \right\}.$$

The temperature for the whole canister field becomes with these approximations

$$T(x,y,z,t) = T_{\text{gl}}(x,y,z,t) - T'_{\text{gl}}(x,y,z,t) + T'_{\text{can}}(x,y,z,t) + T'_{\text{tunnel}}(x,y,z,t). \quad (5.24)$$

## 5.8 Final fast solution

Total temperature solution is now from (5.17), (5.18) and (5.24)

$$\begin{aligned} T_{\text{tot}}(x,y,z,t) = T_{\text{gl}}(x,y,z,t) - T_{\text{gl}}(x,y,z-2D_{\text{gr}},t) - T'_{\text{gl}}(x,y,z,t) + \\ T'_{\text{can}}(x,y,z,t) + T'_{\text{tunnel}}(x,y,z,t) + T_{\text{undist}}(z). \end{aligned} \quad (5.25)$$

Here, $T_{\text{gl}}$ is given by (5.15), $T'_{\text{gl}}$ by (5.21), $T'_{\text{can}}$ by (5.22), $T'_{\text{tunnel}}$ by (5.23) and $T_{\text{undist}}$ by (5.16), right. The solution is applicable around the central canister (or a canister not too close to the periphery of the repository).

# 6 Equations for heat and moisture flow

We consider the radial flow process at the mid-level $z = 0$ of the bentonite annulus surrounding a canister. See Fig. 1.2. The canister boundary lies at $r = r_c$ and the rock boundary at $r = r_r$. The bentonite fills the region $r_c < r < r_r$. See Fig. 6.1.

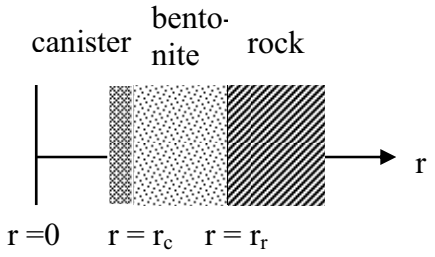


Figure 6.1. Radial flow process in the bentonite annulus.

## 6.1 Flow equations

The radial moisture flux per unit area, $g$ (kg/(m$^2$,s)), in the bentonite has a liquid and a vapor component. The liquid flux $g_{\text{liq}}$ is proportional to the gradient of the pore water pressure $P$ with a hydraulic conductivity $k(S)$ that is a function of the degree of water saturation $S$. The flux is inversely proportional to the temperature-dependent viscosity $\eta(T)$. The water vapor flux $g_{\text{vap}}$ is proportional to the gradient of the water vapor density $\rho_v$ in the gas phases in the pores with a vapor conductivity factor $D_v(S)$ that is a decreasing function of $S$. We have:

$$g = g_{\text{liq}} + g_{\text{vap}}, \qquad g_{\text{liq}} = -\frac{\rho_w k(S)}{\eta(T)} \cdot \frac{\partial P}{\partial r}, \qquad g_{\text{vap}} = -D_v(S) \cdot \frac{\partial \rho_v}{\partial r}. \tag{6.1}$$

The heat or energy flux $q$ (W/m$^2$) has a conductive part with a thermal conductivity $\lambda(S)$, which is a function of $S$. The convective part is equal to the liquid and vapor fluxes multiplied by their respective heat contents (specific enthalpy). We have

$$q = -\lambda(S) \cdot \frac{\partial T}{\partial r} + h_{\text{liq}}(T) g_{\text{liq}} + h_{\text{vap}}(T) g_{\text{vap}}. \tag{6.2}$$

We will see that the convective parts may be neglected.

We consider the total radial flux over the canister height $H_c$. The area of the cylinder at a radius $r$ is $2\pi r H_c$. The total fluxes of heat, $Q$ (W), and moisture, $G$ (kg/s), become

$$Q(r,t) = 2\pi r H_c \cdot q(r,t), \qquad G(r,t) = 2\pi r H_c \cdot g(r,t). \tag{6.3}$$

## 6.2 Data for bentonite and water

We will use the degree of water saturation $S$ in the pores and the temperature $T$ as basic state variables. The degree of saturation lies in the interval $0 < S \le 1$.

The water retention curve $P(S)$ is an important material property. We use the following functions for the bentonite

$$k(S), \quad D_{\mathrm{v}}(S) = D_{\mathrm{v}}(0)\cdot(1-S), \quad \lambda(S), \quad P(S). \tag{6.4}$$

The vapor diffusion coefficient $D_{\mathrm{v}}(S)$ is zero for $S=1$, and it is in a first approximation proportional to $1-S$.

We also need data for water. We will use the saturation water vapor density, the water vapor density as a function of *S* and *T*, the dynamic viscosity, the heat of evaporation, and the heat content of water in liquid and vapor form:

$$\rho_{\mathrm{v,sat}}(T), \qquad \rho_{\mathrm{v}}(S,T), \qquad \eta(T), \qquad L_{\mathrm{evap}}(T), \qquad h_{\mathrm{liq}}(T), \qquad h_{\mathrm{vap}}(T). \tag{6.5}$$

We use certain thermodynamic relations, which are presented in Appendix 4.

All above functions for bentonite and water are represented by explicit formulas with an error below 1% in the interval $10 < T < 100$ °C and $0.3 < S \le 1$. The mathematical program Mathcad is used. All the functions (6.4) and (6.5) are discussed further in Claesson, Hagentoft and Sällfors (2003). The above functions are also given on pages 1-2 in the models in App. 4-6 of this report.

In the reference case we use the following functions and data:

$$\begin{aligned} &k(S) = k(1)\cdot S^3, \qquad k(1) = 1.6\cdot 10^{-20}, \qquad \lambda(S) = 0.6 + 0.6\cdot S \ \text{ W/(mK)}, \\ &D_{\mathrm{v}}(S) = (1-S)\cdot D_{\mathrm{v}}(0), \qquad D_{\mathrm{v}}(0) = 2\cdot 10^{-6} \ \text{ m}^2/\text{s} \qquad S_{\mathrm{in}} = 0.85, \qquad V_{\mathrm{p}} = 0.39. \end{aligned} \tag{6.6}$$

The chosen type of functions and data for bentonite are those of Rutquist, Noorishad and Tsang (1999).

## 6.3 General form for flow equations

The moisture flux *g* and the conductive-convective heat flux *q* may now be written in the following general form

$$g(r,t) = -K_S(S,T)\cdot\frac{\partial S}{\partial r} - K_T(S,T)\cdot\frac{\partial T}{\partial r}. \tag{6.7}$$

$$q(r,t) = -\lambda_S(S,T)\cdot\frac{\partial S}{\partial r} - \lambda_T(S,T)\cdot\frac{\partial T}{\partial r}. \tag{6.8}$$

The flow coefficients for moisture, $K_S$ and $K_T$, and for heat, $\lambda_S$ and $\lambda_T$, are functions of the state variables *S* and *T*. The exact expressions are given by (14.4)-(14.7) in Appendix 2. For $K_S$ and $K_T$ we have:

$$K_S(S,T) = \left(\frac{\rho_{\mathrm{w}}\,k(S)}{\eta(T)} + D_{\mathrm{v}}(S)\cdot\frac{\partial\rho_{\mathrm{v}}}{\partial P}\right)\cdot\frac{dP}{dS}. \tag{6.9}$$

$$K_T(S,T) = K_T'(S)\cdot(1-S), \qquad K_T'(S) = D_{\mathrm{v}}'(0)\cdot\frac{\partial\rho_{\mathrm{v}}}{\partial T}. \tag{6.10}$$

The function $K_T(S,T)$ involves the factor $1-S$ from the vapor diffusivity (6.4). This factor is zero for $S=1$, when the gas phase has vanished. The remaining flow coefficient $K'_T(S,T)$ is has a very much smaller variation with *S* and *T*. The coefficient functions are readily calculated in the mathematical program. See Appendices 4-6.

The general *steady-state* relations are now from (6.7), (6.8) and (6.3) of the following type:

$$g(r)=\frac{G}{2\pi r H_{\mathrm{c}}}=-K_S(S,T)\cdot\frac{dS}{dr}-K_T(S,T)\cdot\frac{dT}{dr}. \tag{6.11}$$

$$q(r)=\frac{Q}{2\pi r H_{\mathrm{c}}}=-\lambda_S(S,T)\cdot\frac{dS}{dr}-\lambda_T(S,T)\cdot\frac{dT}{dr}. \tag{6.12}$$

## 6.4 Temperature over the bentonite annulus

The total heat release from the canister is $Q_{\mathrm{c}}(t)$ (W). It varies in time with a time scale of years. The time scale to establish a steady-state temperature profile over the bentonite annulus is below 24 hours. We may therefore with very good accuracy consider the temperature as quasi steady-state or independent of time. But the value of $Q_{\mathrm{c}}$ and the temperature level and profile in the bentonite will vary slowly with time. In any particular moderate time span, we have a constant value of $Q_{\mathrm{c}}$ and a constant temperature $T_{\mathrm{r}}$ at the rock boundary. The radial temperature profile $T(r)$ satisfies, using (6.3) and (6.2) without the convective terms, the heat balance equation

$$Q_c=-2\pi r H_{\mathrm{c}}\cdot\lambda(S)\cdot\frac{\partial T}{\partial r},\qquad T(r_{\mathrm{r}})=T_{\mathrm{r}}. \tag{6.13}$$

The solution $T(r)$ depends on $Q_{\mathrm{c}}$, $T_{\mathrm{r}}$ and the thermal conductivity $\lambda(S)$ over the annular region. This is discussed further in Appendix 2. Integration in *r*, using an average value for the water saturation $S$, gives $T(r)$:

$$T(r)\approx T_{\mathrm{r}}+\frac{Q_{\mathrm{c}}}{2\pi H_{\mathrm{c}}\cdot\lambda(S_{\mathrm{av}})}\cdot\ln\left(\frac{r_{\mathrm{r}}}{r}\right). \tag{6.14}$$

The canister surface temperature $T_{\mathrm{c}}$ is obtained for $r=r_{\mathrm{c}}$.

## 6.5 Thermo-diffusive coefficient function A(S,T)

The moisture flux *G*, (6.3) and (6.7), may be written in an alternative form that will prove to be very useful for our analysis. We eliminate the temperature gradient by using (6.13). We also use (6.10). Then we may write the flux in the following way

$$G=-2\pi H_{\mathrm{c}}\cdot r\cdot K_S(S,T)\cdot\frac{\partial S}{\partial r}+K'_T(S,T)\cdot\frac{Q_{\mathrm{c}}}{\lambda(S)}\cdot(1-S). \tag{6.15}$$

The first term is of a diffusive character, and the second one of a convective character with a flow coefficient function times $1-S$. We may write the equation in the following way

$$G = -2\pi H_{\mathrm{c}} \cdot K_S(S,T) \cdot \left[ r \cdot \frac{\partial S}{\partial r} - 2 \cdot A(S,T) \cdot (1-S) \right] \tag{6.16}$$

Here, we have introduced the thermo-diffusive coefficient function $2 \cdot A(S,T)$ as the ratio between the functions before $1-S$ and $r \cdot \partial S/\partial r$. We have

$$A(S,T) = \frac{K_T'(S,T)}{4\pi H_{\mathrm{c}} \cdot K_S(S,T)} \cdot \frac{Q_{\mathrm{c}}}{\lambda(\mathrm{S})}. \tag{6.17}$$

The factor 2 is introduced for notational convenience for the solutions in Section 8.2 and following.

The thermo-diffusive coefficient function $A(S,T)$ is of a somewhat intricate character. The first right-hand factor is the ratio between the reduced coefficient $K_T'$, where the factor $1-S$ is taken away, and $K_S$. The second factor involving the heat emission represents the temperature gradient in accordance with (6.13).

Let us note the criterion for zero flux. The factor within the square brackets of (6.16) is then zero. This expression is then zero in steady state. It is also zero at the canister boundary, and at the rock boundary in the dry-rock case. The equation for zero moisture flux is:

$$\text{Zero flux} \quad \Leftrightarrow \quad r \cdot \frac{\partial S}{\partial r} - 2 \cdot A(S,T) \cdot (1-S) = 0. \tag{6.18}$$

## 6.6 Moisture balance equation

The moisture balance equation for the degree of water saturation $S(r,t)$ in the pores of the bentonite in the considered radial, time-dependent case for an annular bentonite region between canister and rock walls is

$$\frac{\partial}{\partial t}\left[ 2\pi r H_{\mathrm{c}} \cdot V_{\mathrm{p}} \rho_{\mathrm{w}} S \right] = -\frac{\partial G}{\partial r}, \qquad r_{\mathrm{c}} < r < r_{\mathrm{r}}, \tag{6.19}$$

or, using (6.16),

$$V_{\mathrm{p}} \rho_{\mathrm{w}} \cdot \frac{\partial S}{\partial t} = \frac{1}{r} \cdot \frac{\partial}{\partial r} \left\{ K_S(S,T) \cdot \left[ r \cdot \frac{\partial S}{\partial r} - 2A(S,T) \cdot (1-S) \right] \right\}, \qquad r_{\mathrm{c}} < r < r_{\mathrm{r}}. \tag{6.20}$$

Here, $V_{\mathrm{p}}$ is the porosity or pore volume per unit volume of bentonite, and $H_{\mathrm{c}}$ the height of the canister.

The above equation involves a diffusivity function $K_S/(V_{\mathrm{p}}\rho_{\mathrm{w}})$ and the thermo-diffusive function. We have arrived at the equation

$$\frac{\partial S}{\partial t} = \frac{1}{r} \cdot \frac{\partial}{\partial r} \left\{ D(S,T) \cdot \left[ r \cdot \frac{\partial S}{\partial r} - 2 \cdot A(S,T) \cdot (1-S) \right] \right\}, \qquad r_{\mathrm{c}} < r < r_{\mathrm{r}}. \tag{6.21}$$

The moisture diffusivity $D(S,T)$ ($m^2/s$) and the flow coefficient function $A(S,T)$ (-) are given by

$$D(S,T) = \frac{K_S(S,T)}{V_p \rho_w}, \qquad A(S,T) = \frac{Q_c(t)}{4\pi H_c} \cdot \frac{K'_T(S,T)}{K_S(S,T) \cdot \lambda(S)}. \tag{6.22}$$

We obtain a *single* equation (6.21) for $S(r,t)$. Any variation of the temperature profile with time is determined from (6.13) and (6.14) with a very slowly varying $Q_c(t)$ and $T_r(t)$. The equation for $S$ is of a convective-diffusive character. The second term involving $1-S$ is caused by the water vapor diffusion due to the temperature gradient.

# 7 Steady-state analyses

As mentioned above, the time scale to approach (exponentially) steady-state moisture conditions is around 4 years in the wet-rock case, and around 1 year in the dry-rock case for the reference data. The temperature and the heat release from the canisters have a distinctly longer time scale. The *steady-state* solutions for the moisture distribution over the bentonite annulus are therefore quite interesting to us. The steady-state solutions are discussed in more detail in the preceding report Claesson, Hagentoft and Sällfors (2003). Here, some new material is added.

## 7.1 General steady-state equations

The general steady-state relations are given by (6.11) and (6.12). The fluxes $G$ and $Q$ are independent of the radius $r$ in steady state. The moisture flux is zero, since it is zero at the canister boundary. We have

$$G = 0, \qquad Q = Q_{\mathrm{c}}(t). \tag{7.1}$$

From (6.11)-(6.12) and (7.1), we get an equation system for the derivatives $dS/dr$ and $dT/dr$. From this equation system we get the derivatives. We have:

$$\frac{dS}{dr} = -\frac{Q_c(t)}{2\pi r H}\cdot\frac{K_T(S,T)}{K_T\lambda_S - K_S\lambda_T},$$

$$\frac{dT}{dr} = \frac{Q_c(t)}{2\pi r H}\cdot\frac{K_S(S,T)}{K_T\lambda_S - K_S\lambda_T}, \qquad r_{\mathrm{c}} \le r \le r_{\mathrm{r}}. \tag{7.2}$$

The four flow coefficients are functions of $S$ and $T$. We have two coupled, strongly nonlinear, ordinary differential equations for $S(r)$ and $T(r)$. We study the solution for any value of $S$ and $T$ at the rock boundary $r = r_{\mathrm{r}}$:

$$S(r_{\mathrm{r}}) = S_{\mathrm{r}}, \qquad T(r_{\mathrm{r}}) = T_{\mathrm{r}}(t). \tag{7.3}$$

Let us first consider the *wet-rock case* with full saturation at the rock boundary: $S(r_{\mathrm{r}}) = 1$. The flow function $K_T(S,T)$ involves the factor $1-S$, (6.10). This means that the value of $K_T$ and the derivative $dS/dr$, (7.2) top, is zero for $S = 1$. From this it follows for the steady-state wet-rock case:

$$K_T(1,T) = 0, \qquad S(r_{\mathrm{r}}) = 1 \;\Rightarrow\; S(r) = 1, \qquad r_{\mathrm{c}} \le r \le r_{\mathrm{r}}. \tag{7.4}$$

The full saturation at the rock boundary is always imposed throughout the bentonite after an initial drying at the canister side. The time scale for this saturation is around 4 years in the reference case.

The situation is very different in the *dry-rock case* (or in a case with partial saturation only at the rock boundary, $S(r_{\mathrm{r}}) = S_{\mathrm{r}} < 1$ ). We will see below that then we always get drying at the canister side. It the rest of this section we consider the dry-rock case.

## 7.2 Coordinate-independent relation between S and T

There is a specific, quite useful, internal structure in the differential equations (7.2) for $S(r)$ and $T(r)$. We divide the first equation by the second one. The differential *dr* and all factors except the *K*-functions cancel. We have in the temperature interval from the rock temperature $T_{\mathrm{r}}$ to the higher temperature $T_{\mathrm{c}}$ at the canister

$$\frac{dS}{dT} = -\frac{K_T(S,T)}{K_S(S,T)}, \qquad T_{\mathrm{r}} \le T \le T_{\mathrm{c}}. \tag{7.5}$$

The relation between *S* and *T* becomes *independent* of the radius *r*. The temperature $T_{\mathrm{c}}$ at the canister boundary is obtained from the steady-state formula (6.14):

$$T_{\mathrm{c}} \approx T_{\mathrm{r}}(t) + \frac{Q_c(t)}{2\pi H \cdot \lambda(S_{\mathrm{av}})} \cdot \ln\left(\frac{r_{\mathrm{r}}}{r_{\mathrm{c}}}\right). \tag{7.6}$$

## 7.3 Solution for the reference case

In the reference case we use the data (2.1) with the heat release $Q_{\mathrm{c}}(0) = 1000$ W. The reference rock temperature is chosen to 70˚C, and the reference value for the degree of saturation at the rock boundary is 0.95. We choose a rather high value for $S_{\mathrm{r}}$ in order to avoid large drying. We take

$$Q_{\mathrm{c}} = 1000 \ \mathrm{W}, \qquad \mathrm{S}_{\mathrm{r}} = 0.95, \qquad T_{\mathrm{r}} = 70 \ ^{\circ}\mathrm{C}. \tag{7.7}$$

The equations (7.2) for $S(r)$ and $T(r)$ are solved in with the program Mathcad. The full solution for the reference case is given in Appendix 4. All data are given explicitly, and the solution should be quite easy to follow without particular knowledge of the program, since direct mathematical notations are used in Mathcad. Pages 1 and 2 in Appendix 4 specify the functions for water and bentonite. The equations are solved at the end of page 2 and the beginning of page 3. Runge-Kutta's solution method is used. The output is three vectors for *r, S* and *T* for the hundred nodes. The computer calculations take a few seconds only.

The results, $S(r)$ and $T(r)$, are shown on page 3 and in Fig. 7.1. The saturation falls from *S*=0.95 at the rock to 0.83 at the canister, while the temperature increases inwards from 70 to 81.8 ˚C. There is a clear but moderate drying of the bentonite in the reference case. The approximation (7.6) gives the canister temperature 70+11.3=81.3. It underestimates the temperature difference over the bentonite by 5%. Figure 7.2 shows the relation $S(T)$ over the bentonite layer for the reference case.

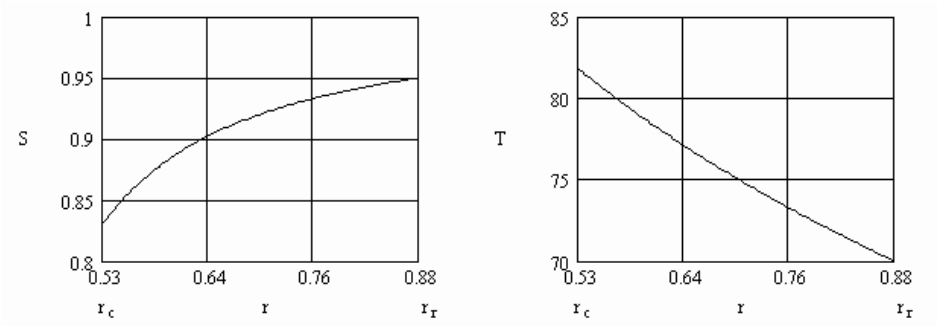


Figure 7.1. Degree of water saturation $S(r)$ and temperature $T(r)$ for the reference case.

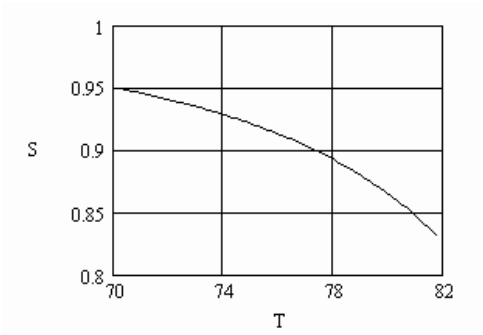


Figure 7.2. The relation $S(T)$ for the reference case.

The vapor and liquid flows are calculated directly on page 4 from the calculated values $S_i$, $T_i$ and $r_i$ at the hundred nodes using the original formulas (6.1). This calculation is a very good test that the program is correct. The result is shown in page 4 and in Fig. 7.3.

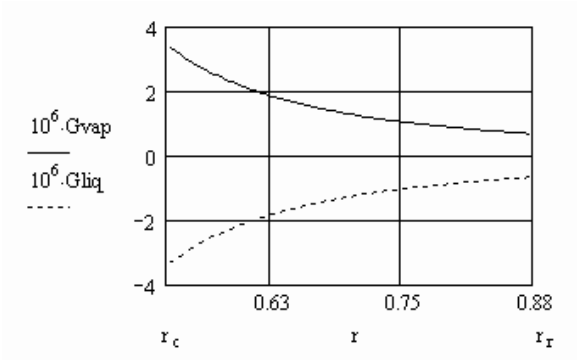


Figure 7.3. Liquid and vapor fluxes for the reference case.

The *accuracy* of the solution is studied in the example. The solution $S_i$, $T_i$ and $r_i$ shall satisfy the original equations (6.1) and (6.2). This is tested directly for the liquid and vapor fluxes on page 3, and for the heat flux on page 5 (in Appendix 4). The relative errors are of the order $10^{-4}$ or smaller. The error becomes of the order $10^{-6}$, when a thousand nodal points are used. A calculation then requires half a minute computer time. This shows that we have obtained a very high and controlled accuracy, which was one of our tasks. There are not *any* approximations in the model.

The ratio between the *convective and conductive* heat flux is calculated on page 5, Appendix 4. The ratio varies between 0.008 and 0.002 in the reference case. This shows that we may quite safely *neglect the convective part* of the heat flux.

## 7.4 Charts for S(T)

The differential equation for the coordinate-independent relations between $S$ and $T$, (7.5), is discussed in Section 7.2. We will here give a complete chart for these relations for the reference case. We will also illustrate the importance of the magnitude of the conductivity ratio by varying $D_v(0)$.

A suitable number of initial saturation degrees are chosen. We have the mathematical problem

$$\frac{dS}{dT} = -\frac{K_T(S,T)}{K_S(S,T)}, \qquad T_{\min} \le T \le T_{\max}, \tag{7.8}$$
$$S(T_{\min}) = S_1,\ S_2, ..., \qquad 1 > S_1 > S_2 > ... > 0.$$

We take the interval $20 \le T \le 100$ °C in order to cover all normal applications. The start values at $T = T_{\min}$ are $S$ = 0.4, 0.5, 0.6, 0.7, 0.8, etc. We choose more closely spaced values near $S = 1$ in order to get curves that cover the upper right-hand region: $S$ = 0.85, 0.90, 0.95, 0.98, 0.99, 0.995, and 0.999. The Mathcad sheet is shown in Appendix 5. The set of curves or chart is shown in Fig. 7.4.

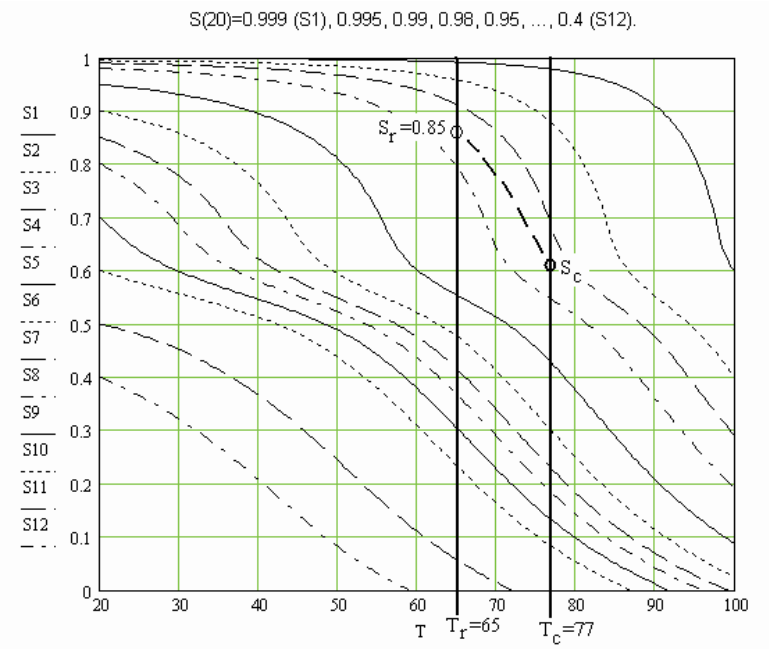


Figure 7.4. Set of curves $S(T)$ to cover all cases in $20 \le T \le 100$ °C for the reference case.

The charts are used in the following way. We have a prescribed rock temperature $T_r$ and a prescribed degree of saturation $S_r$. This point is marked in the chart in Fig. 7.4. We choose the nearest curve on the vertical line $T = T_r$ or the two curves above and below. The solution will follow this curve or lie between the two enclosing curves. We need to know the upper

temperature $T_c$. A good estimate is given by (7.6). An example is shown in Fig. 7.4: $T_r = 65$ and $S_r = 0.85$. We estimate $T_c$ to 77 ˚C from (7.6). We will follow the indicated curve between S3 and S4. The chart is *a very handy way* to estimate the drying.

The set of curves are valid for the reference case. A new chart for another set of input data will require some 10 seconds of computer time (ordinary PC).

Figure 7.5 shows the chart for the higher temperature interval $80 \le T \le 120$ ˚C. The slope of the curves, and hence the drying for a fixed temperature span over the bentonite, increases with the temperature level. This is shown in Fig. 7.4 and in Fig. 7.5 (note the larger *T*-scale in Fig. 6.4).

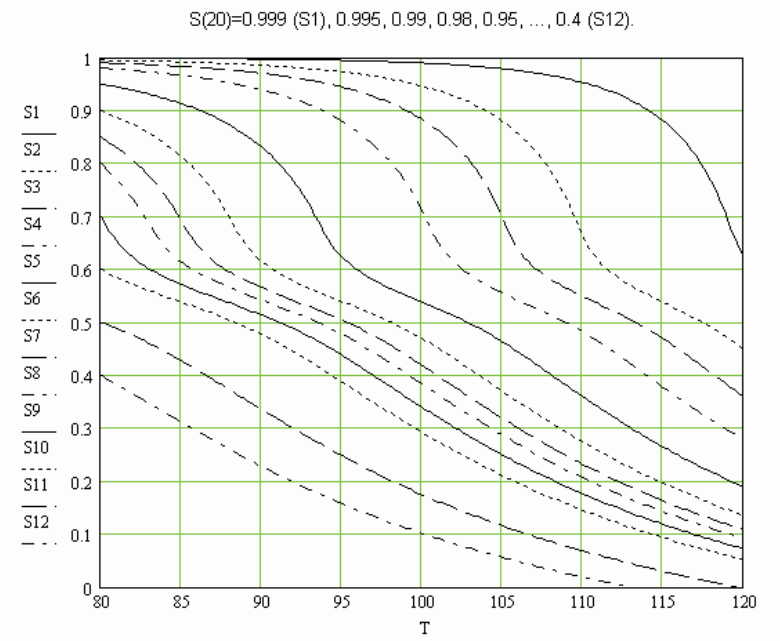


Figure 7.5. Set of curves $S(T)$ to cover all cases in $80 \le T \le 120$ ˚C for the reference case.

Figure 7.6 (on next page) shows the chart for $60 \le T \le 90$ ˚C and $0.6 \le S \le 1$ for a few values of $D_v(0)$:

$$D_v(0) = 1 \cdot 10^{-6}, \quad 2 \cdot 10^{-6}, \quad 4 \cdot 10^{-6}, \quad 8 \cdot 10^{-6}. \tag{7.9}$$

The second value is the reference value. The top, right-hand graph is contained in the larger graph of Figure 7.4. We see how the slope increases with *T*. The slopes increase quite strongly with increasing $D_v(0)$. We see that the magnitude of the conductivity ratio $D_v(0)/k(1)$ is *a critical parameter* for drying of the bentonite.

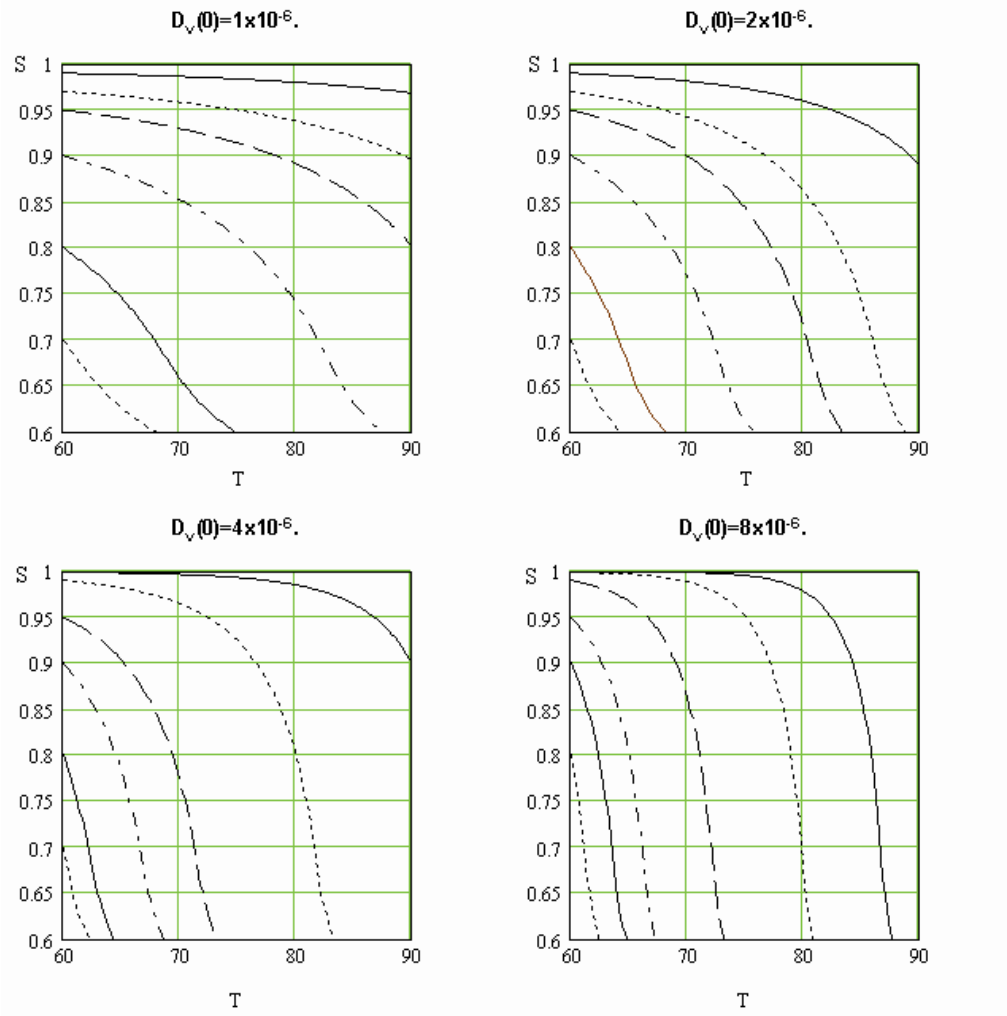


Figure 7.6. Set of curves $S(T)$ for $60 \le T \le 90$ ˚C for the reference case for a few $D_{\mathrm{v}}(0)$.

## 7.5 Linearized equation for S(r)

The equation for the steady-state solution $S(r)$ becomes from (6.18)

$$r \cdot \frac{dS}{dr} - 2 \cdot A(S,T) \cdot (1-S) = 0, \qquad r_{\mathrm{c}} \le r \le r_{\mathrm{r}}. \tag{7.10}$$

A particular solution is $S(r) = 1$ for all $r$. This is the solution in the wet-rock case with $S(r_{\mathrm{r}}) = 1$. In the *dry-rock case,* which is considered from now on in this section, we get a moisture distribution from dry to wet over the annular region.

A linearization of the equation for the degree of saturation $S$ is discussed in Section 8. We will here consider this linearization in the steady-state case. We make as in (8.2) the approximation

$$A(S,T) \approx A(S_0,T_0) = a. \tag{7.11}$$

Here, $S_0$ is a mean water saturation level and $T_0$ the mean temperature in the bentonite for the considered case. The total moisture content, which is given by the integral of $2\pi r H_{\mathrm{c}} \cdot S$ over

$r_c \le r \le r_r$, must be the same for $S = S(r)$ and for $S = S_{in}$ (initial value) in the dry-rock case. We have to solve (7.10) with the approximation (7.11) and an integral relation. We have the problem:

$$r \cdot \frac{dS}{dr} + 2aS = 2a, \qquad r_c \le r \le r_r; \qquad \int_{r_c}^{r_r} r \cdot S(r)\, dr = \int_{r_c}^{r_r} r \cdot S_{in}\, dr. \tag{7.12}$$

The general solution of the differential equation is of the type $S(r) = 1 + F \cdot r^{-2a}$. The constant $F$ is determined from the integral.

The solution is:

$$S_{ss}(r) = 1 - (1 - S_{in}) \cdot \frac{1-a}{1-s_c^{2-2a}} \cdot \frac{1-s_c^2}{(r/r_r)^{2a}}, \qquad r_c \le r \le r_r, \qquad a \ne 1, \qquad (s_c = r_c / r_r). \tag{7.13}$$

Here, we introduce the ratio $s_c = r_c / r_r$, which equals 0.6 in our application. The formula above is not valid for $a = 1$, in which case we get 0/0. This quotient is to be replaced by the limit for $a \to 1$. We have

$$a = 1: \quad \frac{1-a}{1-s_c^{2-2a}} \to \frac{1}{2 \cdot \ln(1/s_c)}, \qquad \frac{1-a}{s_c^{2a} - s_c^2} \to \frac{1}{2 \cdot \ln(1/s_c) \cdot s_c^2}. \tag{7.14}$$

The right-hand alternative form is used below. Figure 6.7 shows the steady-state moisture distribution (7.13) for the reference value $S_{in} = 0.85$ for different values of $a$. This curves give the *largest* drying that may occur in the bentonite.

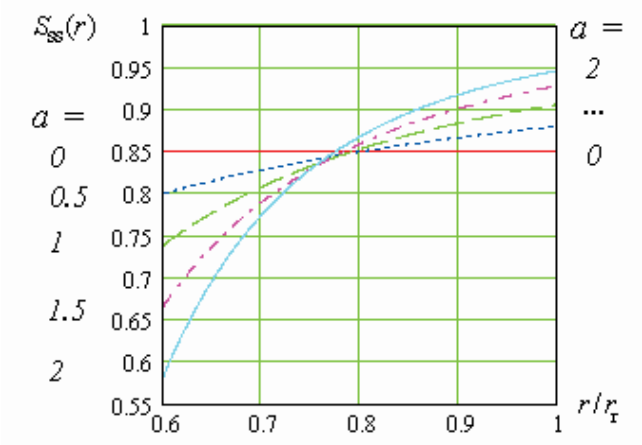


Figure 7.7. Steady-state moisture distribution (7.13) for $S_{in} = 0.85$ for different values of $a$ in the dry-rock case. It gives the largest drying that may occur in the bentonite.

The largest wetting occurs at the rock boundary with $r = r_r$ in (7.13), and the largest drying $S_{ss}(r_c)$ for $r = r_c$. We are in particular interested in the largest drying at the canister wall. We have

$$S_{ss}(r_c) = 1 - (1 - S_{in}) \cdot \frac{1-a}{s_c^{2a} - s_c^2} \cdot \left(1 - s_c^2\right), \qquad a \neq 1. \tag{7.15}$$

The right-hand expression of (7.14) is to be used for $a = 1$. Figure 7.8 shows this largest drying, which may occur in the bentonite as a function of $a$ for different initial degrees of water saturation $S_{in}$ in the bentonite. The curves start at $S_{ss}(r_c) = S_{in}$ for $a = 0$, and they decrease with a larger drying as $a$ increases.

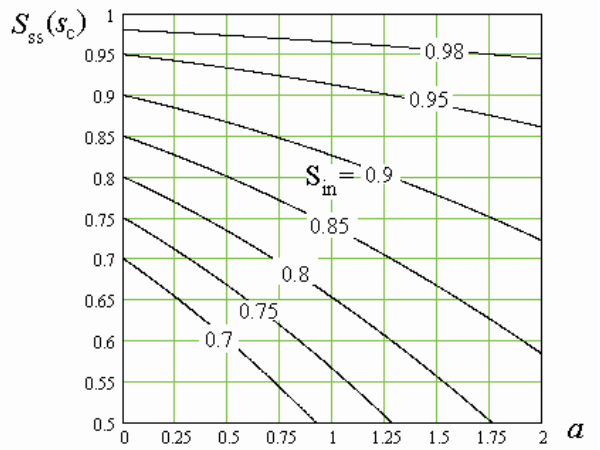


Figure 7.8. Steady-state moisture distribution (7.15) at the canister wall as a function of $a$ for different initial degrees of water saturation $S_{in}$ in the bentonite. These curves give the largest drying that may occur in the bentonite.

The curves in Fig. 7.7 show drying in the left-hand half of $r_c \le r \le r_r$, and wetting above $S = S_{in}$ in the right-hand half of the interval. This is a general feature in the dry-rock case. This means that the outer half of the bentonite annulus *never dries below* $S = S_{in}$.

The above results may be formulated with a new saturation function that is independent of $S_{in}$. We define the steady-state saturation function $\sigma_{ss}(s)$, $s = r / r_r$, by

$$S_{ss}(r) = S_{in} + (1 - S_{in}) \cdot \sigma_{ss}(s), \qquad s_c = r_c / r_r \le s \le 1. \tag{7.16}$$

From (7.13) we get

$$\sigma_{ss}(s) = 1 - \frac{1-a}{1 - s_c^{2-2a}} \cdot \frac{1 - s_c^2}{s^{2a}}, \qquad s_c \le s \le 1, \qquad a \neq 1. \tag{7.17}$$

The left-hand expression of (7.14) is to be used for $a = 1$. Figure 7.9 shows the function $\sigma_{ss}(s)$ for different *a*-values.

In particular, we have at the canister boundary

$$S_{ss}(r_c) = S_{in} + (1 - S_{in}) \cdot \sigma_{ss}(s_c), \qquad s_c = r_c / r_r. \tag{7.18}$$

$$\sigma_{ss}(s_c) = 1 - \frac{1-a}{s_c^{2a} - s_c^2} \cdot \left(1 - s_c^2\right), \qquad a \neq 1. \tag{7.19}$$

The right-hand expression of (7.14) is to be used for $a = 1$. Figure 7.10 shows $\sigma_{ss}(s_c)$ as function of $a$.

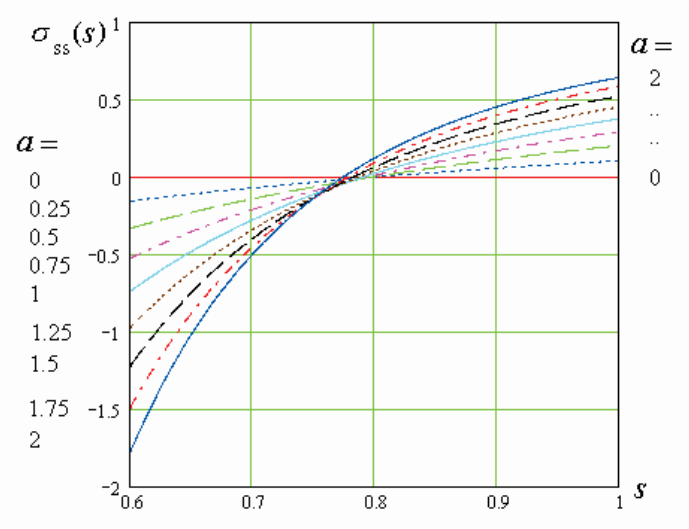


Figure 7.9. The function $\sigma_{ss}(s)$, (7.17), for different $a$-values.

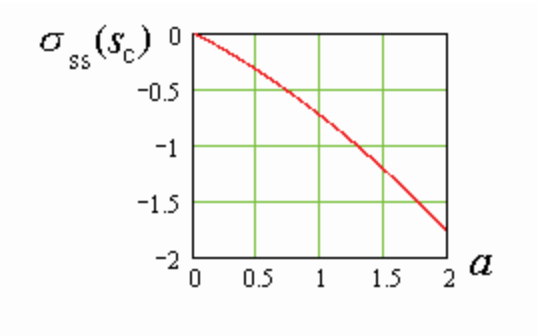


Figure 7.10. The steady-state drying $\sigma_{ss}(s_c)$, (7.19), as function of $a$.

# 8 Assessing drying, wetting and resaturation

The highly non-linear coupled equations may, in the form the equations are formulated below, be linearized with a loss of accuracy of around 10%. The equation for the moisture becomes of a convective-diffusive character. An analytical solution involving Bessel functions may be obtained for the transient drying and saturation of the bentonite annulus, when it is exposed to heating from the canister side and water saturation from the rock side in the wet-rock case. The results are presented in Claesson, 2003A (report) and 2003B (paper). The report presents the study in fuller detail. An analytical solution for the time-dependent radial water and heat flux through the bentonite annular region around the canister is derived. From this it is possible to give explicit formulas for the intensity and time scale of the drying, and for the time scale of the water resaturation process.

A solution in the dry-rock case has also been developed, but it is not yet reported in detail. All formulas and the solution in Mathcad are presented here.

The linearized solution involves two parameters. The first key parameter $t_0$ (or $D_0$) gives a basic time scale for the whole process of drying and wetting. The second key parameter for the initially quite complex coupled process is the thermo-diffusive parameter *a*.

## 8.1 Linearization of the equation for S(r,t)

The general moisture balance equation for $S(r,t)$, (6.21), is

$$\frac{\partial S}{\partial t} = \frac{1}{r}\cdot\frac{\partial}{\partial r}\left\{ D(S,T)\cdot\left[ r\cdot\frac{\partial S}{\partial r} - 2\cdot A(S,T)\cdot(1-S)\right]\right\}, \qquad r_c < r < r_r. \tag{8.1}$$

The moisture diffusivity function $D(S,T)$ and thermo-diffusive parameter $A(S,T)$ depend on the flow properties of the bentonite with its water in the pores, (6.22) and (6.9)-(6.10). The two functions are shown in Figs. 8.1-2 for the reference data. They are calculated with a Mathcad program. See Appendix 6.

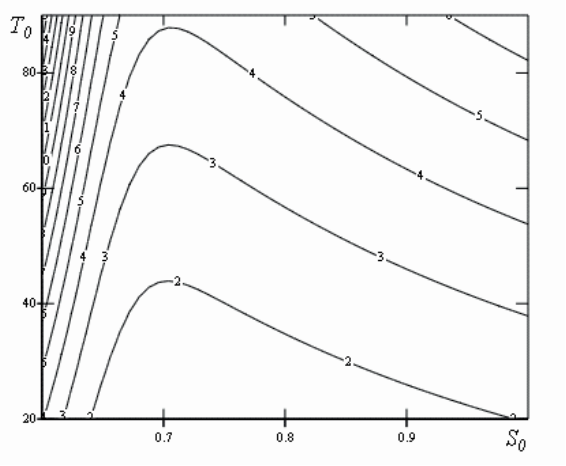


Figure 8.1. Diffusivity function $D(S_0,T_0)\cdot 10^{10}$ ($m^2$/s) using reference bentonite data.
Intervals for saturation and temperature: $0.6 \le S_0 \le 1,\ 20 \le T_0 \le 90^{\circ}$ C.

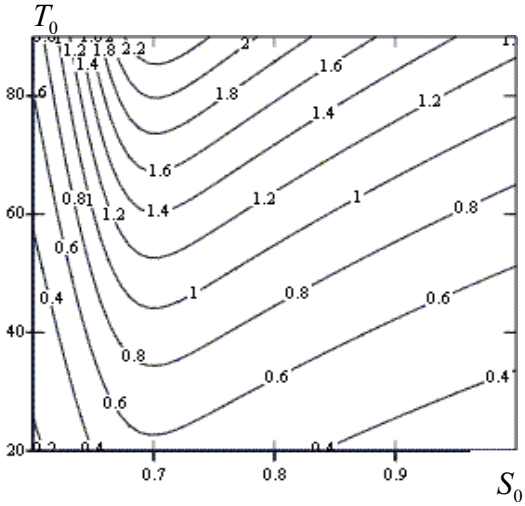


Figure 8.2. The thermo-diffusive function $A(S_0,T_0)$ using reference bentonite data. Intervals for saturation and temperature: $0.6 \le S_0 \le 1$, $20 \le T_0 \le 90$ °C.

Consider as an example the variation of $D(S,T)$ and $A(S,T)$ in the region $0.8<S<1$ and $70<T<80^{o}$C. There is a variation of some $\pm 20\%$ in the considered region. This is quite typical for the type of cases that we will consider. It may be noted that the factor $1-S$ varies much more (by a factor 20 between S=0.8 and S=0.99). This separation of the factor $1-S$ is the key idea to obtain a tractable problem.

The drying and wetting process will in the cases we consider have a variation of the flow coefficients $D(S,T)$ and $A(S,T)$ in the governing equation (8.1) of up to $\pm 20\%$. We may with some caution approximate the two functions by suitable *constant mean values*. We use the approximations:

$$D(S,T) \approx D(S_0,T_0) = D_0, \qquad A(S,T) \approx A(S_0,T_0) = a. \tag{8.2}$$

Here, $S_0$ is a mean water saturation level and $T_0$ the mean temperature in the bentonite for the considered case.

We introduce these approximations in (8.1). The error involved in this approximation is judged to be below 10 %, since the flow functions have values both above and below the approximate constant values. There are now two parameters in (8.1). We get a mean effective diffusivity $D_0$ and a convective-diffusive parameter *a* from the dimensionless factor before $1-S$:

$$D_0 = \frac{K_S(S_0,T_0)}{V_{\mathrm{p}}\rho_{\mathrm{w}}}, \qquad a = \frac{Q_{\mathrm{c}}}{4\pi H_{\mathrm{c}}} \cdot \frac{K_T'(S_0,T_0)}{K_S(S_0,T_0)\lambda(S_0)}. \tag{8.3}$$

Equation (8.1) with the approximations (8.2) may now be written

$$\frac{1}{D_0} \cdot \frac{\partial S}{\partial t} = \frac{1}{r} \cdot \frac{\partial}{\partial r}\left[ r \cdot \frac{\partial S}{\partial r} - 2a \cdot (1-S) \right], \qquad r_{\mathrm{c}} < r < r_{\mathrm{r}}. \tag{8.4}$$

The initial degree of saturation in the bentonite is $S_{\text{in}}$. The moisture flux is zero at the canister boundary. The criterion for zero moisture flux is given by (6.18). At the rock boundary $r = r_{\text{r}}$, the moisture flux zero in the dry-rock case, (6.18), while full saturation *S*=1 is maintained in the wet-rock case. Equation (8.4) for $S(r,t)$ in a slightly modified form together with initial and boundary conditions give the following problem for $S(r,t)$:

$$\frac{1}{D_0}\cdot\frac{\partial S}{\partial t} = \frac{\partial^2 S}{\partial r^2} + \frac{1+2a}{r}\cdot\frac{\partial S}{\partial r}, \qquad r_{\text{c}} < r < r_{\text{r}}; \tag{8.5}$$

$$S(r,0) = S_{\text{in}}, \qquad r_{\text{c}} < r < r_{\text{r}}; \tag{8.6}$$

$$r = r_{\text{c}}: \quad r_{\text{c}}\cdot\left.\frac{\partial S}{\partial r}\right|_{r=r_{\text{c}}} = 2a\left[1 - S(r_{\text{c}},t)\right]; \tag{8.7}$$

$$\begin{gathered} r = r_{\text{r}}: \quad \text{Dry-rock case}: \quad r_{\text{r}}\cdot\left.\frac{\partial S}{\partial r}\right|_{r=r_{\text{r}}} = 2a\cdot\left[1 - S(r_{\text{r}},t)\right], \\ \text{Wet-rock case}: \; S(r_{\text{r}},t) = 1. \end{gathered} \tag{8.8}$$

The problem (8.5)-(8.8) for $S(r,t)$ has a diffusive-convective character, (8.4). It involves one essential dimensionless parameter *a* only. Time is scaled with the diffusivity factor $D_0$.

## 8.2 Solution of linearized equation

The solution $S(r,t)$ of (8.5)-(8.8) is expressed with dimensionless radius $s$ and time $\tau$, and with a new function $\sigma(s,\tau)$ for the degree of saturation:

$$S(r,t) = S_{\text{in}} + (1 - S_{\text{in}})\cdot\sigma(s,\tau), \qquad s = r/r_{\text{r}}, \qquad \tau = t/t_0. \tag{8.9}$$

The dimensionless *saturation* function $\sigma(s,\tau)$ is zero, when the saturation equals the initial level: $S = S_{\text{in}}$. The value is negative when the saturation is below the initial value: $S < S_{\text{in}}$, and it lies in the interval $0 < \sigma \le 1$ for $S_{\text{in}} < S \le 1$. We use the following *basic time scale* $t_0$ for the considered process:

$$t_0 = \frac{4(r_{\text{r}} - r_{\text{c}})^2}{\pi^2 D_0}. \tag{8.10}$$

The solution for $\sigma(s,\tau)$ has in the *dry-rock case* the form

$$\sigma(s,\tau) = \sigma_{\text{ss}}(s) - s^{-a}\cdot\sum_{n=1}^{\infty} A_n\, u_n(s)\, e^{-\nu_n^2\cdot\tau}, \qquad r_{\text{c}}/r_{\text{r}} \le s \le 1. \tag{8.11}$$

Here, the steady-state solution $\sigma_{\text{ss}}(s)$ is given by (7.17). This solution is implemented in Mathcad in Appendix 7. The eigenvalues $\nu_n$ lie, with the choice (8.10), close to $2n$. The first

exponent in (8.11), $-\nu_1^2 \cdot \tau \approx -2^2 \cdot t/t_0 = -t/(t_0/4)$, gives the time scale for the exponential approach to steady-state conditions:

$$t_{\text{dry rock}} = \frac{t_0}{4} = \frac{(r_\text{r} - r_\text{c})^2}{\pi^2 D_0}. \tag{8.12}$$

The solution in the *wet-rock case* for $\sigma(s,\tau)$ has the form

$$\sigma(s,\tau) = 1 - s^{-a} \cdot \sum_{n=1}^{\infty} A_n\, u_n(s)\, e^{-\nu_n^2 \cdot \tau}, \qquad r_\text{c}/r_\text{r} \le s \le 1. \tag{8.13}$$

The steady-state solution is $\sigma(s,\infty) = 1$, or $S(s,\infty) = 1$, in the wet-rock case. This solution is implemented in Mathcad in Appendix 8. The eigenvalues $\nu_n$ lie, with the choice (8.12), close to $2n-1$. The first exponent in (8.13), $-\nu_1^2 \cdot \tau \approx -t/t_0$, gives the time scale for the exponential approach to steady-state conditions:

$$t_{\text{wet rock}} = t_0 = \frac{4(r_\text{r} - r_\text{c})^2}{\pi^2 D_0}. \tag{8.14}$$

It should be noted that the time scale in the dry-rock case is *one fourth* of the time scale in the wet-rock case.

The exact formulas for eigenfunctions $u_n(r)$, coefficients $A_n$, and eigenvalues $\nu_n$ are given in Appendix 3 for the two cases.

## 8.3 An example. The reference case

The two above solution have been implemented in the mathematical computer program Mathcad. The solutions are readily calculated in any particular case requiring moderate computer time. In this example and in all other examples, we have

$$s_\text{c} = r_\text{c}/r_\text{r} = 0.6. \tag{8.15}$$

For these examples in this section, we take

$$a = 0.9, \qquad S_\text{in} = 0.85. \tag{8.16}$$

The value $a$=0.9 corresponds to $S_0 = 0.9$ and $T_0 = 60$ ˚C in Fig. 7.12.

### 8.3.1 Dry-rock case

The full Mathcad solution for the dry-rock case is given in Appendix 7. The degree of water saturation $S$ is shown in Fig. 8.3 as a function of $r/r_\text{r}$ for different dimensionless times $\tau = t/t_0$. The initial value at zero time is $S = 0.85$. We see a drying at the warm canister side and a wetting on the colder rock side, both of which increase with time. The total water content is constant in time, since moisture flux is zero at both boundaries. The solution approaches the steady-state moisture distribution $S_\text{ss}(s)$. It is quite close for $t/t_0 = 0.8$. Fig.

7.7 shows the steady-state distribution given by (7.16)-(7.17) for different *a*-values. The dashed curve for $a = 0.9$ in Fig. 8.3 lies close to the curve for $a = 1$ in Fig. 7.7.

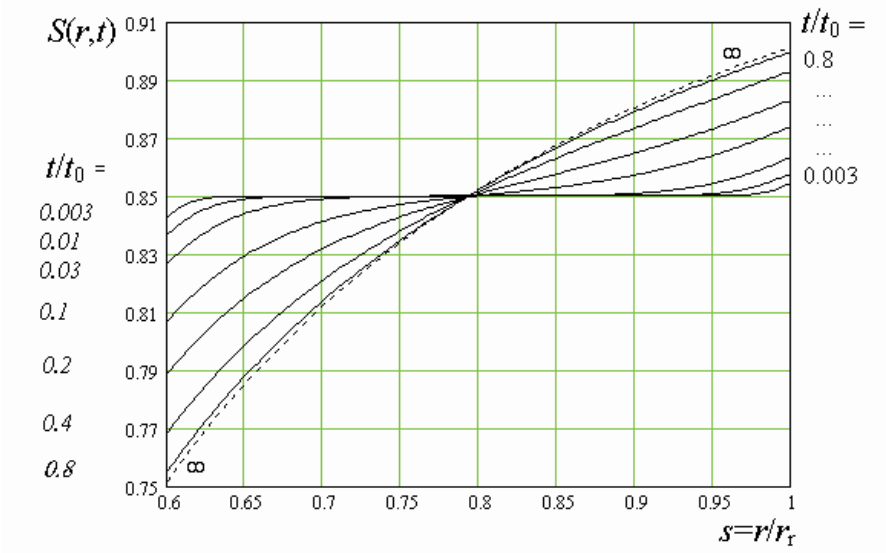


Figure 8.3. The degree of saturation $S(r,\tau)$, $r_c / r_r \le r / r_r \le 1$, for a=0.9.

The strongest drying occurs at the warm canister boundary $r = r_c$. Fig. 8.4 shows the drying from the initial value $S_{in}$ to the final largest drying $S_{ss}(r_c) = 0.752$ (a=0.9) at steady state.

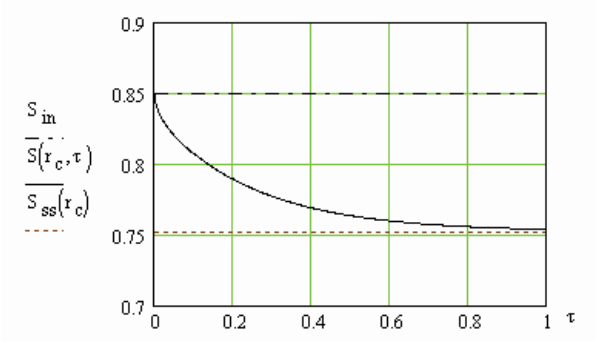


Figure 8.4. Degree of saturation $S(r_c,\tau)$ at the canister boundary, where the strongest drying occurs.

### 8.3.2 Wet-rock case

The calculated drying, wetting and resaturation process is shown in Fig. 8.5 in the wet-rock case. The degree of saturation $S(r,\tau)$ is shown as function of the relative radius $r / r_r$ for a few dimensionless times $\tau = t / t_0$.

The curve for the shortest time $\tau$=0.002 shows a small drying near the canister, and increased saturation from the initial value *S*=0.85 to *S*=1 in a small region near the rock boundary, where full saturation $S = 1$ is maintained. The intermediate region is unchanged. The dried region and the region of increased saturation both increase in time. Water from the dried region is displaced by vapor diffusion through the undisturbed intermediate region to the outer parts. At $\tau \simeq 0.05$ the two regions meet at $r / r_r \simeq 0.8$. The drying in the inner region

continues until the time of largest drying $\tau = 0.216$. Then the wetting process becomes dominant also at the canister wall. There is from this time a steady wetting of all the bentonite. The initial saturation at the canister wall ($S$=0.85) is restored at the time $\tau = 0.694$.

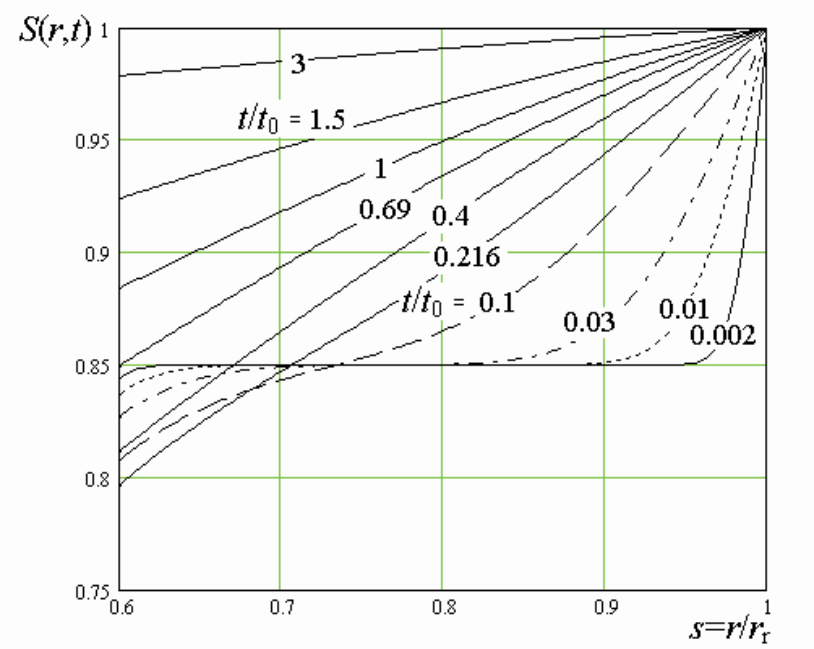


Figure 8.5. The degree of saturation $S(r,\tau)$, $r_c / r_r \le r / r_r \le 1$, for a=0.9. Maximum drying at $\tau = 0.216$. Initial saturation S=0.85 is recovered at canister wall for $\tau = 0.69$.

The strongest drying occurs at the warm canister boundary $r = r_c$. Fig. 8.6 shows the degree of saturation at the canister boundary as function of time. There is an initial drying with the minimum saturation $S = 0.79$ for $\tau = 0.216$. From that time there is a steady increase up to full saturation at, say, $\tau = 5$.

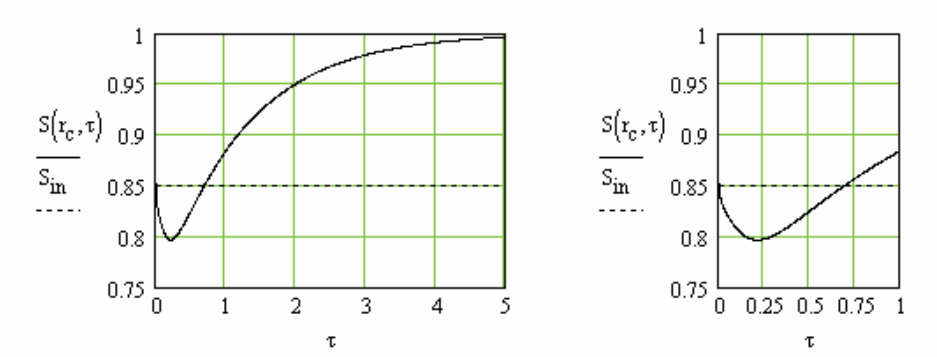


Figure 8.6. Degree of saturation $S(r_c,\tau)$ at the canister boundary, where the strongest drying occurs.

## 8.4 Dependence on saturation and temperature level

The above solution involves the two key parameters $t_0$ and $a$. The time scale $t_0$ is essentially the inverse of $D_0$, (8.10). The basic parameters $D_0$ and $a$ are defined in (8.3). They depend on

the choice of average saturation level $S_0$ and average temperature level $T_0$. The functions $D_0 = D(S_0, T_0)$ and $a = A(S_0, T_0)$ are shown in Figs. 8.1 and 8.2 for the reference data.

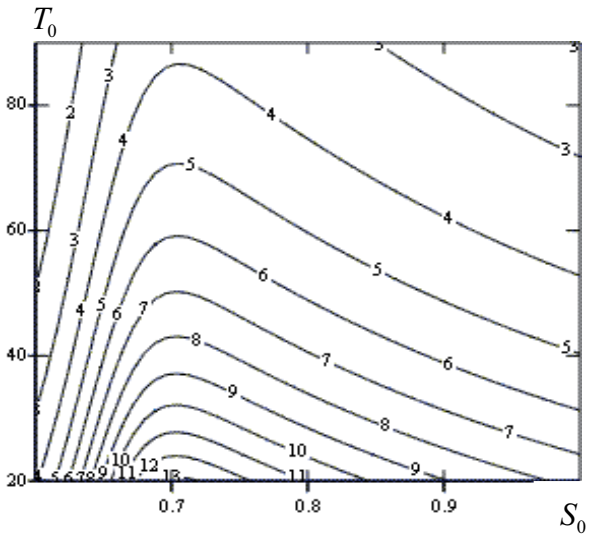


Figure 8.7. The time scale $t_{0y}(S_0, T_0)$ using reference bentonite data. Intervals in degree of saturation and temperature: $0.6 \le S_0 \le 1$, $20 \le T_0 \le 90$ °C.

For the time scale $t_0$, we have from (8.10) and (8.3):

$$t_0 = \frac{4(r_r - r_c)^2}{\pi^2 D_0}, \qquad t_{0y}(S_0, T_0) = \frac{4(r_r - r_c)^2 \cdot V_p \rho_w}{\pi^2 \cdot K_S(S_0, T_0) \cdot t_y}. \tag{8.17}$$

The function $t_0(S_0, T_0)$ is divided by the time of a year $t_y$ = 3600·24·365 s, which means that $t_{0y}$ is the time scale in years. Figure 8.7 shows $t_{0y}(S_0, T_0)$ for the reference data. The Mathcad model for the calculation is given in Appendix 6. The Mathcad program generates such a plot in no time for any bentonite (and water) data.

The time scale $t_0$, (8.17), is determined by the average diffusivity $D_0$, or by $K_S(S_0, T_0)$. The dimensionless parameter *a*, (8.3), is proportional to the heat flux $Q_c / H$. It is also proportional to the ratio between the reduced flow coefficient $K'_T(S_0, T_0)$ for the temperature and the flow coefficient $K_S(S_0, T_0)$ for saturation gradients. It is a thermo-diffusive parameter. It should be noted that the time scale $t_0$ is inversely proportional to the flow coefficient $K_S$, while *a* only depends on the ratio between the two basic flow coefficients.

## 8.5 Graphs for the full solution for different a-values

The degree of saturation $S(r,t)$ is given by the basic relation (8.9):

$$S(r,t) = S_{in} + (1 - S_{in}) \cdot \sigma(s,\tau), \qquad s = r / r_r, \qquad \tau = t / t_0. \tag{8.18}$$

The dimensionless saturation function $\sigma(s,\tau)$ is independent of the initial value $S_{in}$. It is a function of dimensionless radius and time. The *only parameter* is *a* ( and $s_c = r_c / r_r = 0.6$ ) .

By calculation of $\sigma(s,\tau)$ for a suitable set of $a$-values, we have the full solution for all cases of interest.

### 8.5.1 Dry-rock case

The saturation function $\sigma(s,\tau)=\sigma(s,\tau;a)$ is always zero for $\tau=0$, and it is equal to the steady-state solution (7.17) of the dry-rock case for infinite time. The function is zero for $a=1$. We have:

$$\sigma(s,0;a)=0, \qquad \sigma(s,\infty;a)=\sigma_{ss}(s;a), \qquad \sigma(s,\tau;0)=0. \tag{8.19}$$

The solution for $\sigma(s,\tau)$ in the dry-rock case is presented in App. 7. The set of curves from a smallest dimensionless time $\tau=0.003$ up to $\tau=0.3$ is shown for $a=0.5,\ 1,\ 1.5,\ 2$ in Fig. 8.8. The dashed curves show the final steady-state solution (7.17). The different scales for $\sigma$ should be noted. The σ-values lie between –0.3 and 0.2 for $a=0.5$. The span increases with *a.* The values lie between –1.75 and 0.7 for $a=2$.

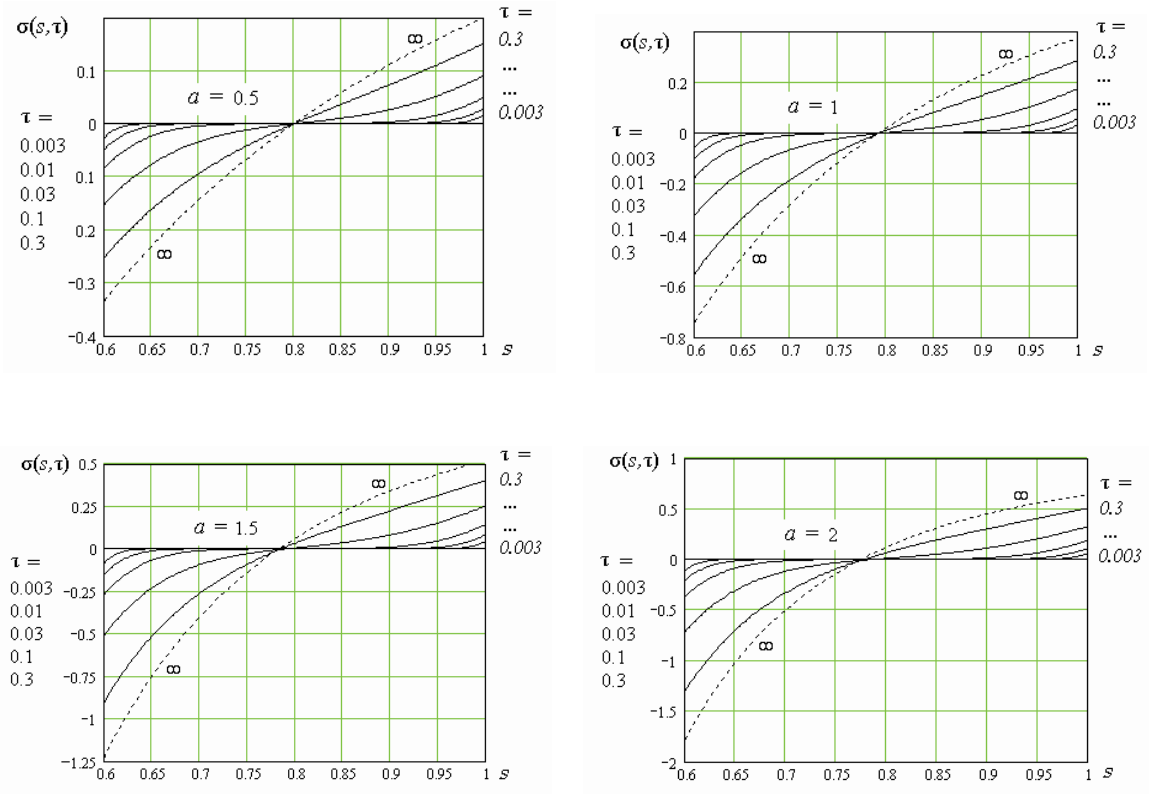


Figure 8.8. The function $\sigma(s,\tau)$ for different values of the convective-diffusive parameter *a*.

### 8.5.2 Wet-rock case

The saturation function $\sigma(s,\tau)=\sigma(s,\tau;a)$ is always zero for $\tau=0$. The steady-state value is equal to full saturation in the wet-rock case for infinite time. We have:

$$\sigma(s,0;a)=0, \qquad \sigma(s,\infty;a)=1. \tag{8.20}$$

For $a = 0$ we have a process of saturation from the rock side without any drying at the canister side.

The solution for $\sigma(s,\tau)$ in the wet-rock case is presented in App. 8. Fig. 8.9 shows the calculated solution in the wet-rock case for $a = 0,\ 0.5,\ 1,\ 1.5,\ 2$.

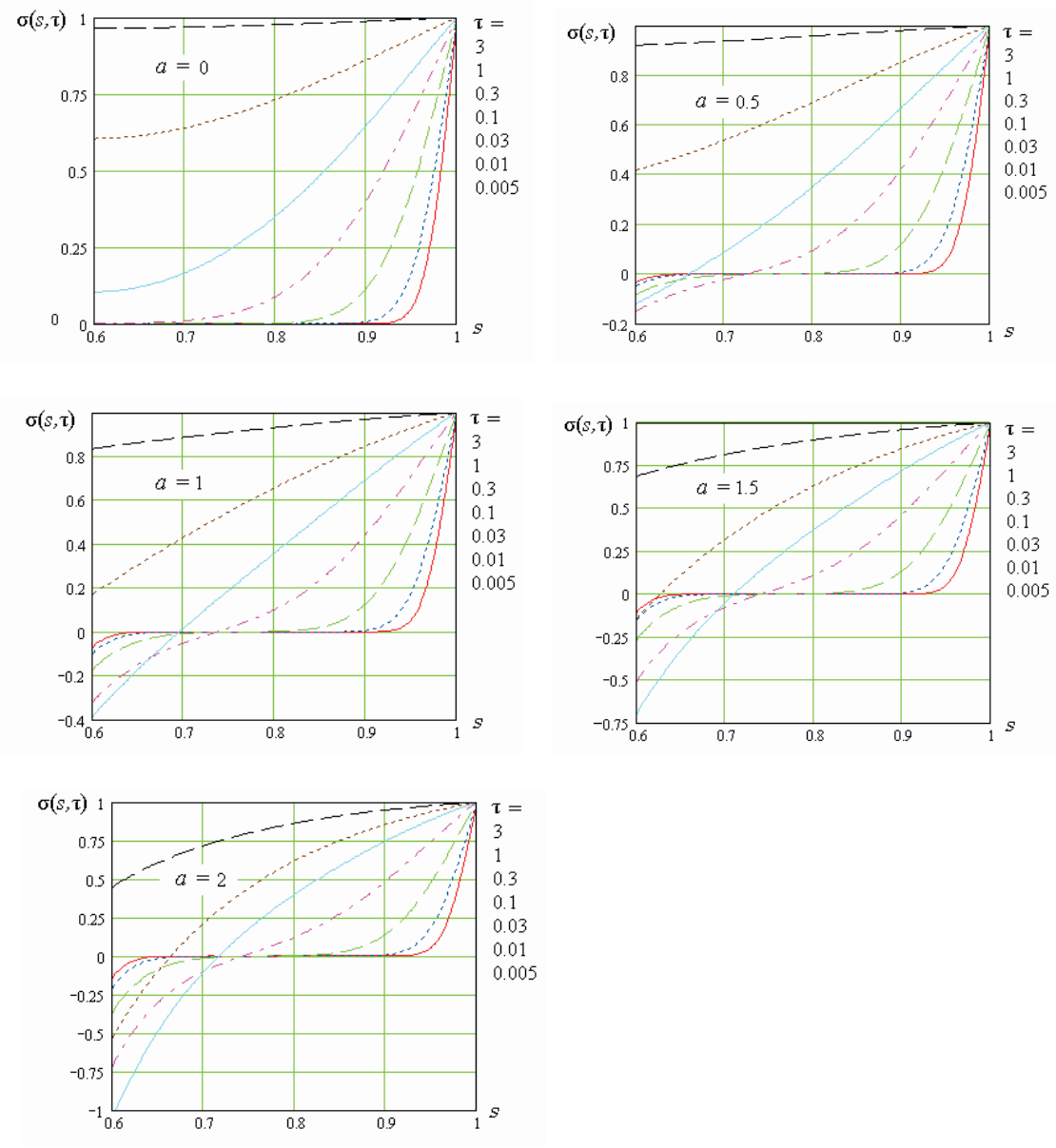


Figure 8.9. The function $\sigma(s,\tau)$ for different values of the convective-diffusive parameter *a*: $a = 0$ (top left), 0.5, 1, 1.5 and 2 (bottom).

The set of curves from a smallest dimensionless time $\tau = 0.005$ up to $\tau = 3$ is shown for the five values $a = 0,\ 0.5,\ 1,\ 1.5,\ 2$. The different scales for $\sigma$ should be noted. The drying phase is longer and deeper as *a* increases.

## 8.6 Drying at the canister wall in the dry-rock case

The strongest drying occurs at the warm canister side $r = r_c$. Figure 8.4 shows this decrease of $S$ in the dry-rock case for the reference case with $a = 0.9$, (8.16). Let $\sigma_c(\tau) = \sigma(s_c, \tau)$ denote value for $\sigma$ at $s = s_c$. This function gives the largest drying that may occur for any boundary condition at the rock boundary. The corresponding degree of water saturation at the canister is, (8.18),

$$S(r_c, t) = S_{in} + (1 - S_{in}) \cdot \sigma_c(t / t_0). \tag{8.21}$$

The function $\sigma_c(\tau)$ starts at zero and falls to the steady-state value (7.19) at infinite time. The function is zero for all times in the case $a = 0$. We have in accordance with (8.19)

$$\sigma_c(0) = 0, \qquad \sigma_c(\infty) = \sigma_{ss}(s_c; a); \qquad a = 0: \quad \sigma_c(\tau) = 0. \tag{8.22}$$

Figure 8.10 shows $\sigma_c(\tau)$ for $a = 0.5,\ 1,\ 1.5,\ 2$ (full lines). The dashed curves, which lie very close except for small $\tau$, show the approximation (8.23)-(8.24).

The function $\sigma_c(\tau)$ is given by (8.11) with $s = s_c$. An approximation, valid for large $\tau$, is to use only the first term in the sum $(n = 1)$. The first eigenvalue $\nu_1 = \nu_1(a)$ as function of $a$ is shown in Fig. 8.11, left. The deviation from $\nu_1 = 2$ is less than 1%. We may use this value in the approximation. We get an approximation of the following type

$$\sigma(s, \tau) \approx \sigma_{ss}(s; a) - A_{c1}(a) \cdot e^{-4 \cdot \tau}, \qquad \tau \geq 0.2. \tag{8.23}$$

The function $A_{c1}(a)$ is shown in Fig. 8.11, right. The following expression is a good approximation

$$A_{c1}(a) \approx -0.5 \cdot a - 0.13 \cdot a^{2.3}, \qquad 0 \leq a \leq 2. \tag{8.24}$$

The error in the approximation (8.23)-(8.24) is less than 2%.

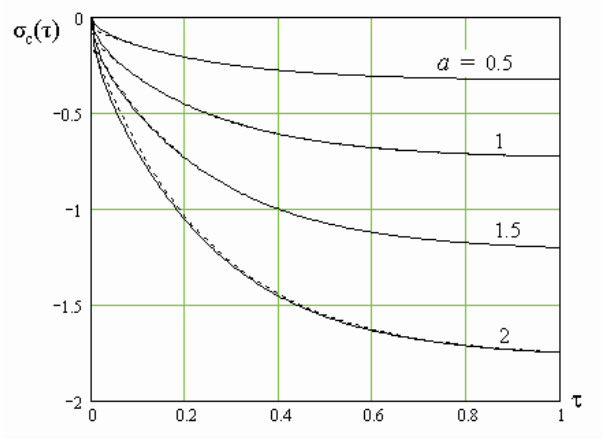


Figure 8.10. The function $\sigma_c(\tau)$ for the drying at the canister wall for different *a*-values (full lines). The dashed curves show the approximation (8.23)-(8.24).

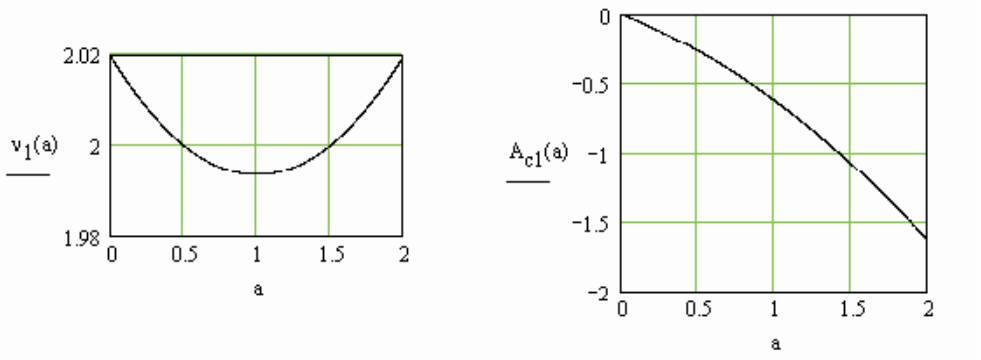


Figure 8.11. The first eigenvalue $\nu_1(a)$ and the coefficient $A_{c1}(a)$ in (8.23) as functions of *a*.

## 8.7 Drying and resaturation at the canister wall in wet-rock case

Fig. 8.5 shows the drying and resaturation in the wet-rock case for the reference case. The largest drying and the slowest resaturation occur at the canister wall $r = r_c$. The degree of saturation at the wall is from (8.9)

$$S(r_c, t) = S_{in} + (1 - S_{in}) \cdot \sigma_c(t / t_0), \qquad \sigma_c(\tau) = \sigma(r_c, \tau). \tag{8.25}$$

The function $\sigma_c(\tau)$, which gives the drying, has *a* as parameter.

### 8.7.1 Drying and resaturation for different a-values

The function $\sigma_c(\tau)$ has been calculated for different values of *a* for the wet-rock case. The curves are shown in Figure 8.12.The curves decrease to a minimum at $\tau = \tau_{md}$ below zero, which gives the largest or *m*aximum *d*rying. Then the curves increase steadily up to +1: $S = S_{in} + (1 - S_{in}) \cdot 1 = 1$ at full saturation. The initial saturation $S = S_{in}$ is reached for $\sigma_c = 0$ at $\tau = \tau_{cin}$.

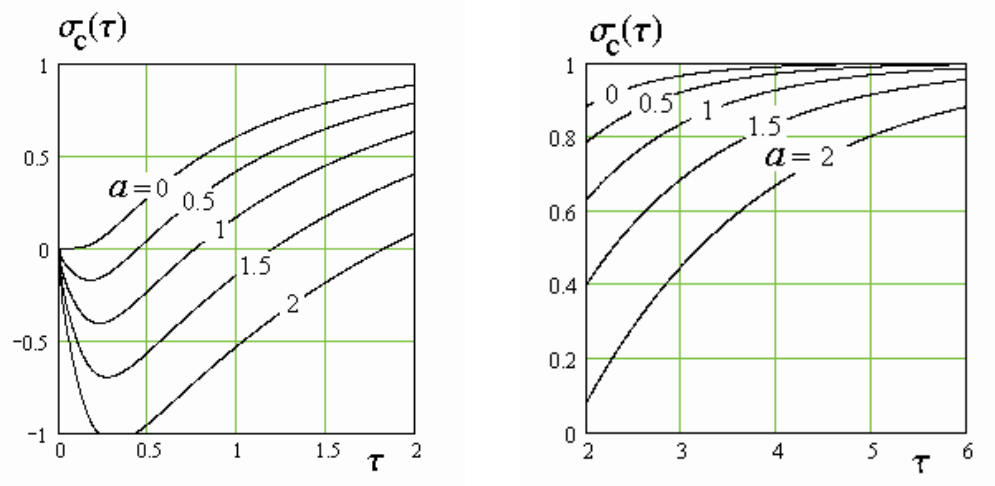


Figure 8.12. Left: The function $\sigma_c(\tau)$, $0 < \tau < 2$, for the degree of saturation at the canister wall, (8.25), for different $a$-values. Drying period when $\sigma < 0$. Right: $\tau > 2$ with resaturation only.

Let us consider an example:

$$a = 0.9 \quad \Rightarrow \quad \tau_{md} \approx 0.22, \quad \sigma_{md} \approx -0.4. \tag{8.26}$$

We get these values by interpolation between the second (a=0.5) and third curve (a=1) from top in Fig. 8.12, left. The maximum drying depends on $S_{in}$. We have for example for $S_{in}$=0.85, (8.16),

$$S_{c,md} = 0.85 + (1 - 0.85) \cdot (-0.4) = 0.79. \tag{8.27}$$

The real time depends on the time scale $t_{0y}$, which is obtained from Fig. 8.7. We have for example

$$t_{0y} = 5 \text{ years} \quad \Rightarrow \quad t_{md} = 5 \cdot 0.22 = 1.1 \text{ y}. \tag{8.28}$$

The value of $\sigma_c(\tau; 0.9)$ has according to Fig. 8.12, left, risen to 0.8 for $\tau = 2.6$. We have

$$t = 5 \cdot 2.6 = 13 \text{ y}, \quad S_c = 1 - (1 - 0.85) \cdot 0.2 = 0.97. \tag{8.29}$$

### 8.7.2 Formulas for drying

The degree of saturation $\sigma_c(\tau)$ at the canister wall $r = r_c$ may be approximated by the first two terms in the sum (8.13). The approximation is valid with good accuracy in the region of minimum drying. The largest drying occurs at the canister at the time when the derivative of $\sigma_c(\tau)$ is zero. From this it is possible to derive a formula for the time $t_{md}$, when minimum during occurs, and a formula for the σ-value $\sigma_{md}(a)$. We have

$$t_{\mathrm{md}} = t_0 \cdot \tau_{\mathrm{md}}(a), \qquad S_{\mathrm{md}} = S_{\mathrm{in}} + (1 - S_{\mathrm{in}}) \cdot \sigma_{\mathrm{md}}(a). \tag{8.30}$$

The functions $\tau_{\mathrm{md}}(a)$ and $\sigma_{\mathrm{md}}(a)$ for the largest drying are shown in Figure 8.13.

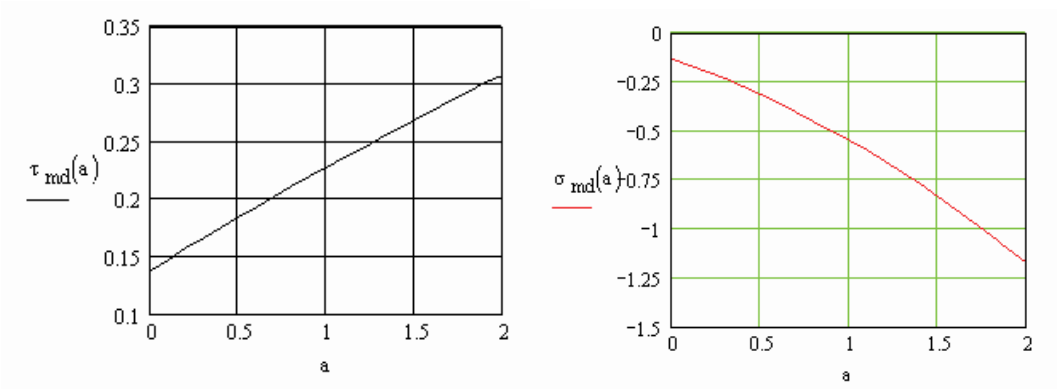


Figure 8.13. The functions $\tau_{\mathrm{md}}(a)$ and $\sigma_{\mathrm{md}}(a)$ to determine the largest drying at the canister wall, (8.30).

### 8.7.3 Formulas for resaturation

The first term $n = 1$ is sufficient for larger times. We have with an error below 2 %

$$\sigma_{\mathrm{c}}(\tau) \approx 1 - A_{\mathrm{c1}} \cdot e^{-\nu_1^2 \cdot \tau}, \quad \tau = t / t_0 > 0.3. \tag{8.31}$$

or from (8.25)

$$S(r_{\mathrm{c}}, t) \approx 1 - (1 - S_{\mathrm{in}}) \cdot A_{\mathrm{c1}} \cdot e^{-\nu_1^2 \cdot t / t_0}, \qquad t > 0.3 \cdot t_0. \tag{8.32}$$

The functions $A_{\mathrm{c1}}(a)$ and $\nu_1^2(a)$ in the above exponential expression are shown in Figure 8.14.

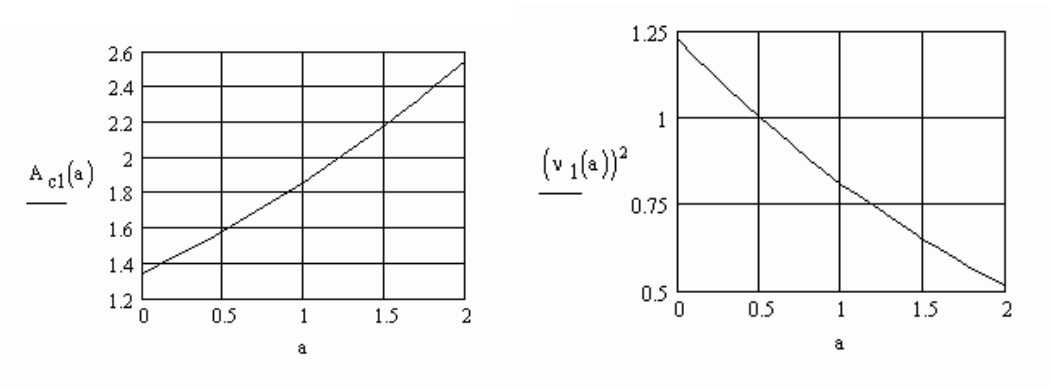


Figure 8.14. The functions $A_{\mathrm{c1}}(a)$ and $(\nu_1(a))^2$ in formula (8.32) for the exponential behavior at large time.

The time when the degree of saturation has retained its initial value after the initial drying is:

$$S_c = S_{\text{in}} \quad \Rightarrow \quad t_{\text{cin}} = t_0 \cdot \tau_{\text{cin}}(a). \tag{8.33}$$

The function $\tau_{\text{cin}}(a)$ is shown in Figure 8.15.

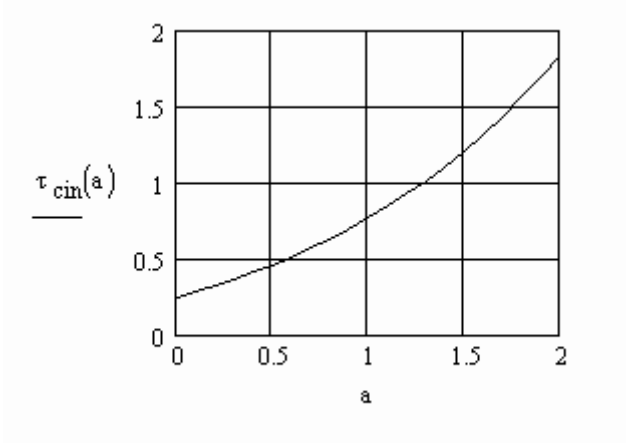


Figure 8.15. The function $\tau_{\text{cin}}(a)$ in formula (8.33) for the time when the initial degree of saturation is recovered.

# 9 Key parameters and sensitivity analysis

A sensitivity analysis is presented in Claesson, Hagentoft and Sällfors (2003). These results are not reported here again.

We have seen that the potential drying depends on the two parameters $a$ and $t_0$ only. The two parameters depend in turn on the flow properties of bentonite, on the temperature level and gradient, and on properties of water. We will here present a rule of thumb to assess the key factors.

## 9.1 Key factors for the thermo-diffusive parameter a

The thermo-diffusive parameter $a$ is defined by (8.3). It is proportional to the various key factors in the following way:

$$a \propto \frac{Q_c}{H_c}, \quad a \propto \frac{1}{\lambda(S_0)} \approx \frac{1}{\lambda(1)}, \quad a \propto K_T'(S_0,T_0) \propto D_v(0), \quad a \propto \frac{1}{K_S(S_0,T_0)} \propto \frac{1}{k(1)}. \qquad (9.1)$$

In the third proportionality, (6.10) is used. In the fourth one, (6.9) is used. Here, the last proportionality giving $1/k(1)$ may in case of doubt be tested with model that gives $A(S,T)$ in App. 6. The factors above show how $a$ depends on four key factors. Let us define the key product $f$ as

$$f = \frac{Q_c}{H_c \lambda(1)} \cdot \frac{D_v(0)}{k(1)}, \qquad f_{ref} = \left( \frac{Q_c}{H_c \lambda(1)} \cdot \frac{D_v(0)}{k(1)} \right)_{ref}. \qquad (9.2)$$

Here, $a_{ref}$ is the *a*-value in the reference case, which has to be calculated by the model in App. 6, for example.

A rule of sum to *assess the variation* of $a$ with the key factors is now

$$a \approx \frac{f}{f_{ref}} \cdot a_{ref}. \qquad (9.3)$$

This means that $a$ is doubled, when the vapor diffusivity for bentonite $D_v(0)$ or the heat flux $Q_c$ is doubled. The parameter $a$ is approximately doubled, when thermal conductivity of fully saturated bentonite $\lambda(1)$ or the hydraulic conductivity of fully saturated bentonite $k(1)$ is halved.

## 9.2 Key factors for the time scale $t_0$

The basic time scale $t_0$ is inversely proportional to the mean diffusivity $D_0$, (8.10), which is proportional to $K_S(S_0,T_0)$, (8.3). We have as in (9.1), right,

$$t_0 \propto \frac{1}{D_0} \propto \frac{1}{K_S(S_0,T_0)} \propto \frac{1}{k(1)}. \qquad (9.4)$$

As a rule of thumb we have that the key factor to determine the basic time scale is the inverse of the hydraulic conductivity of fully saturated bentonite $k(1)$:

$$t_0 \approx \frac{k(1)\big|_{\text{ref}}}{k(1)} \cdot t_{0,\text{ref}}. \tag{9.5}$$

Here, $t_{0,\text{ref}}$ is the value in the reference case, which may be calculated by the model in App. 6. The time scale decreases by a factor 10, when $k(1)$ is increased by a factor 10.

# 10 Survey of models

A number of small computer models has been developed as handy tools of analysis to understand and assess the potential drying under various conditions. All models are implemented in Mathcad. They are shown in full in App. 4-8. The models, which consist of a moderate set of formulas and computations, should be reasonable straight forward to implement in other mathematical programs as Matlab or Maple.

1. *General steady-state solution for S and T.* Eqs. (7.2)-(7.3) are solved. App. 4.
2. *Chart for S(T).* Eqs. (7.8) are solved. App. 5.
3. *Key parameters D, A and $t_0$ as functions of S and T.* The functions (6.22) and (8.17) are calculated. App. 6.
4. *Solution S(r,t) in dry-rock case.* The function from (8.9) and (8.11) with the specifications in App.3 is calculated. App.7.
5. *Solution S(r,t) in dry-rock case.* The function from (8.9) and (8.13) with the specifications in App.3 is calculated. App.8.

The formulas for water and bentonite are used in the first three models.

# 11 Boltzmann solution

## 11.1 General step-response problem

Computer models are used to predict the intricate water-temperature-pressure processes in the bentonite layer between canisters and rock in nuclear waste repositories. The property functions involved in the calculations may vary strongly with the state variables. There is a need for independent solutions to control the results. The *purpose* of this study is to provide such a critical solution, which is quite accurate and obtained in a different, semi-analytical way. Here, only a brief summary is given. Claesson (2003C) presents more details.

The solutions will also provide further insight into the complicated coupled, highly non-linear processes with water evaporation and condensation. The effects and relative importance of particular assumptions and choice of data may be analyzed.

Let $S(x,t)$ and $T(x,t)$ be the solution to the following problem:

$$\frac{\partial}{\partial t}\big[w(x,t)\big] = \frac{\partial}{\partial x}\cdot\left(K_S(S,T)\cdot\frac{\partial S}{\partial x} + K_T(S,T)\cdot\frac{\partial T}{\partial x}\right). \tag{11.1}$$

$$\frac{\partial}{\partial t}\big[e(x,t)\big] = \frac{\partial}{\partial x}\cdot\left(\lambda_S(S,T)\cdot\frac{\partial S}{\partial x} + \lambda_T(S,T)\cdot\frac{\partial T}{\partial x}\right). \tag{11.2}$$

Here, the moisture and heat contents are given functions of the chosen state variables:

$$w = w(S,T), \qquad e = e(S,T). \tag{11.3}$$

The particular initial and boundary conditions for Boltzmann solutions are:

$$S(x,0) = S_{\text{in}}, \qquad T(x,0) = T_{\text{in}}, \qquad 0 < x < \infty; \tag{11.4}$$

$$T(0,t) = T_0, \qquad S(0,t) = S_0 \quad \text{or} \quad \text{zero water flux}, \qquad t > 0. \tag{11.5}$$

Here, $T$ is the temperature, and $S$ is the chosen state variable for water or moisture in the pores such as degree of water saturation (or water pressure). The flow coefficients and the capacity factors are (apart from some thermodynamic restrictions) any functions of $S$ and $T$.

## 11.2 Boltzmann solution

The solution to this so-called Boltzmann problem depends on a single variable $s$:

$$S(x,t) = \tilde{S}(s), \qquad T(x,t) = \tilde{T}(s), \qquad s = \frac{x}{\sqrt{4t}}. \tag{11.6}$$

Here, $\tilde{S}(s)$ and $\tilde{T}(s)$ are the solution to

$$\begin{aligned}
&\frac{d}{ds}\left( K_S(\tilde{S},\tilde{T})\cdot\frac{d\tilde{S}}{ds} + K_T(\tilde{S},\tilde{T})\cdot\frac{d\tilde{T}}{ds}\right) + 2s\cdot\frac{d}{ds}\Big[\, w(\tilde{S},\tilde{T})\,\Big] = 0, \\
&\frac{d}{ds}\left( \lambda_S(\tilde{S},\tilde{T})\cdot\frac{d\tilde{S}}{ds} + \lambda_T(\tilde{S},\tilde{T})\cdot\frac{d\tilde{T}}{ds}\right) + 2s\cdot\frac{d}{ds}\Big[\, e(\tilde{S},\tilde{T})\,\Big] = 0, \qquad 0 < s < \infty.
\end{aligned} \tag{11.7}$$

The boundary and initial conditions (11.4) and (11.5) become:

$$\tilde{S}(\infty) = S_{\text{in}}, \qquad \tilde{T}(\infty) = T_{\text{in}}, \qquad \tilde{T}(0) = T_0, \tag{11.8}$$

$$\tilde{S}(0) = S_0 \quad \text{or} \quad \left( K_S(\tilde{S},\tilde{T})\cdot\frac{d\tilde{S}}{ds} + K_T(\tilde{S},\tilde{T})\cdot\frac{d\tilde{T}}{ds}\right)\Bigg|_{s=0} = 0. \tag{11.9}$$

This is a system of two coupled nonlinear *ordinary* differential equations, which is much simpler to solve with three-digit accuracy using a modern mathematical program (such as Mathcad).

Mathcad programs for this Boltzmann problem have been developed. They have been used as a benchmark test for models for coupled heat and moisture flow in building applications CEN-norms.

# 12 Conclusion

The aim of this study has been to develop tools of analysis to assess the drying of the bentonite. A few small models based on a number of equations are available in Mathcad. They should be quite easy to translate to other mathematical programs.

The key parameters are a time scale $t_0$ and a thermo-diffusive parameter *a*. These depend in a rather complicated way on flow properties of bentonite, properties of water, level of degree of water saturation and temperature in the bentonite annulus, and on the temperature gradient. But they are readily calculated with the models.

At the outer boundary $r = r_r$, there are two limits. The rock may be sufficiently wet to maintain full saturation at the surface of the bentonite, the wet-rock case. The other limit, which is the worst possible case, is that the water flow to the rock is zero, the dry-rock case.

The bentonite will always start to dry at the warmer canister side (except for case of full saturation initially when nothing happens), and the saturation will increase on the rock side from the initial saturation $S_{in}$. In the wet-rock case, wetting from the fully saturated rock side will stop the drying after a certain time, and a successive wetting of all bentonite continues toward full saturation in the whole annulus after, say, $3 \cdot t_0$. See Fig. 8.5. In the dry-rock case, drying on the canister side and wetting on the rock side continue until a steady-state moisture distribution is established. See Fig. 8.3. Then water vapor flow outwards and liquid water flow inwards balance each other at all points in the bentonite.

The curves in Figs. 8.3 and 8.5 show drying in the left-hand half of $r_c \le r \le r_r$, and wetting above $S = S_{in}$ in the right-hand half of the interval. This is a general feature. This means that the outer half of the bentonite annulus *never dries below* the initial degree of water saturation $S_{in}$. The strongest drying occurs in a rather thin layer near the canister.

The steady-state moisture distributions, which are attained after the time $t_0$ in the dry-rock case, are analyzed in detail. Models for the exact moisture profiles are available. A handy tool is a chart for the coordinate-independent relations $S = S(T)$.

The steady-state solutions are simplified in the linearized case. We get very handy formulas to assess the largest drying. Formula (7.15) and Fig. 7.8 give the largest possible drying as function of the two parameters $S_{in}$ and $a$, only.

The complete process is obtained for any *a*-value in the linearized case from new analytical solutions. See Figs. 8.8 and 8.9. Then we also have formulas and graphs that give the drying at the canister side. See Section 8.6-7.

# References

Claesson J. and Th. Probert, (1996). Temperature Field Due to Time-dependent Heat Sources in a Large Rectangular grid. Derivation of Analytical Solution**.** *SKB, Technical Report 96-12,* Swedish Nuclear and Waste Management Co, P.O. Box 5864, S-11248 Stockholm, Sweden.

Claesson, J., (2003A). Drying and resaturation of the bentonite barrier in a nuclear waste repository. Analyses based on an analytical solution. Detailed report. *Report for SKI*, Nov. 2003 (available from Building Physics, Chalmers).

Claesson, J., C.-E. Hagentoft and G. Sällfors, (2003). Analyses of highly nonlinear, coupled moisture and heat flow in bentonite based on radial, steady-state solutions. *Report for SKI*, Nov. 2003 (available from Building Physics, Chalmers).

Claesson, J., (2003B)**.** Drying and Resaturation of the Bentonite Barrier in a Nuclear Waste Repository. Analyses Based on an Analytical Solution. *GeoProc 2003, Int. Conf on Coupled T-H-M-C Processes in Geosystems*, Oct. 2003, KTH, Stockholm, Sweden.

Claesson, J., (2003C). Generalized Boltzmann solutions for coupled, highly nonlinear diffusion equations. *Report for SKI*, Dec. 2003 (available from Building Physics, Chalmers).

Claesson J., (2007). Temperature field in a nuclear waste repository. Formulas from canister heat sources. *Report for SKI*, Dec. 2007 (available from Building Physics, Chalmers).

Hökmark H., and J. Claesson, (2005). Use of an Analytical Solution for Calculating Temperatures in Repository Host Rock. J. of Engineering Geology, 81, 353-364. (Also presented at *Key Issues in Waste Isolation research*, 6th International Workshop, Ecole National des Ponts et Chaussées, Paris.)

Probert, Th., and J. Claesson, (1997). Temperature Field Due to Time-dependent Heat Sources in a Large Rectangular grid. II. Application for the KBS-3 repository. SKB, *Technical Report 97-27,* Swedish Nuclear and Waste Management Co, P.O. Box 5864, S-11248 Stockholm, Sweden.

Rutqvist J., J. Noorishad and C-F. Tsang (1999). Coupled Termohydromechanical Analysis of a Heater Test in Unsaturated Clay and Fractured Rock at the Kamaishi Mine. *SKI report 99:50*, the Swedish Nuclear Power Inspectorate.

# Nomenclature

| | | |
|---|---|---|
| $A(S,T)$ | Thermo-diffusive flow function, Eq. (6.22) | - |
| $a$ | Thermo-diffusive parameter, $\left( a = A(S_0,T_0) \right)$ | - |
| $a_\mathrm{r}$ | Thermal diffusivity of rock, $a_\mathrm{r} = \lambda_\mathrm{r} /(\rho_\mathrm{r} c_\mathrm{r})$ | $\mathrm{m}^2/\mathrm{s}$ |
| $B$ | Half length of repository tunnels | m |
| $c_\mathrm{r}$ | Heat capacity of rock | J/(kgK) |
| $D_\mathrm{c}$ | Distance between canisters in a tunnel | m |
| $D_\mathrm{gr}$ | Distance from ground surface to the repository area | m |
| $D_\mathrm{t}$ | Distance between tunnels | m |
| $D(S,T)$ | Diffusivity function, Eq. (6.22) | $\mathrm{m}^2/\mathrm{s}$ |
| $D_0$ | Mean diffusivity, $\left( D_0 = D(S_0,T_0) \right)$ | $\mathrm{m}^2/\mathrm{s}$ |
| $D_\mathrm{v}(S)$ | Water vapor diffusivity in the bentonite, Eq. (6.4) | $\mathrm{m}^2/\mathrm{s}$ |
| $D_\mathrm{v}'(0)$ | Water vapor diffusivity in the bentonite for $S = 0$ | $\mathrm{m}^2/\mathrm{s}$ |
| $\mathrm{erf}(x)$ | Error function | - |
| $g$ | Moisture flux per unit area (with liquid and vapor components) | $\mathrm{kg}/(\mathrm{m}^2\mathrm{s})$ |
| $G$ | Total moisture flux, Eq. (6.3) | kg/s |
| $h(T)$ | Enthalpy of water (liquid, vapor) | J/kg |
| $H_\mathrm{c}$ | Height of canisters | m |
| $k(S)$ | Hydraulic conductivity | $\mathrm{m}^2$ |
| $K_S(S,T)$ | Moisture flow coefficient for gradient in $S$, Eq. (6.7) | kg/(ms) |
| $K_T(S,T)$ | Moisture flow coefficient for gradient in $T$, Eq. (6.7) | kg/(msK) |
| $L$ | Half width of rectangular repository area | m |
| $P$ | Pore water pressure | Pa |
| $P(S)$ | Water retention curve | Pa |
| $q$ | Heat flux per unit area | $\mathrm{W}/\mathrm{m}^2$ |
| $Q$ | Total heat flux, Eq. (6.3) | W |
| $Q_\mathrm{c}(t)$ | Heat emission from a canister | W |
| $r$ | Local radial distance from the central canister, $\sqrt{x^2 + y^2}$ | m |
| $r_\mathrm{c}$ | Canister radius, inner radius of bentonite annulus | m |
| $r_\mathrm{r}$ | Rock radius, outer radius of bentonite annulus | m |
| $s_\mathrm{c}$ | Ratio between radii: $s_\mathrm{c} = r_\mathrm{c} / r_\mathrm{r}$ | - |
| $S$ | Degree of water saturation in the bentonite, $0 \le S \le 1$ | - |
| $S_\mathrm{c}$ | Degree of water saturation at the canister radius | - |
| $S_\mathrm{in}$ | Initial degree of water saturation in the bentonite | - |
| $S_\mathrm{r}$ | Degree of water saturation at the rock radius | - |
| $S_0$ | Chosen mean level for the degree of saturation in Eq. (8.2) | - |
| $t$ | Time | s |
| $t_0$ | Basic time scale, Eq. (8.10) | s |
| $t_{0\mathrm{y}}$ | Basic time scale in years, Eq. (8.17) | years |
| $T$ | Temperature | ºC |
| $T_\mathrm{c}$ | Temperature in the bentonite at the canister radius | ºC |

| | | |
|---|---|---|
| $T_r$ | Temperature in the bentonite at the rock radius | ºC |
| $T_{rep}$ | Undisturbed rock temperature at the repository level, $(=T_u(0))$ | ºC |
| $T_0$ | Chosen mean temperature level in Eq. (8.2) | ºC |
| $V_p$ | Pore volume of bentonite | - |
| $x$ | Horizontal coordinate perpendicular to the tunnels | m |
| $y$ | Horizontal coordinate parallel with the tunnels | m |
| $z$ | Vertical coordinate from repository level | m |

| | | |
|---|---|---|
| $\phi$ | Relative humidity | - |
| $\eta(T)$ | Dynamic viscosity of water | kg/(ms) |
| $\lambda(S)$ | Thermal conductivity of bentonite | W/(mK) |
| $\lambda_r$ | Thermal conductivity of rock | W/(mK) |
| $\lambda_S(S,T)$ | Heat flow coefficient for gradient in *S*, Eq. (6.8) | W/m |
| $\lambda_T(S,T)$ | Heat flow coefficient for gradient in *T*, Eq. (6.8) | W/(mK) |
| $\rho_r$ | Density of rock | kg/m$^3$ |
| $\rho_v$ | Density of water vapor in the pores | kg/m$^3$ |
| $\rho_{v,sat}(T)$ | Density of water vapor at saturation | kg/m$^3$ |
| $\rho_w$ | Density of water, (=1000) | kg/m$^3$ |
| $\sigma(r,\tau)$ | Function for water saturation, Eq. (8.9) | - |
| $\sigma_c(\tau)$ | Function for water saturation, Eq. (8.25) | - |
| $\tau$ | Dimensionless time, $(\tau = t/t_0)$ | - |

# Appendix 1. Temperature field

The canisters of the repository lie in large a rectangular area, $-L < x < L$, $-B < y < B$, $z = 0$ at a depth $D_{\mathrm{gr}}$ below the ground surface. The canisters are placed along tunnels at a distance $D_c$. The distance between the parallel tunnels is $D_{\mathrm{t}}$. See Figs. 1.1 and 2.1. The canisters have the height $H_{\mathrm{c}}$, and each of them emits the heat $Q_{\mathrm{c}}(t)$ (W).

## A1.1 Temperature field from heat emitting canisters

Let $T(x,y,z,t)$ denote the temperature field in the ground with the array of heat emitting canisters. The undisturbed ground temperature without canisters is $T_{\mathrm{undist}}(z)$. There is a line heat source along each canister $(-H_{\mathrm{c}}/2 < z' < H_{\mathrm{c}}/2)$ with the heat emission $Q_{\mathrm{c}}(t)/H_{\mathrm{c}}$ (W/m).

The temperature field from the central canister alone is obtained by integration in time and in space along the canister axis of a point source. We have

$$T_{\mathrm{can}}(x,y,z,t) = \int_0^t dt' \int_{-H_{\mathrm{c}}/2}^{H_{\mathrm{c}}/2} dz' \frac{Q_{\mathrm{c}}(t')/H_{\mathrm{c}}}{\rho_{\mathrm{r}} c_{\mathrm{r}} \left[4\pi a_{\mathrm{r}}(t-t')\right]^{1.5}} \cdot \exp\left[\frac{x^2+y^2+(z-z')^2}{4a_{\mathrm{r}}(t-t')}\right]. \qquad (13.1)$$

The total temperature field becomes

$$T(x,y,z,t) = T_{\mathrm{undist}}(z) + \sum_m \sum_n T_{\mathrm{can}}(x - mD_{\mathrm{t}}, y - nD_{\mathrm{c}}, z, t). \qquad (13.2)$$

The sum may involve some 6000 canisters in the positions $(mD_{\mathrm{t}}, nD_{\mathrm{c}}, 0)$. For each canister there is integration in time and along the line source. The central canister lies along $(0,0,z)$. The temperature due to the canisters is zero to be zero at $z = D_{\mathrm{gr}}$. This is obtained by using negative mirror sources above the ground surface at $z = 2D_{\mathrm{gr}}$. Then we subtract a double sum with $z$ replaced by $2D_{\mathrm{gr}} - z$. After very long time when the effect of the ground surface is accounted for we have

$$T(x,y,z,t) = T_{\mathrm{u}}(z) + \sum_m \sum_n \left[T_{\mathrm{can}}(x - mD_{\mathrm{t}}, y - nD_{\mathrm{c}}, z, t) - T_{\mathrm{can}}(x - mD_{\mathrm{t}}, y - nD_{\mathrm{c}}, 2D_{\mathrm{gr}} - z, t)\right]. \qquad (13.3)$$

The double sum is zero at the ground surface $z = D_{\mathrm{gr}}$

The integral in $z'$ may be expressed with the error function. The integration in time may be somewhat neater by a suitable variable substitution. We get the following simpler expression for the temperature (13.1)

$$T_{\mathrm{can}}(x,y,z,t) = \frac{1}{4\pi\lambda_{\mathrm{r}} H_{\mathrm{c}}} \cdot \int_{r/\sqrt{4a_{\mathrm{r}}t}}^{\infty} Q_{\mathrm{c}}\left(t - \frac{r^2}{4a_{\mathrm{r}}s^2}\right) \cdot e^{-s^2} \cdot \frac{1}{s} \cdot E\, ds,$$

$$E = \mathrm{erf}\left[\frac{s}{r}\cdot\left(\frac{H_c}{2}-z\right)\right]+\mathrm{erf}\left[\frac{s}{r}\cdot\left(\frac{H_c}{2}+z\right)\right]. \qquad (13.4)$$

We are in particular interested in the temperature at the bentonite at the mid-level of the canister in the very center of the field of canisters, i.e. for $\sqrt{x^2+y^2}=r_r$ and $z=0$. The line source from the central canister gives essentially an ellipsoidal temperature field in the vicinity of the canister. The cylindrical surface is approximated by a suitable ellipsoid (with the same volume and general shape). As rock temperature $T_r$, we choose

$$T_r(t) = T(0, y_r, 0, t), \qquad y_r = \sqrt{1.5}\cdot r_r. \qquad (13.5)$$

There is a small correction to (13.1) and (13.4) from the local temperature field due to the local design in and around the canister. These minor contributions would require a local three-dimensional calculation for the temperature field, the result of which is not important for our purposes.

## A1.2 Temperature during the first years

During the first few years [$t < D_t^2/(4a)$], it is sufficient to consider the contributions from canisters below the distance $2D_t$ from the central canister. Here, $D_t$ is the distance between two adjacent tunnels, Fig. 2.1. We get a line of canisters along the central tunnel ($n = \pm 1, ..., \pm N, \quad N \approx \mathrm{int}\left[2D_t / D_c\right]$). The line of canister heat sources from the two adjacent tunnels may be replaced by a line heat source along the tunnels with the strength $Q_c(t)/D_c$ (W/m). With these assumptions, we get the following formula for the rock temperature $T_r(t)$ at the bentonite

$$T_r(t) \approx T_{rep} + T_{can}(0, y_r, 0, t) + 2\cdot\sum_{n=1}^{N} T_{can}(0, nD_c, 0, t) + 2\cdot T_{line}(t). \qquad (13.6)$$

$$T_{line}(t) = \frac{1}{4\pi\lambda_r D_c}\cdot\int_{D_t/\sqrt{4a_r t}}^{\infty} Q_c\left(t-\frac{D_t^2}{4a_r s}\right)\cdot\frac{1}{s}\cdot e^{-s}\,ds \qquad (13.7)$$

$$T_{can}(0, y, 0, t) = \frac{1}{4\pi\lambda_r H_c}\cdot\int_{|y|/\sqrt{4a_r t}}^{\infty} Q_c\left(t-\frac{y^2}{4a_r s^2}\right)\cdot e^{-s^2}\cdot\frac{1}{s}\cdot\mathrm{erf}\left(\frac{sH_c}{2|y|}\right)ds, \qquad (13.8)$$

The undisturbed ground temperature at the repository level $z=0$ is $T_u(0) = T_{rep}$. The first integral is the contribution from the central canister, and the sum of integrals the contribution from the canisters along the central tunnel. The error function and the complementary error function are defined by the integrals

$$\mathrm{erf}(x) = \frac{2}{\sqrt{\pi}}\int_0^x e^{-s^2}\,ds, \qquad \mathrm{erfc}(x) = 1-\mathrm{erf}(x) = \frac{2}{\sqrt{\pi}}\int_x^{\infty} e^{-s^2}\,ds. \qquad (13.9)$$

## A1.3 Simplified formula

After the first year (or two), we may use the following remarkably simple formula.

$$T_{\mathrm{r}}(t) \approx T_{\mathrm{rep}} + T_{\mathrm{global}}(t) + Q_{\mathrm{c}}(t) \cdot R_{\mathrm{local}}. \tag{13.10}$$

Here, we have a global temperature field obtained from a surface heat source over $z = 0$, $-L < x < L$, $-B < y < B$ with the strength $Q_{\mathrm{c}}(t)/(DD')$ (W/m$^2$). See Figure A1.1

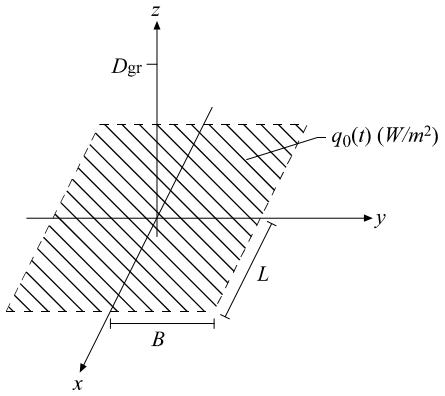


Figure A1.1. Surface heat source with the strength $q_0(t) = Q_{\mathrm{c}}(t)/(D_{\mathrm{c}} \cdot D_{\mathrm{t}})$ (W/m$^2$) over the repository area.

The temperature field from the rectangular surface heat source of Fig. A1.1 is

$$T_{\mathrm{rec}}(x,y,z,t) = \int_0^t \frac{Q_{\mathrm{c}}(t')/(D_{\mathrm{c}}D_{\mathrm{t}})}{4\rho_{\mathrm{r}}c_{\mathrm{r}}\sqrt{\pi}\cdot s} \cdot \left[\mathrm{erf}\left(\frac{\mathrm{L}-x}{s}\right) + \mathrm{erf}\left(\frac{\mathrm{L}+x}{s}\right)\right] \cdot \left[\mathrm{erf}\left(\frac{B-y}{s}\right) + \mathrm{erf}\left(\frac{B+y}{s}\right)\right] \cdot \left(e^{-z^2/s^2} - e^{-(z-2D_{\mathrm{gr}})^2/s^2}\right) dt', \tag{13.11}$$

$$s = \sqrt{4a_{\mathrm{r}}(t-t')}\,.$$

The temperature is the center, $x = 0$, $y = 0$, $z = 0$ in (13.11), is the global temperature of (13.10). We have:

$$T_{\mathrm{global}}(t) = \int_0^t \frac{Q_{\mathrm{c}}(t')/(D_{\mathrm{c}}D_{\mathrm{t}})}{\rho_{\mathrm{r}}c_{\mathrm{r}}\sqrt{\pi}\cdot s} \cdot \mathrm{erf}\left(\frac{\mathrm{L}}{s}\right) \cdot \mathrm{erf}\left(\frac{B}{s}\right) \cdot \left(1 - e^{-4D_{\mathrm{gr}}^2/s^2}\right) dt', \qquad s = \sqrt{4a_{\mathrm{r}}(t-t')}\,. \tag{13.12}$$

We have replaced the array of line sources as defined in (13.2) by smearing out the heat sources evenly over the corresponding rectangle, Fig. A1.1. The remaining temperature field involves *balanced* heat sources between the array of line sources and the rectangular source with negative sign. This part may, after rather intricate calculations, be represented by a single thermal resistance in the last term of (13.10):

$$R_{\mathrm{local}} = \frac{1}{2\pi\lambda_{\mathrm{r}}} \cdot \left\{ \frac{1}{H_{\mathrm{c}}} \cdot \ln\left(\frac{\mathrm{H_c}}{y_{\mathrm{r}}}\right) + \frac{1}{D_{\mathrm{c}}} \cdot \left[\gamma + \ln\left(\frac{D_{\mathrm{t}}}{4\pi D_{\mathrm{c}}}\right)\right] \right\}. \tag{13.13}$$

Here, $\gamma = 0.577$ is Euler's constant.

The solution (13.10),(13.12) and (13.13) is valid with good accuracy compared to the full expression (13.3) after a year or two until infinite time. The effects of spacing $D_t$ between tunnels and spacing $D_c$ between canisters along a tunnel are shown in a very clear way

Let us note that formula (13.10) may be extended to the case when the repository area consists of more than one rectangular array of canisters. Let index A denote a second rectangle $-L_A < x - x_A < L_A$, $-B_A < y - y_A < B_A$, $z = z_A$. Then we just have to the rectangular global temperature at the initial central canister to (13.10):

$$T_{recA}(t) = \int_0^t \frac{Q_c(t')/(D_c D_t)}{\rho_r c_r \sqrt{\pi}\cdot s} \cdot \left[ \mathrm{erf}\left( \frac{L_A + x_A}{s} \right) + \mathrm{erf}\left( \frac{L_A - x_A}{s} \right) \right] \cdot$$
$$\cdot \left[ \mathrm{erf}\left( \frac{B_A + y_A}{s} \right) + \mathrm{erf}\left( \frac{B_A - y_A}{s} \right) \right] \cdot \left( e^{-z_A^2/s^2} - e^{-(z_A + 2D_{grA})^2/s^2} \right) dt', \qquad (13.14)$$
$$s = \sqrt{4a_r(t - t')}\,.$$

# Appendix 2. Equations for heat and moisture flow

The equations for heat and moisture flow in the bentonite are discussed in Section 6. Here, some additional things are presented.

## A2.1 Data for water

Kelvin's equation relates the pore water pressure $P$ to the relative humidity $\phi$ of adjacent water vapor:

$$P = R_{\mathrm{w}}(273+T)\rho_{\mathrm{w}} \cdot \ln(\phi), \qquad \phi = \rho_v / \rho_{\mathrm{v,sat}}(T). \tag{14.1}$$

Here, $R_{\mathrm{w}} = R / M_{\mathrm{w}}$ =8.314/0.018 J/(kgK) is the gas constant for water, and $\rho_{\mathrm{w}}$ =1000 kg/m$^3$ the density of water. The water vapor density $\rho_{\mathrm{v}} = \rho_{\mathrm{v}}(S,T)$ becomes a function of $P(S)$ and $T$:

$$\rho_{\mathrm{v}}(S,T) = e^{P(S)/[R_{\mathrm{w}}(273+T)\rho_{\mathrm{w}}]} \cdot \rho_{\mathrm{v,sat}}(T). \tag{14.2}$$

The heat of evaporation of water is temperature dependent, and it equals the enthalpy difference between vapor and liquid:

$$L_{\mathrm{evap}}(T) = h_{\mathrm{vap}}(T) - h_{\mathrm{liq}}(T). \tag{14.3}$$

## A2.2 Flow coefficient functions

The flow coefficients $K_S$, $K_T$, $\lambda_S$ and $\lambda_T$ in (6.7)-(6.8) are obtained from (6.1)-(6.2). We get

$$K_S(S,T) = \left( \frac{\rho_{\mathrm{w}} k(S)}{\eta(T)} + D_{\mathrm{v}}(S) \cdot \frac{\partial \rho_{\mathrm{v}}}{\partial P} \right) \cdot \frac{dP}{dS}. \tag{14.4}$$

$$K_T(S,T) = D_{\mathrm{v}}(S) \cdot \frac{\partial \rho_{\mathrm{v}}}{\partial T} = D_{\mathrm{v}}(0) \cdot (1-S) \cdot \frac{\partial \rho_{\mathrm{v}}}{\partial T} = K_T'(S) \cdot (1-S). \tag{14.5}$$

$$\lambda_S(S,T) = \left( h_{\mathrm{liq}}(T) \frac{\rho_{\mathrm{w}} k(S)}{\eta(T)} + h_{\mathrm{vap}}(T) D_{\mathrm{v}}(S) \frac{\partial \rho_{\mathrm{v}}}{\partial P} \right) \cdot \frac{dP}{dS}. \tag{14.6}$$

$$\lambda_T(S,T) = \lambda(S) + h_{\mathrm{vap}}(T) D_{\mathrm{v}}(S) \frac{\partial \rho_{\mathrm{v}}}{\partial T}. \tag{14.7}$$

The coefficient $K_T(S,T)$ involves the water vapor diffusivity $D_{\mathrm{v}}(S)$ as factor. The vapor diffusion is zero at full saturation. This means that $K_T$ is zero for $S = 1$:

$$D_{\mathrm{v}}(S) = D_{\mathrm{v}}(0) \cdot (1-S) \quad \Rightarrow \quad K_T(1,T) = 0. \tag{14.8}$$

## A2.3 Temperature solution

Integration of (6.13) gives

$$T(r;t) = T_{\mathrm{r}} + \frac{Q_{\mathrm{c}}(t)}{2\pi H_{\mathrm{c}}} \cdot \int_{r}^{r_{\mathrm{r}}} \frac{1}{\lambda(S(r')) \cdot r'} dr' \approx T_{\mathrm{r}} + \frac{Q_{\mathrm{c}}(t)}{2\pi H_{\mathrm{c}} \cdot \lambda(S_{\mathrm{av}})} \cdot \ln\left(\frac{r_{\mathrm{r}}}{r}\right). \tag{14.9}$$

The temperature $T_{\mathrm{r}}$ will also change slowly with time due to the influence from other canisters. Here, $S_{\mathrm{av}}$ is a suitable average value.

## A2.4 Moisture balance equation

We will write Eq. (6.19) in an alternative way. Inserting (6.15), we have

$$V_{\mathrm{p}}\rho_{\mathrm{w}} \cdot \frac{\partial S}{\partial t} = \frac{1}{r} \cdot \frac{\partial}{\partial r}\left[ K_S(S,T) \cdot \left( r \cdot \frac{\partial S}{\partial r} + \frac{K_T(S,T)}{K_S(S,T)} \cdot r \frac{\partial T}{\partial r} \right) \right], \qquad r_{\mathrm{c}} < r < r_{\mathrm{r}}. \tag{14.10}$$

From (6.13) and (6.10), we have

$$r \cdot \frac{\partial T}{\partial r} = -\frac{Q_c}{2\pi H_{\mathrm{c}} \lambda(S)}, \qquad K_T(S,T) = K_T'(S,T) \cdot (1-S). \tag{14.11}$$

Eq. (14.10) may then be written

$$\frac{\partial S}{\partial t} = \frac{1}{r} \cdot \frac{\partial}{\partial r}\left\{ D(S,T) \cdot \left[ r \cdot \frac{\partial S}{\partial r} - 2 \cdot A(S,T) \cdot (1-S) \right] \right\}, \qquad r_{\mathrm{c}} < r < r_{\mathrm{r}}. \tag{14.12}$$

Here, we have introduced the functions

$$D(S,T) = \frac{K_S(S,T)}{V_{\mathrm{p}}\rho_{\mathrm{w}}}, \qquad A(S,T) = \frac{Q_{\mathrm{c}}(t)}{4\pi H_{\mathrm{c}}} \cdot \frac{K_T'(S,T)}{K_S(S,T) \cdot \lambda(S)}. \tag{14.13}$$

The total moisture flux is given by the expression inside the curly brackets in (14.12) multiplied by $-2\pi H_{\mathrm{c}}$:

$$Q(r,t) = -2\pi H_{\mathrm{c}} \cdot D(S,T) \cdot \left[ r \cdot \frac{\partial S}{\partial r} - 2 \cdot A(S,T) \cdot (1-S) \right], \qquad r_{\mathrm{c}} \le r \le r_{\mathrm{r}}. \tag{14.14}$$

The flux is zero at the canister boundary, at the rock boundary in the dry-rock case, and throughout the annulus in steady state. The expression within the square brackets is then zero. We have:

$$\text{Zero moisture flux} \quad \Leftrightarrow \quad r \cdot \frac{\partial S}{\partial r} - 2 \cdot A(S,T) \cdot (1-S) = 0. \tag{14.15}$$

# Appendix 3. Transient solution for dry and wet rock

In this appendix, complete formulas for the solutions in Section 8 are presented. The full derivations for wet-rock solution are presented in Claesson (2003A). The dry-rock solution is not yet reported, but the solution is well tested in Mathcad, so it is certainly correct.

## A3.1. Dimensionless form of linearized equation

We seek the solution $S(r,t)$ of (8.5)-(8.7) for the rock boundary condition (8.8) in the dry-rock case and in the wet-rock case. The problem involves the parameters $S_{\text{in}}$, $a$, $r_{\text{c}}$ and $r_{\text{r}}$. In order to reduce the number of parameters as much as possible, we introduce dimensionless coordinates:

$$\tau = t/t_0, \qquad s = r/r_{\text{r}}, \qquad s_{\text{c}} \le s \le 1, \qquad s_{\text{c}} = r_{\text{c}}/r_{\text{r}}. \tag{15.1}$$

The time $t_0$ is chosen as, (8.10):

$$t_0 = \frac{4(r_{\text{r}} - r_{\text{c}})^2}{\pi^2 D_0}. \tag{15.2}$$

We also introduce a new function $\sigma(r/r_{\text{r}}, t/t_0)$ for the degree of saturation:

$$S(r,t) = S_{\text{in}} + (1 - S_{\text{in}}) \cdot \sigma(s,\tau), \qquad \sigma(s,\tau) = \frac{S(r,t) - S_{\text{in}}}{1 - S_{\text{in}}}. \tag{15.3}$$

The function $\sigma(r/r_{\text{r}}, t/t_0)$ is zero, when the saturation equals the initial level: $S = S_{\text{in}}$. The value is negative when the saturation is below the initial value: $S < S_{\text{in}}$, and it lies in the interval $0 < \sigma \le 1$ for $S_{\text{in}} < S \le 1$:

$$\sigma = 0 \;\Leftrightarrow\; S = S_{\text{in}}, \qquad \sigma < 0 \;\Leftrightarrow\; S < S_{\text{in}}, \qquad 0 < \sigma \le 1 \;\Leftrightarrow\; S_{\text{in}} < S \le 1. \tag{15.4}$$

The problem for $\sigma(s,\tau)$ becomes from (8.5)-(8.8) and (15.3):

$$f_{\text{r}}^2 \cdot \frac{\partial \sigma}{\partial \tau} = \frac{\partial^2 \sigma}{\partial s^2} + \frac{1 + 2a}{s} \cdot \frac{\partial \sigma}{\partial s}, \qquad s_{\text{c}} < s < 1. \tag{15.5}$$

$$\tau = 0, \quad (t = 0): \quad \sigma(s,0) = 0, \qquad s_{\text{c}} < s < 1. \tag{15.6}$$

$$s = s_{\text{c}}, \quad (r = r_{\text{c}}): \quad s_{\text{c}} \cdot \left.\frac{\partial \sigma}{\partial s}\right|_{s = s_{\text{c}}} = 2a\left[1 - \sigma(s_{\text{c}}, \tau)\right]. \tag{15.7}$$

$$s=1,\quad (r=r_{\mathrm{r}}):\quad \text{Dry-rock case}:\quad 1\cdot\left.\frac{\partial\sigma}{\partial s}\right|_{s=1}=2a\cdot\left[1-\sigma(1,\tau)\right],$$
$$\text{Wet-rock case}:\ \sigma(1,\tau)=1. \tag{15.8}$$

This problem is independent of the parameter $S_{\mathrm{in}}$. It has $a$ and the ratio $s_{\mathrm{c}}$ ($s_{\mathrm{c}}=0.6$ in our application) as parameters. The constants $s_{\mathrm{c}}$, $f_{\mathrm{r}}^2$, and $f_{\mathrm{r}}$ (using (15.2) ) are given by

$$s_{\mathrm{c}}=\frac{r_{\mathrm{c}}}{r_{\mathrm{r}}},\qquad f_{\mathrm{r}}^2=\frac{r_{\mathrm{r}}^2}{D_0 t_0},\qquad f_{\mathrm{r}}=\frac{\pi r_{\mathrm{r}}}{2(r_{\mathrm{r}}-r_{\mathrm{c}})}. \tag{15.9}$$

## A3.2. Solution for the wet-rock case

A full derivation of the solution in the wet-rock case is given in Claesson (2003A). The solution for $\sigma(s,\tau)$ has the form

$$\sigma(s,\tau)=1-s^{-a}\cdot\sum_{n=1}^{\infty}A_n\,u_n(s)\,e^{-\nu_n^2\cdot\tau}\ . \tag{15.10}$$

Here, $s=r/r_{\mathrm{r}}$ is the dimensionless radial coordinate, and $\tau=t/t_0$ the dimensionless time, (15.1). The steady-state solution after long time is

$$\sigma_{\mathrm{ss}}(s)=\sigma(s,\infty)=1. \tag{15.11}$$

The right-hand boundary value $\sigma=1$, (15.8), is imposed throughout the annulus in steady state.

The eigenvalues $\alpha_n=\nu_n\cdot f_{\mathrm{r}}$ are obtained from the equation

$$J_a(f_{\mathrm{r}}\nu_n)\cdot Y_{a-1}(f_{\mathrm{c}}\nu_n)-Y_a(f_{\mathrm{r}}\nu_n)\cdot J_{a-1}(f_{\mathrm{c}}\nu_n)=0,\qquad 0<\nu_1<\nu_2<\ldots. \tag{15.12}$$

Here, we use the notations

$$\alpha_n=\nu_n\cdot f_{\mathrm{r}},\qquad \alpha_n'=\alpha_n\cdot\frac{r_{\mathrm{c}}}{r_{\mathrm{r}}}=\nu_n\cdot f_{\mathrm{c}},\qquad f_{\mathrm{c}}=\frac{\pi r_{\mathrm{c}}}{2(r_{\mathrm{r}}-r_{\mathrm{c}})}. \tag{15.13}$$

Then values $\nu_n$ become roughly equal to 1, 3, 5, etc, :

$$\nu_1\sim 1,\qquad \nu_2\approx 3,\qquad \nu_3\approx 5,\qquad \ldots. \tag{15.14}$$

This is the reason to choose $t_0$ according to (15.2).

The eigenfunctions $u_n(s)$ are given by

$$u_n(s)=\frac{J_a(\alpha_n s)}{J_a(\alpha_n)}-\frac{Y_a(\alpha_n s)}{Y_a(\alpha_n)},\qquad s_{\mathrm{c}}\le s\le 1. \tag{15.15}$$

The coefficients $A_n$ are given by

$$A_n = \pi \cdot \frac{\mathrm{J}_a(\alpha_n)\,\mathrm{Y}_{a-1}(\alpha'_n)}{B_n^2 - 1} \cdot \left[ B_n - \frac{2a}{\alpha_n} \cdot s_\mathrm{c}^{\,a-1} \right], \qquad B_n = \frac{\mathrm{J}_{a-1}(\alpha'_n)}{\mathrm{J}_a(\alpha_n)}. \tag{15.16}$$

## A3.3. Steady-state solution for the dry-rock case

In the dry-rock case, we first determine the steady-state solution. The equation for the steady-state solution $S(r)$ becomes from (8.4):

$$\frac{d}{dr}\left[ r \cdot \frac{dS}{dr} - 2a \cdot (1 - S) \right] = 0, \qquad r_\mathrm{c} \le r \le r_\mathrm{r}. \tag{15.17}$$

This means that the expression within the brackets (essentially the moisture flux) is constant over the interval in *r*. The value is zero at both boundaries according to (8.7) and (8.8), which means that the moisture flux is zero for all *r* in accordance with (7.12). The total moisture content in steady state must be equal to the initial amount. We have to solve

$$r \cdot \frac{dS}{dr} + 2aS = 2a, \qquad r_\mathrm{r} \le r \le r_\mathrm{c}; \qquad \int_{r_c}^{r_r} r \cdot S(r)\, dr = \int_{r_c}^{r_r} r \cdot S_\mathrm{in}\, dr. \tag{15.18}$$

With the transformation (15.3)

$$S(r) = S_\mathrm{in} + (1 - S_\mathrm{in}) \cdot \sigma(s), \qquad s = r / r_\mathrm{r}, \tag{15.19}$$

we get rid of the initial degree of saturation as parameter. The problem (15.18) becomes

$$s \cdot \frac{d\sigma}{ds} + 2a \cdot \sigma = 2a, \qquad s_\mathrm{c} = r_\mathrm{c} / r_\mathrm{r} \le s \le 1; \qquad \int_{s_c}^{1} s \cdot \sigma(s)\, ds = 0. \tag{15.20}$$

The general solution is of the differential equation is

$$\sigma(s) = 1 + F \cdot s^{-2a} \tag{15.21}$$

The condition of zero integral determines the constant *F*. We get the steady-state solution $\sigma(s) = \sigma_\mathrm{ss}(s)$ in the dry-rock case:

$$\sigma_\mathrm{ss}(s) = \begin{cases} 1 - \dfrac{1 - s_\mathrm{c}^2}{1 - s_\mathrm{c}^{2-2a}} \cdot \dfrac{1 - a}{s^{2a}}, & a \ne 1 \\ 1 - \dfrac{1 - s_\mathrm{c}^2}{2 \cdot \ln\left(1 / s_\mathrm{c}\right)} \cdot \dfrac{1}{s^2}, & a = 1 \end{cases} \tag{15.22}$$

The largest wetting $\sigma_\mathrm{ss}(1)$ occurs at the rock boundary. We are in particular interested in the largest drying, which occurs at the warm canister boundary. We have for $s = s_\mathrm{c}$ from (15.22):

$$\sigma_{\rm ss}(s_{\rm c}) = \begin{cases} 1 - \dfrac{1-s_{\rm c}^2}{s_{\rm c}^{2a}-s_{\rm c}^2}\cdot(1-a), & a \neq 1 \\ 1 - \dfrac{1-s_{\rm c}^2}{2s_{\rm c}^2\cdot\ln\left(1/s_{\rm c}\right)}, & a = 1 \end{cases} \tag{15.23}$$

The corresponding degree of saturation is from (15.23) and (15.19)

$$S_{\rm ss}(s_{\rm c}) = \begin{cases} 1-(1-S_{\rm in})\cdot\dfrac{1-s_{\rm c}^2}{s_{\rm c}^{2a}-s_{\rm c}^2}\cdot(1-a), & a \neq 1 \\ 1-(1-S_{\rm in})\cdot\dfrac{1-s_{\rm c}^2}{2s_{\rm c}^2\cdot\ln\left(1/s_{\rm c}\right)}, & a = 1 \end{cases} \tag{15.24}$$

## A3.4. Solution for the dry-rock case

The solution $\sigma(r,t)$ has in the dry-rock case the form

$$\sigma(s,\tau) = \sigma_{\rm ss}(s) - s^{-a}\cdot\sum_{n=1}^{\infty} A_n\, u_n(s)\; e^{-\nu_n^2\cdot\tau}\,. \tag{15.25}$$

Here, $\sigma_{\rm ss}(s) = \sigma(s,\infty)$ is the steady-state solution (15.22).

The equation for the eigenvalues $\alpha_n = \nu_n\cdot f_{\rm r}$ is in the dry-rock case

$$J_{a-1}(f_{\rm r}\nu_n)\cdot Y_{a-1}(f_{\rm c}\nu_n) - Y_{a-1}(f_{\rm r}\nu_n)\cdot J_{a-1}(f_{\rm c}\nu_n) = 0, \qquad 0<\nu_1<\nu_2<\ldots\,. \tag{15.26}$$

Here, we use the notations in (15.13) and (15.9). The values $\nu_n$ become in the dry-rock case roughly equal to 2, 4, 6, etc, :

$$\nu_1 \approx 2, \qquad \nu_2 \approx 4, \qquad \nu_3 \approx 6, \qquad \ldots\,. \tag{15.27}$$

This is again the reason to choose $t_0$ according to (15.2).

The eigenfunctions $u_n(s)$ are given by

$$u_n(s) = \frac{J_a(\alpha_n s)}{J_{a-1}(\alpha_n)} - \frac{Y_a(\alpha_n s)}{Y_{a-1}(\alpha_n)}, \qquad s_{\rm c} \le s \le 1. \tag{15.28}$$

The coefficients $A_n$ are given by

$$A_n = \frac{2\pi a}{\alpha_n}\cdot\frac{B_n - s_{\rm c}^{\rm a-1}}{B_n^2-1}\cdot Y_{a-1}(\alpha_n)J_{a-1}(\alpha_n'), \qquad B_n = \frac{\mathrm{J}_{a-1}(\alpha_n')}{\mathrm{J}_{a-1}(\alpha_n)}. \tag{15.29}$$

## Appendix 4. Steady-state solution of coupled nonlinear equations for water saturation S(r) and temperature T(r), $r_c<r<r_r$.

Claesson

**Canister data:**

$Q_c := 1000$ $H_c := 6$ $r_c := 0.525$ $r_r := 0.875$

**Formulas and data for water and water vapor:**

SI units

$$Exp(T) := \frac{19.625 \cdot T}{270.1 + T} - \frac{0.00463 \cdot T^2}{142.15 + T} \qquad p_{sat}(T) := 610.8 \cdot e^{Exp(T)}$$

Saturation water vapor pressure $p_{sat}(T)$

$$L_{ev}(T) := 10^6 \cdot \left[ 2.5016 - \frac{T}{422} - \left( \frac{T}{342} \right)^4 \right]$$

Latent heat of evaporation $L_{ev}(T)$

$$R_w := \frac{8.314}{0.018} \qquad \rho_w := 997 \qquad \rho_{vsat}(T) := \frac{p_{sat}(T)}{R_w \cdot (T + 273.15)}$$

Saturation vapor density $\rho_{v,sat}(T)$

$$h_{liq}(T) := 4186 \cdot T \qquad h_v(T) := L_{ev}(T) + h_{liq}(T)$$

Enthalpy

$$\eta(T) := 1.75 \cdot 10^{-3} \cdot \left( \frac{0.629}{1 + \frac{T}{29.5}} + 0.371 \cdot e^{\frac{-T}{31.8}} \right)$$

Dynamic viscosity

$$\rho_v(P,T) := e^{\frac{P}{R_w \cdot (T+273.15) \cdot \rho_w}} \cdot \rho_{vsat}(T)$$

Vapor density $\rho_v(P,T)$, from Kelvin's relation.

$$\rho_{vP}(P,T) := \frac{\rho_v(P,T)}{R_w \cdot (T + 273.15) \cdot \rho_w}$$

Derivative of $\rho_v(P,T)$ with respect to P .

$$\rho_{vT}(P,T) := \frac{d}{dT}\left(\rho_v(P,T)\right)$$

Derivative of $\rho_v(P,T)$ with respect to T .

**Data and formulas for bentonite, reference case:**

Water retention curve P(S) and its derivative:

$$f(S) := 17.82 - 3.204 \cdot S + (1.621 \cdot S - 1.28) \cdot \mathrm{erf}[14.4 \cdot (S - 0.568)] \qquad P(S) := -e^{f(S)} + e^{f(1)}$$

$$\mathrm{derP}(S) := (-1) \cdot e^{f(S)} \cdot \left[ -3.204 + 1.621 \cdot \mathrm{erf}[14.4 \cdot (S - 0.568)] + (1.621 \cdot S - 1.28) \cdot 14.4 \cdot \frac{2}{\sqrt{\pi}} \cdot e^{-14.4^2 \cdot (S - 0.568)^2} \right]$$

Functions for vapor and liqiud flow coefficients:

$$D_v(S) := 2 \cdot 10^{-6} \cdot (1 - S) \qquad k_{sat} := 1.6 \cdot 10^{-20} \qquad k(S) := k_{sat} \cdot S^3$$

Thermal conductivity: $\lambda(S) := 0.6 + 0.6 \cdot S$

**Flow coefficient functions:**

Eqs. 6.9, 6.10: $K_S(S,T) := \left( \frac{\rho_w \cdot k(S)}{\eta(T)} + D_v(S) \cdot \rho_{vP}(P(S),T) \right) \cdot \mathrm{derP}(S) \qquad K_T(S,T) := D_v(S) \cdot \rho_{vT}(P(S),T)$

Eq. 14.6 $\lambda_S(S,T) := \left( h_{liq}(T) \cdot \frac{\rho_w \cdot k(S)}{\eta(T)} + h_v(T) \cdot D_v(S) \cdot \rho_{vP}(P(S),T) \right) \cdot \mathrm{derP}(S)$

Eq. 14.7 $\lambda_T(S,T) := \lambda(S) + h_v(T) \cdot D_v(S) \cdot \rho_{vT}(P(S),T)$

Eq. 7.2 $\mathrm{Det}(S,T) := K_T(S,T) \cdot \lambda_S(S,T) - K_S(S,T) \cdot \lambda_T(S,T)$

**Input and solution of differential equations starting at the outer boundary:**

Eq. 7.2

$$q := \frac{Q_c}{2\pi \cdot H_c}$$

$$D(r1, ST) := \begin{pmatrix} \frac{q}{r_r - r1} \cdot \frac{K_T(ST_0, ST_1)}{\mathrm{Det}(ST_0, ST_1)} \\ \frac{q}{r_r - r1} \cdot \frac{K_S(ST_0, ST_1)}{\mathrm{Det}(ST_0, ST_1)} \end{pmatrix}$$

( =dS/dr, $ST_0$=S )

( =dT/dr; $ST_1$=T )

Note: r=r.r - r1

( 0<r1<r.r -r.c )

Reference case: $S_r := 0.95 \qquad T_r := 70$

Eq. 7.3

(Initial values)

$$ST := \begin{pmatrix} S_r \\ T_r \end{pmatrix} \qquad I := 100 \qquad Out := rkfixed(ST, 0, r_r - r_c, I, D)$$

$$r := r_r - Out^{\langle 0 \rangle} \qquad S := Out^{\langle 1 \rangle} \qquad T := Out^{\langle 2 \rangle} \qquad i := 0..I$$

Figure 7.1, left

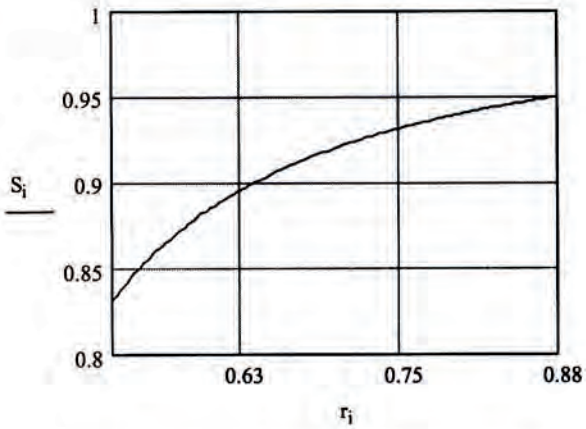


$S_0 = 0.95$

$S_I = 0.83$

Figure 7.1, right

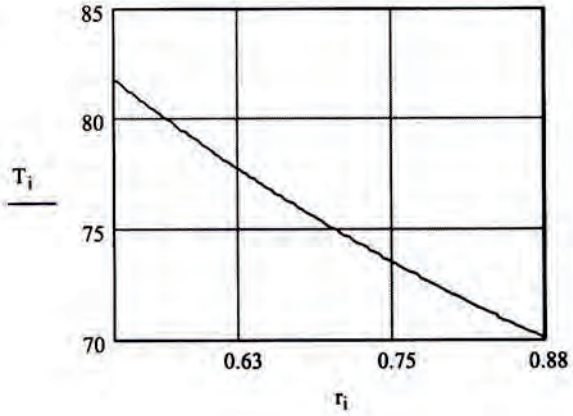


$T_0 = 70$

$T_I = 81.8$

Figure 7.2

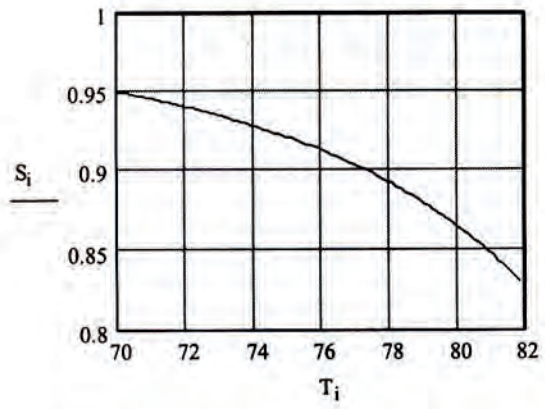


$T_I - T_0 = 11.8$

**Control of original equations for vapor and liquid flow**

$i := 1..I-1$

$$Gv_i := -2\cdot\pi\cdot H_c\cdot r_i\cdot D_v\left(S_i\right)\cdot\frac{\rho_v\left(P\left(S_{i+1}\right),T_{i+1}\right)-\rho_v\left(P\left(S_{i-1}\right),T_{i-1}\right)}{r_{i+1}-r_{i-1}}$$

Eqs. 6.1 and 6.5

$$Gliq_i := -2\cdot\pi\cdot H_c\cdot r_i\cdot\frac{\rho_w\cdot k\left(S_i\right)}{\eta\left(T_i\right)}\cdot\frac{P\left(S_{i+1}\right)-P\left(S_{i-1}\right)}{r_{i+1}-r_{i-1}}$$

$G_i := Gliq_i + Gv_i$

$Gliq_{I-1} = -3.34\times 10^{-6}$ $Gv_{I-1} = 3.34\times 10^{-6}$ $Gvap_i := Gv_i$

Figure 7.3

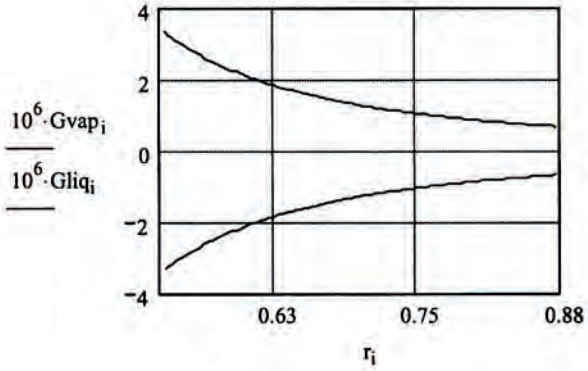


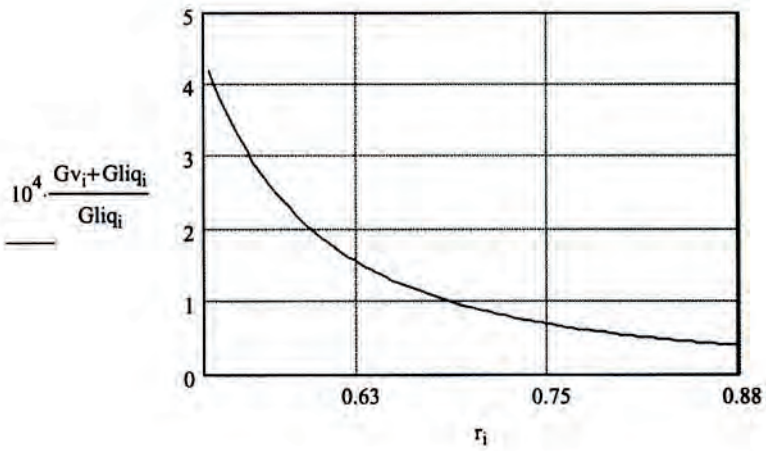


Error of the order $10^{-4}$.

**Control of original heat flow equation**

Eqs. 6.1-3 $Qcond_i := -2\cdot\pi\cdot H_c\cdot r_i\cdot\lambda\left(S_i\right)\cdot\frac{T_{i+1}-T_{i-1}}{r_{i+1}-r_{i-1}}$ $Qconv_i := h_{liq}\left(T_i\right)\cdot Gliq_i + h_v\left(T_i\right)\cdot Gv_i$

$Q_i := Qcond_i + Qconv_i$

$Q_1 = 1\times 10^3$ $Q_{50} = 1\times 10^3$ $Q_{l-1} = 1\times 10^3$ $Q_c = 1000$

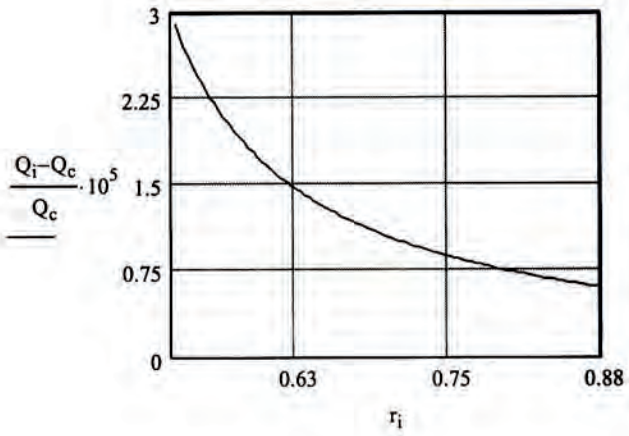


Error of the order $10^{-5}$.

**Ratio between convective and conductive heat flow**

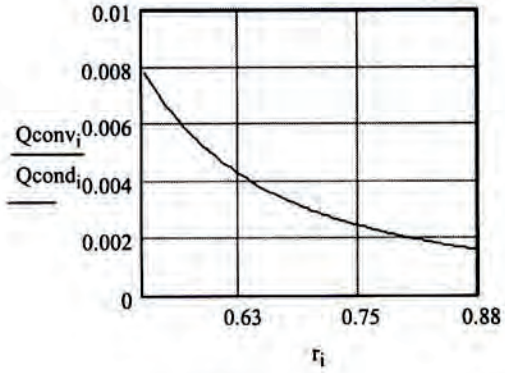


Ratio between 0.008 and 0.002.

## Appendix 5. Steady-state solution of coupled nonlinear equations to give $S(T;S_0)$ for $T>T_0$, $S(T_0;S_0)=S_0$.

**Formulas and data for water and water vapor:**

SI units

$$Exp(T) := \frac{19.625 \cdot T}{270.1 + T} - \frac{0.00463 \cdot T^2}{142.15 + T} \qquad p_{sat}(T) := 610.8 \cdot e^{Exp(T)}$$

Saturation water vapor pressure $p_{sat}(T)$

$$L_{ev}(T) := 10^6 \cdot \left[ 2.5016 - \frac{T}{422} - \left( \frac{T}{342} \right)^4 \right]$$

Latent heat of evaporation $L_{ev}(T)$

$$R_w := \frac{8.314}{0.018} \qquad \rho_w := 997 \qquad \rho_{vsat}(T) := \frac{p_{sat}(T)}{R_w \cdot (T + 273.15)}$$

Saturation vapor density $\rho_{v,sat}(T)$

$$h_{liq}(T) := 4186 \cdot T \qquad h_v(T) := L_{ev}(T) + h_{liq}(T)$$

Enthalpy

$$\eta(T) := 1.75 \cdot 10^{-3} \cdot \left( \frac{0.629}{1 + \frac{T}{29.5}} + 0.371 \cdot e^{\frac{-T}{31.8}} \right)$$

Dynamic viscosity

$$\rho_v(P,T) := e^{\frac{P}{R_w \cdot (T+273.15) \cdot \rho_w}} \cdot \rho_{vsat}(T)$$

Vapor density $\rho_v(P,T)$, from Kelvin's relation.

$$\rho_{vP}(P,T) := \frac{\rho_v(P,T)}{R_w \cdot (T + 273.15) \cdot \rho_w}$$

Derivative of $\rho_v(P,T)$ with respect to P.

$$\rho_{vT}(P,T) := \frac{d}{dT}\left(\rho_v(P,T)\right)$$

Derivative of $\rho_v(P,T)$ with respect to T.

**Data and formulas for bentonite, reference case:**

Water retention curve P(S) and its derivative:

$$f(S) := 17.82 - 3.204 \cdot S + (1.621 \cdot S - 1.28) \cdot \mathrm{erf}[14.4 \cdot (S - 0.568)] \qquad P(S) := -e^{f(S)} + e^{f(1)}$$

$$\mathrm{derP}(S) := (-1) \cdot e^{f(S)} \cdot \left[ -3.204 + 1.621 \cdot \mathrm{erf}[14.4 \cdot (S - 0.568)] + (1.621 \cdot S - 1.28) \cdot 14.4 \cdot \frac{2}{\sqrt{\pi}} \cdot e^{-14.4^2 \cdot (S - 0.568)^2} \right]$$

Functions for vapor and liqiud flow coefficients:

$$D_v(S) := 2 \cdot 10^{-6} \cdot (1 - S) \qquad k_{sat} := 1.6 \cdot 10^{-20} \qquad k(S) := k_{sat} \cdot S^3$$

Thermal conductivity: $\lambda(S) := 0.6 + 0.6 \cdot S$

**Flow coefficient functions:**

Eq. 6.9 $$K_S(S, T) := \left( \frac{\rho_w \cdot k(S)}{\eta(T)} + D_v(S) \cdot \rho_{vP}(P(S), T) \right) \cdot \mathrm{derP}(S)$$

Eq. 6.10 $$K_T(S, T) := D_v(S) \cdot \rho_{vT}(P(S), T)$$

**Input and solution of differential equations starting at the outer boundary:**

Eq. 7.5 $$D(T, S) := \frac{K_T(S_0, T)}{K_S(S_0, T)}$$ ( =dS/dT; S.0=S ) $I := 200$

| | | | |
|---|---|---|---|
| $S_0 := 0.999$ | $\mathrm{Out} := \mathrm{rkfixed}(S, 20, 100, I, D)$ | $S1 := \mathrm{Out}^{\langle 1 \rangle}$ | $T := \mathrm{Out}^{\langle 0 \rangle}$ |
| $S_0 := 0.995$ | $\mathrm{Out} := \mathrm{rkfixed}(S, 20, 100, I, D)$ | $S2 := \mathrm{Out}^{\langle 1 \rangle}$ | |
| $S_0 := 0.99$ | $\mathrm{Out} := \mathrm{rkfixed}(S, 20, 100, I, D)$ | $S3 := \mathrm{Out}^{\langle 1 \rangle}$ | |
| $S_0 := 0.98$ | $\mathrm{Out} := \mathrm{rkfixed}(S, 20, 100, I, D)$ | $S4 := \mathrm{Out}^{\langle 1 \rangle}$ | |
| $S_0 := 0.95$ | $\mathrm{Out} := \mathrm{rkfixed}(S, 20, 100, I, D)$ | $S5 := \mathrm{Out}^{\langle 1 \rangle}$ | |

$S_0 := 0.9$ Out := rkfixed(S, 20, 100, I, D) S6 := $Out^{\langle 1 \rangle}$

$S_0 := 0.85$ Out := rkfixed(S, 20, 100, I, D) S7 := $Out^{\langle 1 \rangle}$

$S_0 := 0.8$ Out := rkfixed(S, 20, 100, I, D) S8 := $Out^{\langle 1 \rangle}$

$S_0 := 0.7$ Out := rkfixed(S, 20, 100, I, D) S9 := $Out^{\langle 1 \rangle}$

$S_0 := 0.6$ Out := rkfixed(S, 20, 100, I, D) S10 := $Out^{\langle 1 \rangle}$

$S_0 := 0.5$ Out := rkfixed(S, 20, 100, I, D) S11 := $Out^{\langle 1 \rangle}$

$S_0 := 0.4$ Out := rkfixed(S, 20, 100, I, D) S12 := $Out^{\langle 1 \rangle}$

$i := 0..I$

**S=S(T) for 20<T<100 for different initial S(20). Reference data.**

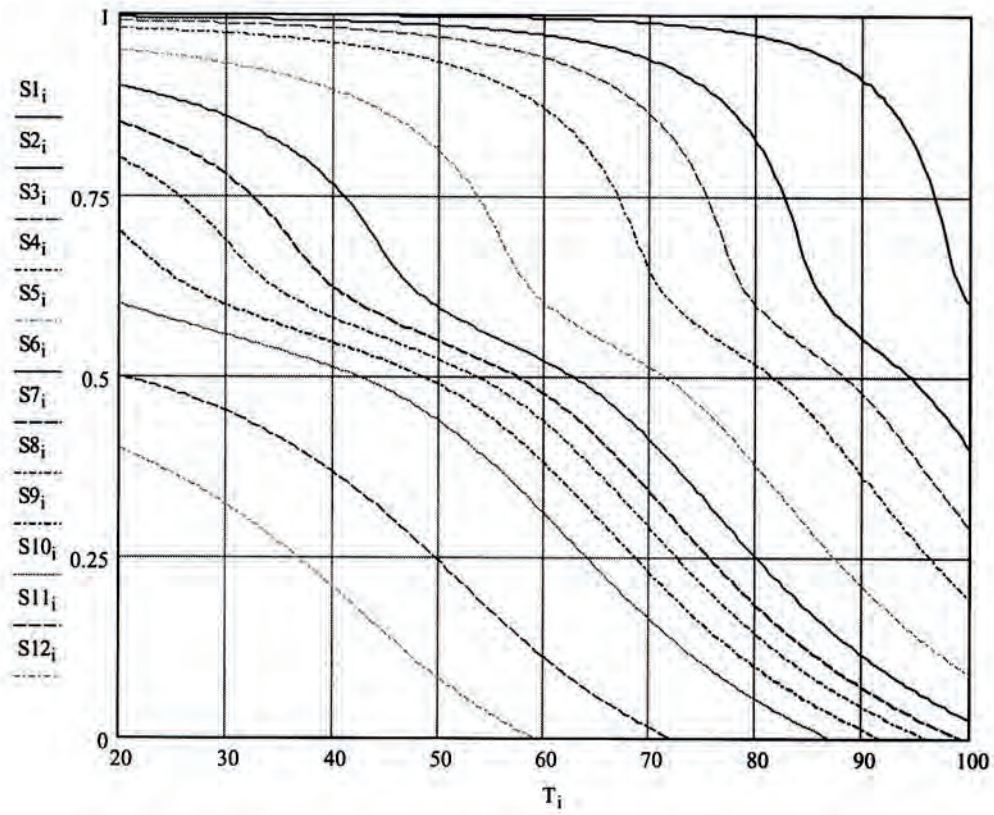


S(20)=0.999 (S1), 0.995, 0.99, 0.98, 0.95, ..., 0.4 (S12).

## Appendix 6. Calculation of thermal diffusivity D, basic time scale $t_{0y}$ and thermodiffusive parameter A as functions of S and T.

Claesson

**Canister data:**

$Q_c := 1000$ $H_c := 6$ $r_c := 0.525$ $r_r := 0.875$

**Formulas and data for water and water vapor:**

SI units

$$Exp(T) := \frac{19.625 \cdot T}{270.1 + T} - \frac{0.00463 \cdot T^2}{142.15 + T} \qquad p_{sat}(T) := 610.8 \cdot e^{Exp(T)}$$

Saturation water vapor pressure $p_{sat}(T)$

$$L_{ev}(T) := 10^6 \cdot \left[ 2.5016 - \frac{T}{422} - \left( \frac{T}{342} \right)^4 \right]$$

Latent heat of evaporation $L_{ev}(T)$

$$R_w := \frac{8.314}{0.018} \qquad \rho_w := 997 \qquad \rho_{vsat}(T) := \frac{p_{sat}(T)}{R_w \cdot (T + 273.15)}$$

Saturation vapor density $\rho_{v,sat}(T)$

$$h_{liq}(T) := 4186 \cdot T \qquad h_v(T) := L_{ev}(T) + h_{liq}(T)$$

Enthalpy

$$\eta(T) := 1.75 \cdot 10^{-3} \cdot \left( \frac{0.629}{1 + \frac{T}{29.5}} + 0.371 \cdot e^{\frac{-T}{31.8}} \right)$$

Dynamic viscosity

$$\rho_v(P,T) := e^{\frac{P}{R_w \cdot (T+273.15) \cdot \rho_w}} \cdot \rho_{vsat}(T)$$

Vapor density $\rho_v(P,T)$, from Kelvin's relation.

$$\rho_{vP}(P,T) := \frac{\rho_v(P,T)}{R_w \cdot (T + 273.15) \cdot \rho_w}$$

Derivative of $\rho_v(P,T)$ with respect to P .

$$\rho_{vT}(P,T) := \frac{d}{dT}\left(\rho_v(P,T)\right)$$

Derivative of $\rho_v(P,T)$ with respect to T .

**Data and formulas for bentonite, reference case:**

Water retention curve P(S) and its derivative:

$$f(S) := 17.82 - 3.204 \cdot S + (1.621 \cdot S - 1.28) \cdot \mathrm{erf}[14.4 \cdot (S - 0.568)] \qquad P(S) := -e^{f(S)} + e^{f(1)}$$

$$\mathrm{derP}(S) := (-1) \cdot e^{f(S)} \cdot \left[ -3.204 + 1.621 \cdot \mathrm{erf}[14.4 \cdot (S - 0.568)] + (1.621 \cdot S - 1.28) \cdot 14.4 \cdot \frac{2}{\sqrt{\pi}} \cdot e^{-14.4^2 \cdot (S - 0.568)^2} \right]$$

Functions for vapor and liqiud flow coefficients:

$$D_v(S) := 2 \cdot 10^{-6} \cdot (1 - S) \qquad k_{sat} := 1.6 \cdot 10^{-20} \qquad k(S) := k_{sat} \cdot S^3$$

Thermal conductivity: $\lambda(S) := 0.6 + 0.6 \cdot S$ Porosity: $V_p := 0.389$

**Flow coefficient functions:**

Eqs. 6.9-10: $$K_S(S,T) := \left( \frac{\rho_w \cdot k(S)}{\eta(T)} + D_v(S) \cdot \rho_{vP}(P(S),T) \right) \cdot \mathrm{derP}(S) \qquad \mathrm{Kprim}_T(S,T) := D_v(0) \cdot \rho_{vT}(P(S),T)$$

Eqs. 6.21, 8.17

$$\mathrm{Dexp10}(S,T) := \frac{K_S(S,T)}{V_p \cdot \rho_w} \cdot 10^{10} \qquad A(S,T) := \frac{Q_c}{4 \cdot \pi \cdot H_c} \cdot \frac{\mathrm{Kprim}_T(S,T)}{K_S(S,T) \cdot \lambda(S)} \qquad t_{0y}(S,T) := \frac{4 \cdot (r_r - r_c)^2 \cdot V_p \cdot \rho_w}{\pi^2 \cdot K_S(S,T) \cdot 3600 \cdot 24 \cdot 365}$$

**Diagrams:**

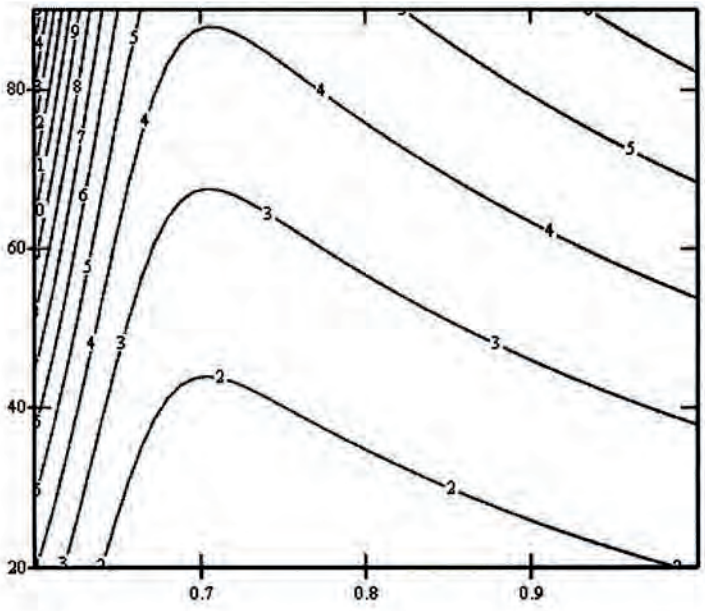


Dexp10

Fig. 8.1

Fig. 8.2

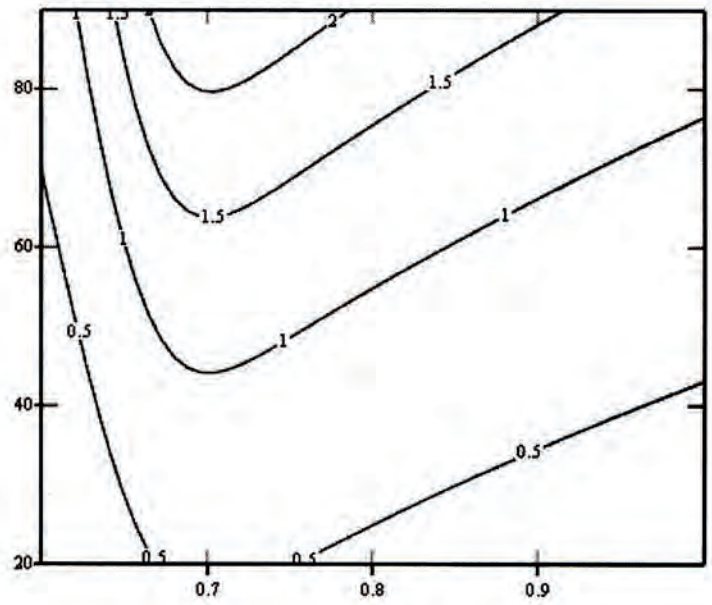


A

Fig.8.7

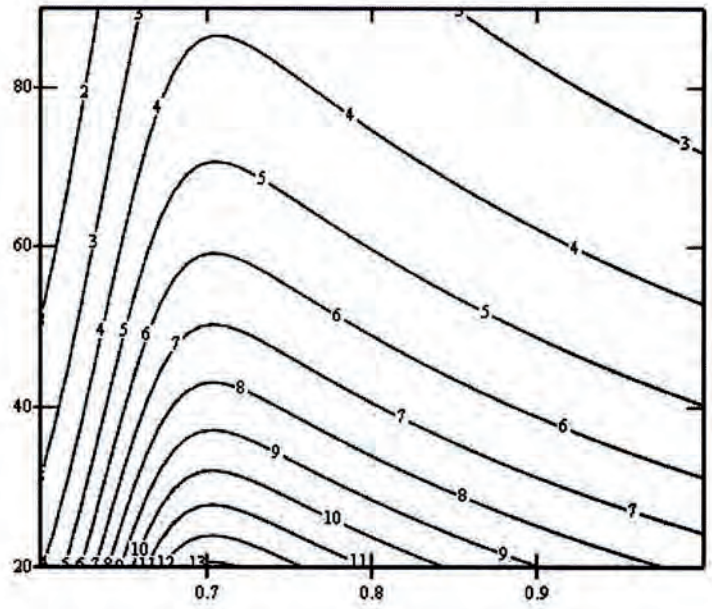


$t_{0y}$

## Appendix 7. Core formulas for $\sigma(s,\tau)$ in the dry-rock case. The solution $S(r,\tau)$. Figure for $S(r,t)$ in reference case.

J. Claesson

Input data

$r_c := 0.525 \qquad r_r := 0.875 \qquad N := 30 \qquad a := 0.9$

**Core formulas for $\sigma(r,\tau)$:**

Bessel functions:
$$Ja(x,a) := \frac{1}{\pi}\cdot\int_0^{\pi}\cos(x\cdot\sin(s)-a\cdot s)\,ds - \frac{\sin(a\cdot\pi)}{\pi}\cdot\int_0^{10} e^{-x\cdot\sinh(s)-a\cdot s}\,ds$$

$$Ya(x,a) := \frac{1}{\pi}\cdot\int_0^{\pi}\sin(x\cdot\sin(s)-a\cdot s)\,ds - \frac{1}{\pi}\cdot\int_0^{10}\left(e^{-x\cdot\sinh(s)+a\cdot s}+\cos(a\cdot\pi)\cdot e^{-x\cdot\sinh(s)-a\cdot s}\right)ds$$

Eigenfunctions:
$$f_r := \frac{\pi\cdot r_r}{2(r_r-r_c)} \qquad f_c := \frac{\pi\cdot r_c}{2(r_r-r_c)} \qquad u(s,\nu,a) := \frac{Ja(\nu\cdot f_r\cdot s,a)}{Ja(\nu\cdot f_r,a-1)} - \frac{Ya(\nu\cdot f_r\cdot s,a)}{Ya(\nu\cdot f_r,a-1)}$$

Eigenvalue equation:
$$eig(\nu,a) := Ja(\nu\cdot f_r,a-1)\cdot Ya(\nu\cdot f_c,a-1) - Ya(\nu\cdot f_r,a-1)\cdot Ja(\nu\cdot f_c,a-1)$$

First N eigenvalues:
$$vvec := \left|\begin{array}{l}\text{for } n\in 1..N\\ \quad var\leftarrow n\cdot 2\\ \quad vvec_n\leftarrow root(eig(var,a),var)\\ vvec\end{array}\right.$$

$$\alpha := vvec\cdot f_r \qquad \alpha' := vvec\cdot f_c \qquad s_c := \frac{r_c}{r_r}$$

Fourier coefficients:
$$i := 1..N \qquad B_i := \frac{Ja(\alpha'_i,a-1)}{Ja(\alpha_i,a-1)} \qquad A_i := \frac{2\cdot\pi\cdot a}{\alpha_i}\cdot Ya(\alpha_i,a-1)\cdot Ja(\alpha'_i,a-1)\cdot\frac{B_i-\left(\frac{r_c}{r_r}\right)^{a-1}}{(B_i)^2-1}$$

Steady-state solution:
$$\sigma_{ss}(s,a) := \left|\begin{array}{ll}1-\dfrac{1-s_c^{\,2}}{1-s_c^{\,2-2\cdot a}}\cdot\dfrac{1-a}{s^{2\cdot a}} & \text{if } a\neq 1\\ 1-\dfrac{1-s_c^{\,2}}{2\cdot\ln\left(\frac{1}{s_c}\right)}\cdot\dfrac{1}{s^{2\cdot a}} & \text{if } a=1\end{array}\right.$$

Solution σ(s,τ):

$$\sigma(s,\tau) := \left| \begin{array}{l} N\tau \leftarrow \operatorname{ceil}\left(\frac{2}{\sqrt{\tau + 0.001}} + \frac{1}{2}\right) \\ Nm \leftarrow \text{if}(N\tau < N, N\tau, N) \\ \sigma_{ss}(s,a) - s^{-a} \cdot \sum_{n=1}^{Nm} A_n \cdot u(s, vvec_n, a) \cdot e^{-(vvec_n)^2 \cdot \tau} \end{array} \right.$$

(End of core formulas)

Solution S(r,t):

$$S_{in} := 0.85 \qquad D_0 := \frac{4 \cdot (r_r - r_c)^2}{\pi^2} \qquad t_0 := \frac{4 \cdot (r_r - r_c)^2}{\pi^2 \cdot D_0} \qquad t_0 = 1$$

( We choose t.0=1, i.e. t=τ: )

$$S(r,t) := S_{in} + (1 - S_{in}) \cdot \sigma\left(\frac{r}{r_r}, \frac{t}{t_0}\right) \qquad S_{ss}(r) := S_{in} + (1 - S_{in}) \cdot \sigma_{ss}\left(\frac{r}{r_r}, a\right)$$

S(r,t) for the reference case:

$$I := 200 \qquad i := 1..I + 1 \qquad rl_i := r_c + \frac{i-1}{I} \cdot (r_r - r_c) \qquad sl_i := \frac{rl_i}{r_r}$$

(Calculation for I points)

**Figure 8.3**

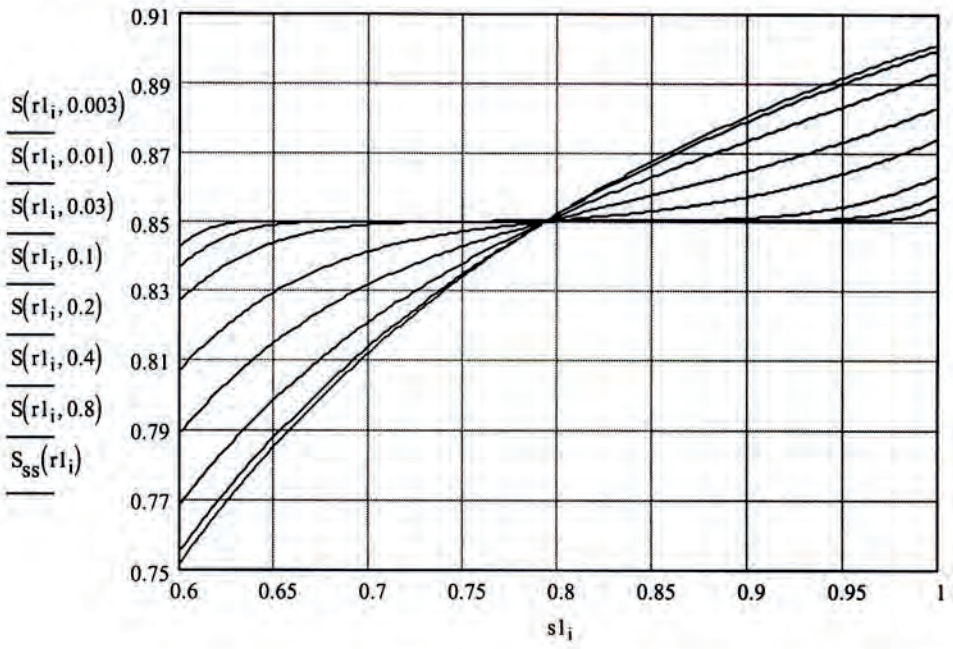

Calculation of S(r.c,t) in the reference case

$Il := 500 \qquad il := 2..Il + 1 \qquad \tau l_{il} := \frac{il - 1}{Il} \qquad \tau l_1 := 0$

$il := 1..Il + 1$

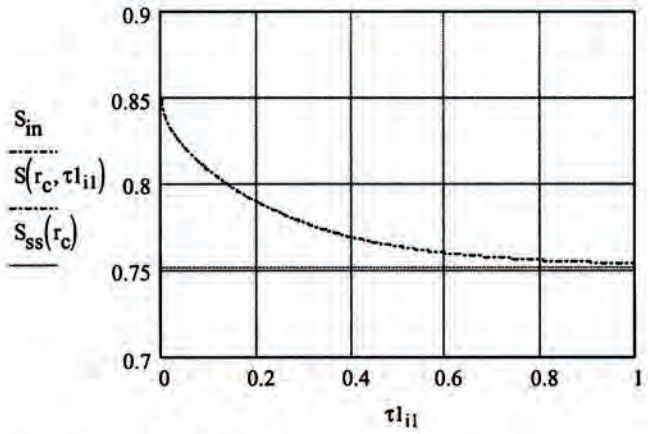


$S_{ss}(r_c) = 0.752$

**Figure 8.4**

## Appendix 8. Core formulas for $\sigma(s,\tau)$ in the wet-rock case. The solution $S(r,\tau)$. Figure for $S(r,\tau)$ in reference case.

J. Claesson

Input data

$r_c := 0.525 \qquad r_r := 0.875 \qquad N := 50 \quad a := 0.9$

**Core formulas for $\sigma(r,\tau)$:**

Bessel functions:

$$Ja(x,a) := \frac{1}{\pi}\cdot\int_0^{\pi}\cos(x\cdot\sin(s)-a\cdot s)\,ds - \frac{\sin(a\cdot\pi)}{\pi}\cdot\int_0^{10} e^{-x\cdot\sinh(s)-a\cdot s}\,ds$$

$$Ya(x,a) := \frac{1}{\pi}\cdot\int_0^{\pi}\sin(x\cdot\sin(s)-a\cdot s)\,ds - \frac{1}{\pi}\cdot\int_0^{10}\left(e^{-x\cdot\sinh(s)+a\cdot s}+\cos(a\cdot\pi)\cdot e^{-x\cdot\sinh(s)-a\cdot s}\right)ds$$

Eigenfunctions:

$$f_r := \frac{\pi\cdot r_r}{2(r_r-r_c)} \qquad f_c := \frac{\pi\cdot r_c}{2(r_r-r_c)} \qquad u(s,\nu,a) := \frac{Ja(\nu\cdot f_r\cdot s,a)}{Ja(\nu\cdot f_r,a)} - \frac{Ya(\nu\cdot f_r\cdot s,a)}{Ya(\nu\cdot f_r,a)}$$

Eigenvalue equation:

$$eig(\nu,a) := Ja(\nu\cdot f_r,a)\cdot Ya(\nu\cdot f_c,a-1) - Ya(\nu\cdot f_r,a)\cdot Ja(\nu\cdot f_c,a-1)$$

First N eigenvalues:

$$vvec := \left|\begin{array}{l}\text{for } n\in 1..N\\ \quad var \leftarrow 2\cdot n-1\\ \quad vvec_n \leftarrow root(eig(var,a),var)\\ vvec\end{array}\right.$$

$$\alpha := vvec\cdot f_r \qquad \alpha' := vvec\cdot f_c$$

$$s_c := \frac{r_c}{r_r}$$

Fourier coefficients:

$$n := 1..N \qquad B_n := \frac{Ja(\alpha'_n,a-1)}{Ja(\alpha_n,a)} \qquad A_n := \pi\cdot\frac{Ja(\alpha_n,a)\cdot Ya(\alpha'_n,a-1)}{(B_n)^2-1}\cdot\left(B_n - \frac{2\cdot a}{\alpha_n}\cdot s_c^{\,a-1}\right)$$

Solution $\sigma(s,\tau)$:

$$\sigma(s,\tau) := \left|\begin{array}{l}N\tau \leftarrow ceil\left(\frac{2}{\sqrt{\tau+0.001}}+\frac{1}{2}\right)\\ Nm \leftarrow if(N\tau < N, N\tau, N)\\ 1 - s^{-a}\cdot\sum_{n=1}^{Nm} A_n\cdot u(s,vvec_n,a)\cdot e^{-(vvec_n)^2\cdot\tau}\end{array}\right.$$

(End of core formulas)

Solution S(r,t):

$$S_{in} := 0.85 \qquad D_0 := \frac{4\cdot(r_r - r_c)^2}{\pi^2} \qquad t_0 := \frac{4\cdot(r_r - r_c)^2}{\pi^2 \cdot D_0} \qquad t_0 = 1$$

( We choose t.0=1, i.e. t=τ: )

$$S(r,t) := S_{in} + (1 - S_{in})\cdot\sigma\left(\frac{r}{r_r}, \frac{t}{t_0}\right)$$

S(r,t) for the reference case, Figure 7.5

$$I := 200 \qquad i := 1..I+1 \qquad rl_i := r_c + \frac{i-1}{I}\cdot(r_r - r_c) \qquad sl_i := \frac{rl_i}{r_r}$$

(Calculation for I points)

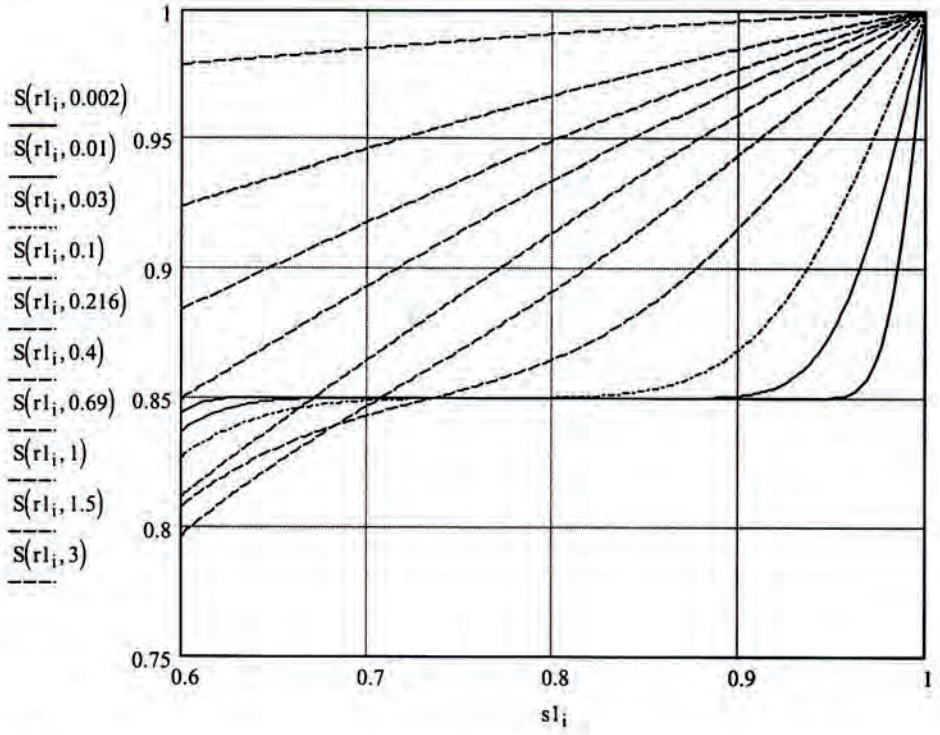


**Fig. 8.5**

Calculation of S(r.c,t) in the reference case

$$I1 := 1000 \qquad i1 := 2..I1 + 1 \qquad \tau l_{i1} := 5 \cdot \frac{i1 - 1}{I1} \qquad \tau l_1 := 0$$

$$i1 := 1..I1 + 1$$

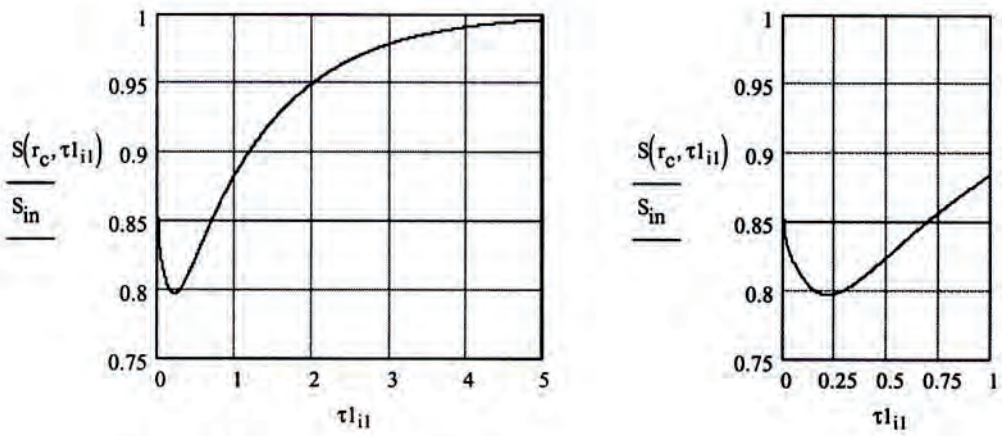


**Figure 8.6**

www.ski.se

**STATENS KÄRNKRAFTINSPEKTION**
Swedish Nuclear Power Inspectorate

**POST/POSTAL ADDRESS** SE-106 58 Stockholm
**BESÖK/OFFICE** Klarabergsviadukten 90
**TELEFON/TELEPHONE** +46 (0)8 698 84 00
**TELEFAX** +46 (0)8 661 90 86
**E-POST/E-MAIL** ski@ski.se
**WEBBPLATS/WEB SITE** www.ski.se